Highlights:

- There is a connection between chironomid functional traits, expressed through feeding guilds, and simulated annual air temperature

- The chironomid July air temperature transfer function from Lough Nakeeroge is not solely reconstructing air temperature from than mid- to late Holocene, but is being driven by a complicated range of influencing variables

- Several important Holocene climate phases and events can be identified from the Irish palaeoclimate records

- There is a clear contradiction between the proxy records and climate model hindcasts over the mid- to late Holocene, which supports the hypothesis that the North Atlantic may be responsible for the Holocene climate 'conundrum'

1   **Complexities in interpreting chironomid-based temperature reconstructions over the**

2   **Holocene from a lake in Western Ireland**

3   Michelle M. McKeown*[1,2], Chris J. Caseldine[3], Gareth Thompson[4], Graeme T. Swindles[5,6],

4   Ruza F. Ivanovic[7], Thomas P. Roland[4], Paul J. Valdes[8], Aaron P. Potito[2]

5   [1]Manaaki Whenua – Landcare Research, 54 Gerald Street, Lincoln, New Zealand

6   [2]Palaeoenvironmental Research Unit, School of Geography and Archaeology, National

7   University of Ireland Galway, Galway, Ireland

8   [3]Centre for Geography, Environment and Society, Penryn Campus, University of Exeter,

9   Penryn, UK

10   [4]Department of Geography, College of Life and Environmental Sciences, Amory Building,

11   University of Exeter, Exeter, UK

12   [5]School of Geography, University of Leeds, Leeds, UK

13   [6]Ottawa-Carleton Geoscience Centre, Department of Earth Sciences, Carleton University,

14   Ottawa, Ontario, Canada

15   [7]School of Earth and Environment, University of Leeds, Leeds, UK

16   [8]School of Geographical Sciences, University of Bristol, Bristol, UK

17   ***Corresponding author**

18   Michelle McKeown, Manaaki Whenua—Landcare Research, 54 Gerald Street, Lincoln 7608,

19   New Zealand.

20   mckeownm@landcareresearch.co.nz

21   **Abstract**:

22   Investigation of Holocene climate variability remains challenging. This is largely due

23   to chronological uncertainties and complexities associated with proxies and their

24   relationship with climatic drivers. Pertinent questions still exist regarding the Holocene

25   climate in Ireland, particularly in the early Holocene. We present a mean July air

26   temperature reconstruction based on fossil chironomidae (non-biting midge flies), along

27   with an assessment of chironomid functional traits from five guilds (based on their feeding

28   habits) from Lough Nakeeroge, a small glacial lake in western Ireland. These records span

29   the early to late Holocene (c. 10,000 - 1500 cal. yr BP). The chironomid record is

30   supplemented with pollen data to determine landscape vegetation dynamics, and compared

31   to climate model simulations of the same period. As reliable models are essential for robust

32   analysis of long-term climate change, we critically assess the value of the chironomid

33   transfer function and explore the use of chironomid functional traits to infer past climate

34   variability. While this study demonstrates the complexities of chironomid-based

35   temperature reconstruction in Irish lakes, it endeavours to i) disentangle a complicated

36   Holocene climate history through the exploration of other long-term Holocene records from

37   the island; and ii) improve our understanding of environmental responses to climate

38   variability in Ireland. The findings of this study suggest that the interpretation of

39   chironomid-based temperature transfer functions can be challenging. However, our results

40   demonstrate the influence of climate on the functioning of lake ecosystems over the

41   Holocene, with the promising performance of the collector-filterer feeding guild as a

42   palaeothermometer.

43   **Keywords**

44   Holocene, Palaeoclimatology, Palaeolimnology, Ireland, Chironomidae, Functional Traits,

45   Pollen, Climate Models

46   **1. Introduction**

47   It is now well recognised that the climate of the Holocene, the last ~ 11,500 cal. yr

48   BP, has been far from stable (Marcott et al., 2013; Marsicek et al., 2018). Broadly speaking,

49   the Holocene climate is widely considered to have transitioned from the cooler Younger

50   Dryas to a warmer climate between 11,500 and 7000 cal. yr BP, followed by a warm middle

51   Holocene with higher humidity between c. 8000 to 7000 cal. yr BP and c. 6000 to 4000 cal.

52   yr BP, depending on the region, in the Northern Hemisphere (Bond et al., 2001; Blaauw et

53   al., 2004; Diefendorf et al., 2006; Daley et al., 2011; Renssen et al., 2012; Blaschek and

54   Renssen, 2013; Marcott et al., 2013; Brooks and Langdon, 2014; Marsicek et al., 2018).

55   These warmer phases were interrupted by numerous multi-decadal- to centennial-scale cold

56   reversals (Wanner et al., 2011). Cooling in the late Holocene is well-documented from proxy

57   reconstructions in the North Atlantic region; however, model reconstructions continuously

58   simulate long-term warming associated with retreating ice-sheets and increasing carbon

59   dioxide concentrations (Baker et al., 2017; Marsicek et al., 2018). From the discrepancies

60   between these proxy reconstructions and the transient climate simulations, pertinent

61   questions regarding climate evolution during the Holocene arise.

62   In recent years, there has been a proliferation of Holocene palaeoclimate research in

63   Ireland (Caseldine et al., 2005; Caseldine and Fyfe, 2006; Langdon et al., 2012; Swindles et

64   al., 2013). Only a small number of records continuously span the early to late Holocene

65   (McDermott et al., 1999; Ahlberg et al., 2001; McDermott et al., 2001; Holmes et al., 2007).

66   The majority of work tends to focus on the mid- to late Holocene (Caseldine et al., 2005;

67   Swindles et al., 2007; Holmes et al., 2010; Langdon et al., 2012; Swindles et al., 2013; Roland

68   et al., 2014; Roland et al., 2015; Taylor et al., 2018), with few targeted reconstructions

69   exploring short-term phases over the early Holocene, (Daley et al., 2011; Ghilardi and

70   O'Connell, 2013; Holmes et al., 2016), and the transition from the Last Glacial Maximum

71   (LGM) to the early/mid-Holocene (Diefendorf et al., 2006; Watson et al., 2010; van Asch et

72   al., 2012). Most of these data are derived from peatlands (Caseldine et al., 2005; Plunkett,

73   2006; Swindles et al., 2010), speleothems (McDermott et al., 1999; McDermott et al., 2001),

74   and lacustrine sediments (Diefendorf et al., 2006; Schettler et al., 2006; Holmes et al., 2007;

75   Holmes et al., 2010; Ghilardi and O'Connell, 2013; Taylor et al., 2018). Despite this progress,

76   a consensus on the prevailing pattern of Holocene climate variability in Ireland has not been

77   reached.

78   The potential of chironomids (non-biting midge, Insecta; Diptera) as a Holocene

79   palaeoclimatic proxy in Ireland has been demonstrated by Potito et al. (2014), McKeown

80   and Potito (2016), and Taylor et al. (2018). As chironomids can track major and minor

81   changes in temperature through time, independently of precipitation (Eggermont and Heiri,

82   2012), they have the potential to capture summer air temperature fluctuations inherent to

83   the Irish climate system. Chironomid-based climate research in Ireland has largely

84   concentrated on quantitative temperature reconstructions over the Pleistocene-Holocene

85   transition (Watson et al., 2010; van Asch et al., 2012), using chironomid-temperature

86   transfer functions generated from Scandinavian-based training sets (Heiri et al., 2011).

87   When no transfer function is available for a region, calibration models from other regions

88   can be used (Watson et al., 2010; van Asch et al., 2012). However, these models do not

89   consider several factors that may undermine the reconstruction when applied to the

90   Holocene, such as regional differences in chironomid biogeography and ecology, and

91　　possible lack of modern analogues (Heiri and Millet, 2005). With the development of the

92　　regional Ireland-based chironomid transfer function (Potito et al., 2014; Taylor et al., 2018),

93　　localised quantitative estimates of July air temperature can be reconstructed for the island.

94　　While the Irish-based training set has many benefits for reconstructing chironomid-inferred

95　　air temperatures for local sites through the Holocene, the Scandinavian-based training set

96　　allows a longer temperature gradient to be captured. Chironomid-inferences using the Irish

97　　model may not have good modern analogues in the earliest portion of the Holocene. Thus,

98　　the development of a European, and even hemisphere-wide, chironomid-air temperature

99　　transfer function would allow the biogeographical patterns of species and their temperature

100　　optima to be more comprehensively understood, along with maximising modern analogues.

101　　This has been successfully achieved using peatland testate amoebae for palaeohydrological

102　　reconstructions (Amesbury et al., 2016; Amesbury et al., 2018)

103　　　　The complexity and sensitivity of the transfer function approach has been discussed

104　　in recent studies (Juggins, 2013; Luoto et al., 2014). The choice of parameters, calibration

105　　set, and regression method can alter reconstructed temperature models and caution should

106　　be exercised in the interpretation of transfer-functions in climate reconstructions (Velle et

107　　al., 2010; Brooks et al., 2012). Ecological systems are rarely as simple as transfer functions

108　　would imply. Criticisms suggest that variables other than the one being reconstructed have

109　　a negligible effect on abiotic assemblages (Juggins, 2013). To complicate matters further,

110　　the chironomid-temperature relationship can be decoupled by non-climate variables such as

111　　human activities in the lake catchment (McKeown, 2013; McKeown and Potito, 2016; Taylor

112　　et al., 2017; Chique et al., 2018). Pollen can be used as an indicator of human activity

113　　through the identification of cereal-type pollen, *Plantago* sp. - which is primarily used as an

114　　indicator of pastoral farming in Europe - and other pastoral indicators (Behre, 1981). This

115   multi-proxy approach to reconstructing palaeo-environments can allow

116   vegetation/landscape changes to be tracked alongside chironomid community change,

117   while also allowing a critical assessment of the transfer function during periods of notable

118   human impacts.

119   Comparing pollen and chironomid records can be difficult in many cases, as the

120   response of terrestrial (and aquatic) plants to fluctuations in climate will likely lag behind

121   chironomid community shifts. While climate fluctuations directly influence the adult

122   chironomids through changes in air temperature, the larval stage is driven by indirect

123   climate effects, such as changes in water temperature, fluctuations in lake level, and

124   alterations in the catchment (e.g., hydrology, vegetation, erosion). As chironomid larvae

125   provide a vital role in biogeochemical cycling in lakes via the food web structure (Palmer et

126   al., 1997), the feeding habits for chironomids have been identified as the most useful

127   functional trait for ecological studies (Pinder, 1995; Schmera et al., 2017). Recent studies

128   have demonstrated that chironomid functional traits are excellent indicators of nutrient

129   enrichment and climate variability (Luoto et al., 2014; Luoto et al., 2016; Árva et al., 2017;

130   Gomes et al., 2018; Luoto and Ojala, 2018). The potential to explore functional traits to

131   characterise long-term environmental change has long been known (Jeppesen et al., 2001),

132   but has recently gained momentum in chironomid research (Fournier et al., 2015; Gałka et

133   al., 2017; Nevalainen and Luoto, 2017; Van Bellen et al., 2017; Luoto and Ojala, 2018), along

134   with other palaeoecological indicators such as testate amoebae (Fournier et al., 2015;

135   Marcisz et al., 2016; Lamentowicz et al., 2017; Van Bellen et al., 2017; Koenig et al., 2018)

136   and diatoms (O'Donnell et al., 2017; McGowan et al., 2018; Stenger-Kovács et al., 2018).

137   Thus, shifts in chironomid functional traits, explored through their feeding guilds, may

138   provide a useful link between the faster response of the chironomid community and the

139   slower plant response to climate fluctuations, as changes in various feeding guilds will, at

140   times, be dependent on plant abundance.

141   To examine key periods of Holocene climate change, we statistically compare the

142   chironomid records with other palaeoclimate reconstructions from fossil archives and

143   climate model simulations for Ireland. This is an important and necessary exercise for

144   bridging gaps in our knowledge of how to interpret climate proxies robustly (Marcott and

145   Shakun, 2015). However, this process is challenging in and of itself. Palaeoclimate

146   reconstructions present several technical challenges including chronological uncertainties

147   (resulting from radiometric dating techniques), and variable temporal resolution of proxy

148   records (variable sedimentation rates in lakes, differing growth rates in speleothem

149   records). Additionally, different proxies respond to different climate variables and local-

150   scale variations can occur (Hu et al., 2017; Sweeney et al., 2018). Thus, combining and

151   comparing several climate proxies for a long-term climate synthesis can be challenging.

152   Recent palaeoenvironmental reconstructions are associated with better chronologies, and

153   many records have been compiled through 'tuning' and 'stacking' (Swindles et al., 2013).

154   Running correlation analysis between forcing parameters and climate proxy data can also be

155   applied to interrogate the temporal variation of correlations (Turner et al., 2016).

156   Well-documented disparities also exist between observed and simulated Holocene

157   climate, particularly from the mid- to late Holocene period. Here, climate proxies have been

158   interpreted to show long-term cooling (Marcott and Shakun, 2015), whereas computer-

159   generated climate simulations show warming as a physically robust response to retreating

160   ice sheets and rising atmospheric CO_2 (Liu et al., 2014). Marsicek et al. (2018) and Baker et

161   al. (2017) suggest that late Holocene cooling, evident in proxy reconstructions, is limited to

162   the North Atlantic records. As large areas of continental regions are under-represented in

163   Holocene global climate studies, it is plausible that the North Atlantic is responsible for the

164   contradiction. Furthermore, this discrepancy could be an over-representation of indicators

165   towards summer temperatures (Baker et al., 2017). However, pollen-based Holocene

166   temperatures from continental regions in the Northern Hemisphere follow the warming

167   trend simulated by climate models (Marsicek et al., 2018). In order to fully understand the

168   climate evolution over the Holocene, and reasons behind the Holocene 'conundrum', more

169   research is needed comparing new palaeoclimate records and climate simulations (Marsicek

170   et al., 2018).

171   This study endeavours to improve our understanding of Holocene climate variability

172   in Ireland. The aims of this study are fourfold: 1) to investigate the potential of chironomid-

173   July air temperature transfer functions to accurately reconstruct temperature change

174   through the early to late Holocene, supplemented with pollen data to track landscape

175   change; 2) to explore the use of chironomid functional traits as a tool for reconstructing

176   ecosystem functioning and stability, along with testing the sensitivity of chironomid feeding

177   guilds to modelled climate; 3) to assess the coherence with other well-established

178   palaeoclimate records in Ireland spanning the Holocene and various climate model

179   hindcasts, which have been downscaled and bias corrected to the west coast of Ireland; 4)

180   to evaluate if there is a link between the Irish palaeoclimate records and climate forcing

181   parameters, such as total solar irradiance and ice rafted debris from the North Atlantic.

182   **2. Regional setting**

183   Ireland's geographic position on the eastern seaboard of the Atlantic Ocean makes it

184   an important location to investigate climate variability over the Holocene due to its

185   sensitivity to oceanic conditions and air masses affecting thermal characteristics of the

186   adjacent land. The climate of the island is characterised by low annual temperatures

187   (between 9 $^{\circ}$C and 10 $^{\circ}$C mean annual temperature), low summer temperatures (14 $^{\circ}$C

188   mean July temperature), and high precipitation (between 1000 and 1400 mm of rainfall per

189   annum along with west coast, and ~ 750 to 1000 mm of rainfall per annum on the eastern

190   half of the island) (McKeown et al., 2012; Met Éireann, 2018).

191   Lough Nakeeroge (53 $^{\circ}$ 59.53 'N, 10 $^{\circ}$ 08.25 'W) is located on the northern coast of

192   Achill Island, Co. Mayo, in the west of Ireland. Achill Island's geology is composed of acidic

193   Dalradian and Moinian schists, which have been folded into the dominating peaks of the

194   island, with summit heights of up to 671 m a.s.l. (Chew et al., 2003). The region was

195   extensively glaciated during the last ice age by inland and local ice sheets (Knight, 2015).

196   Sea-levels have been modelled close to Achill Island, which was at the boundary of the Celtic

197   Ice sheet (Patton et al., 2017). They were estimated to be around minus 80 m by 20,000 cal.

198   yr BP, and rose rapidly to minus 30 m by 10,000 cal. yr BP, reaching around minus 5 m by

199   8000 cal. yr BP (Shennan et al., 2018).

200   Achill Island has been subject to several palaeoenvironmental studies (Caseldine et

201   al., 2005; Caseldine et al., 2007; Head et al., 2007). The present landscape is covered with

202   extensive ombrotrophic blanket peat, and it is suggested that peat initiation began in the

203   early Holocene and became a dominant form on the landscape by the late-Holocene

204   (Caseldine et al., 2007). The treeless landscape of the island bears little resemblance to that

205   of the early to mid-Holocene, when Achill Island was covered with extensive forest of *Pinus*,

206   *Quercus*, *Betula*, *Corylus*, *Alnu*s, and *Ulmus* (Caseldine et al., 2007). Lough Nakeeroge is

207   adjacent to the coast at 20 m a.s.l. (Annagh Beach, located only meters to the north) with

208   steep hill slopes to the south, east and west (Fig 1). No bathymetric maps were generated,

209   but spot measurements were taken on the day of coring. The maximum depth of the water

210   column is 9 m towards the centre of the larger basin and 4 m towards the centre of the

211   smaller one, which is located at the western edge of the lake. The lake is 0.65 km long and

212   0.2 km wide with two basins. The catchment slopes consist of shallow peat soils on granite

213   schist bedrock. *Molinia caerulea*, *Schoenus nigricans* and *Sphagnum* spp. are dominant

214   along the slopes and the lower plateaus. There are limited areas of *Phragmites* around the

215   periphery of the lake. Despite the lake's remote location, prehistoric features such as

216   unclassified megalithic tombs and a stone circle have been identified on the nearby

217   headlands (archaeology.ie, 2018).

218   Figure 1 here

219   **3. Materials and methods**

220   3.1 Lake coring strategy and core realignment

221   Two overlapping cores, core A and core B, were extracted in June 2009 in 1 m

222   segments to a maximum depth of 4 m, from the smaller basin of the Lough Nakeeroge. This

223   was carried out using a Livingstone corer (Wright Jr, 1980) from an anchored boat. The

224   smaller basin was selected to avoid slumping from steeper slopes. The cores were labelled

225   and wrapped in plastic film and aluminium foil before being transported to the Geography

226   Department's laboratory at the University of Exeter, where they were stored at c. 4°C to

227   minimise biological activity.

228   During the analysis of the Lough Nakeeroge sediment core, uncertainties in core

229   recovery were identified from an evaluation of the ^{14}C dating model, percentage weight of

230   loss-on-ignition after being dried at 550 ºC and 950 ºC (LOI$_{550}$ and LOI$_{950}$), and chironomid

231   assemblages from core A and core B (see Sup Fig. 1-2, supplementary material).

232   3.2 Age-depth model

233   Age-depth models for the Lough Nakeeroge core were based on AMS ^{14}C ages of

234   bulk sediment, due to the absence of suitable macrofossils. Humic acid and bulk humin were

235   the fractions chosen for dating and samples were pre-treated according to Lowe et al.

236   (2004). Five AMS radiocarbon dates were obtained along the sediment master core (Table

237   1). The five dates for this lake were calibrated using IntCal 13 (Reimer et al. 2013) on *Bacon*

238   version 2.2 (Blaauw and Christen, 2013) and R version 3.5.2. (R Core Team, 2018). Dates for

239   this lake are reported throughout the paper in calibrated years before present and rounded

240   to the nearest 10 years (cal. yr BP).

241   Table 1 Here

242   3.3 Laboratory analyses

243   Sediment organic (LOI$_{550}$) and inorganic content (LOI$_{950}$) was calculated using loss-on-

244   ignition, following using standard methods (Heiri et al. 2001). This was carried out at

245   continuous 1 cm intervals. Chironomid analysis was carried out at 2 cm intervals at the top

246   of core A from 50 cm to 66 cm, and at 4 cm intervals hereafter. Chironomid analysis

247   followed standard procedures outlined by Walker (2001). Chironomids were handpicked

248   with forceps using 10-40 x magnification and permanently mounted on slides for

249   identification. A minimum of 150 chironomid head capsules was picked for each sample.

250   Chironomid identifications were made using a compound microscope at 100-400 x

251   magnification. Taxa were identified to genus, sub-genus and species-type based on

252   Wiederholm (1983), Rieradevall and Brooks (2001), and Brooks et al. (2007). Samples for

253   pollen analysis were taken volumetrically (0.4 cm^3) at 4 cm intervals and prepared using

254   standard methods including KOH digestion, HF treatment and acetylation (Moore et al.,

255   1991).

256   3.4 Numerical and statistical analysis

257   A chironomid stratigraphy was created using C2 version 1.4, and stratigraphic

258   changes in the composition of chironomid and pollen assemblages were assessed by sum-

259   of-squares partitioning and statistically significant zones were identified using Psimpoll 4.27

260   (Bennett, 2009). All ordinations were produced using square-root transformed chironomid

261   percentage data for all common taxa. Common taxa were identified as those present in at

262   least two samples with a relative abundance of > 2 % in at least one sample (Heiri and

263   Lotter, 2001).

264   Chironomid-inferred temperatures were reconstructed from the chironomid

265   assemblages using an inference model generated using the 50-lake training set from

266   Western Ireland (Potito et al., 2014; Taylor et al., 2018). Based on a weighted-average (WA)

267   classic model of lake characteristics, chironomid assemblages were deemed a good

268   predictor of summer air temperature in west of Ireland region (r^2_{jack} = 0.63, RMSEP = 0.56

269   °C) (Potito et al., 2014, Taylor et al., 2018). The reliability of the chironomid-inferred

270   temperature model was assessed with a chi-squared 'goodness-of-fit' to temperature test

271   whereby fossil samples were passively positioned on a Canonical Correspondence Analysis

272   (CCA) of the modern training set constrained solely against July air temperature (Heiri and

273   Lotter, 2001). Any fossil samples that had a squared residual distance value within the 10th

274   percentile of values in the modern training set were considered to have a poor fit-to-

275   temperature (Birks, 1998). Chi chord-squared distances were calculated, and CCA were

276   performed using CANOCO version 4.54 (Ter Braak and Smilauer, 2002). Non-metric

277   multidimensional scaling (NMDS) was performed on the chironomid community data to

278   further explore changes through time using vegan version 2.5-4 (Oksanen et al., 2015) in R

279   version 3.5.2. Chironomids were divided into five guilds based on their primary feeding

280   preferences: collector-gatherers, collector-filterers, scrapers, shredders, and predators

281   (Merritt and Cummins, 1996; Luoto and Nevalainen, 2015b).

282   3.6 Data compilation

283   The Lough Nakeeroge chironomid-inferred temperature model (C-IT) and functional

284   trait (using collector-filterer guild) records were compared with Holocene palaeoclimate

285   data from Ireland to test the strength of coherence, if any, between the reconstructions.

286   The Irish palaeoclimate data is composed of peatland water table reconstructions combined

287   and detrended from eight sites across Ireland (Swindles et al., 2013), and the $\delta^{18}O$ record

288   sourced from the Crag Cave speleothem (McDermott et al., 1999; McDermott et al., 2001).

289   Although palaeoclimate evidence differs in the degree to which it records specific climate

290   parameters, statistical comparisons between the proxy reconstructions and palaeoclimate

291   simulations from a coupled atmosphere-ocean-vegetation general circulation model, the

292   Hadley Centre Coupled Model, version 3 (HadCM3; Valdes et al., 2017), was carried out to

293   explore connections between the different climate parameters and the proxy datasets.

294   Whilst this climate model is not in the latest generation of general circulation or earth

295   system models, its relatively fast integration speed on few cores (e.g. achieving ~100 model

296   years per wall-clock day on 24 processors of a Tier 3, i.e. University, supercomputing facility)

297   makes it feasible to carry out the number of simulations required for comparison to the

298   climate proxy data presented here. Furthermore, HadCM3 performs well, simulating mean

299   present-day climate and Last Glacial Maximum climate (21 ka) with comparable skill to other

300   and more recent models (DiNezio and Tierney, 2013; Valdes et al., 2017). The climate model

301   also performs well when compared to a range of palaeoenvironmental records over the last

302   glacial cycle (120 ka to present) (Singarayer et al., 2011; Hoogakker et al., 2016; Davies-

303   Barnard et al., 2017).

304   The equilibrium-type simulations used in this study were run at intervals of 500 years

305   from 12,500 to 0 yr BP and are the same simulations as those used by Gandy et al. (2018),

306   Swindles et al. (2018) and Morris et al. (2018). The simulations are based on the previous

307   1750-year long runs performed by Singarayer et al. (2011) with model developments and

308   the dynamic vegetation module described by Davies-Barnard et al. (2017) as

309   HadCM3BM2.1aD. For each time interval, the model setup was updated to be broadly

310   consistent with the Paleoclimate Model Intercomparison Project Phase Four (PMIP4)

311   protocol for the last deglaciation (Ivanovic et al., 2016) and run for a further 500 years with

312   the new boundary conditions (such as orbital parameters, atmospheric trace gases,

313   bathymetry, land sea mask, ice mask, orography) held constant through time. The climate

314   means used in this study were calculated from the last 50 years of the simulations, by which

315   time the model had reached near steady-state. The model outputs were then regionally

316   downscaled and bias corrected to 0.5° x 0.5° resolution using bi-cubic spline (see Morris et

317   al., 2018; SI Materials and Methods for more details), which is c. 50 x 50 km in the mid-

318   latitudes. This provided estimates of climate to be localised to northern Achill Island. For this

319   study, five climate variables were extracted from the simulation output: 1) annual air

320   temperature at 2 m above the ground surface (°C); 2) July air temperature at 2 m above the

321   ground surface (°C); 3) total annual precipitation (mm); 4) total July precipitation (mm); 5)

322   total annual potential evaporation (mm). Each variable was statistically assessed with each

323   of the Irish proxy reconstructions by placing all records on the same 500-year window. The

324   climate proxy data were tested for normality using the Sharpo-Wilk test and Pearson

325   correlations were performed across all datasets. Running correlations were then performed

326   to statistically interrogate the relationship among the proxy records, and then with the five

327   computer simulated climate variables. This was carried out between 9500 to 2000 cal. yr BP

328   for all records, apart from the standardised water table compilation (Swindles et al., 2013),

329   which was assessed between 6000 and 2000 cal. yr BP.

330   All palaeoclimate records (proxy and simulated) were used to determine the

331   correlation between each variable and two climate forcing datasets, Total Solar Irradiance

332   (TSI) (Steinhilber et al., 2009), and Ice Rafted Debris (IRD) in the North Atlantic (Bond et al.,

333   2001), and then with the $\delta^{18}O$ from the Greenland NGRIP record (North Greenland Ice Core

334   Project members, 2004). TSI was selected as a forcing parameter to determine if solar

335   signals are present in the proxy reconstructions. The IRD record has been recently linked to

336   storm activity throughout the Holocene in Denmark, where shifts in North Atlantic

337   westerlies and storm tracks were modulated by persistent North Atlantic Oscillation-like

338   phases (Goslin et al., 2018). The IRD record was chosen to determine if we see similar links

339   in the Irish palaeoclimate data, given that Lough Nakeeroge is a high-energy lake adjacent to

340   the coast. The $\delta^{18}O$ of the Greenland NGRIP record was used to determine if we can see

341   wider regional-scale teleconnections in Holocene climate.

342   **4. Results**

343   4.1 Age-Depth Model

344   The sedimentation rate throughout the dated levels of the master core maintains a

345   relatively consistent pattern based on the weighted mean of the age model, with no

346   significant irregularities. Between 10,050 cal. yr BP and 2050 cal. yr BP (389 cm to 76 cm),

347   the sedimentation rate was modelled at an average rate of 0.045 cm yr^{-1} (26 yr cm^{-1}).

348   Figure 2 Here

349   4.2 Organic Carbon (LOI_{550})

350   Organic carbon (LOI_{550}) ranges from 3.2 % to 39.1 % over the length of the master

351   core (Fig 3). The section of the core that is > 10,000 cal. yr BP is marked by the lowest values

352   of organic carbon (~ 4-9 %). By 9960 cal. yr BP, LOI_{550} increases to ~ 17 % and continues to

353   rise hereafter, reaching an average of 25 % between 9300 and 8100 cal. yr BP. LOI_{550} values

354   decrease to ~ 10 to 17 % between 7860 and 7600. This is followed by a marked rise in

355   organic carbon, where LOI_{550} reaches a maximum of 39 % by 6500 cal. yr BP. LOI_{550} values

356   largely stabilise from the mid-Holocene, fluctuating between 25 and 30 %. However, two

357   notable drops in LOI_{550} values occur at 3900 and 1700 cal. yr BP.

358   4.3 Chironomid community analysis and functional traits

359   The succession was divided into five statistically significant chironomid assemblage

360   zones (CAZs). In total, 54 different taxa were identified in Lough Nakeeroge, with 36

361   common taxa (Fig. 3). There was an average of 17 different taxa per sample.

362   Figure 3 Here

363   4.3.1 CAZ1 ca. > 10,000 cal. yr BP (404 – 393 cm)

364   *Micropsectra insignilobus*-type (64 %), *Tanytarsus lugens*-type (8 %), *Tanytarsus*

365   *chinyensis*-type (8 %) and *Protanypus* (4 %) comprise 84 % of the taxa in this zone.

16

366 *Microtendipes pedellus*-type (3 %), *Polypedilum nubifer*-type (3 %) and *Cladopelma* (2 %) are

367 present, albeit in low numbers. These samples lie below the last radiocarbon date in the

368 inorganic portion of the core, and denoted > 10,000 cal. yr BP. Collector-filterers are the

369 largest guild in this zone (84 %), while predators (7 %), shredders (5 %), collector-gatherers

370 (2 %) are present but at low abundance. Scrapers are not present in this zone.

371   4.3.2 CAZ2 ca. 10,050 – 8400 cal. yr BP (389 – 320 cm)

372   CAZ2 is characterised by a rise in *M. pedellus*-type (6%), *Psectrocladius*

373 *sordidellus/psilopterus*-type (6 %) and *Procladius* (6 %). *Dicrotendipes nervosus*-type (20 %)

374 and *Ablabesmyia* (10 %) appear for the first time in this zone and are the most dominant

375 taxa. These taxa make up around half of the chironomid community in CAZ2. *M.*

376 *insignilobus*-type (3 %), *T. lugens*-type (<1 %) and *Protanypus* (<1 %) notably decrease.

377 *Heterotanytarsus* (3.5 %) appears for the first time in this zone. Collector-gatherers (49 %),

378 predators (19 %) and shredders (6 %) show a sharp increase at the start of the zone, while

379 collector-filterers show a notable decline by 10,050 cal. yr BP and a progressive decline

380 through the rest of the zone (33 – 22 %). Scrapers appear for the first time in the record (1

381 %).

382   4.3.3 CAZ3 ca. 8310 – 7760 cal. yr BP (317 – 300 cm)

383   In CAZ3 there is an increase in *P. septentrionalis*-type (19 %), *H. marcidus*-type (6 %),

384 *Pseudochironomus* (5 %) and *M. insignilobus*-type (4 %). *P. septentrionalis*-type reaches its

385 highest abundance between 8100 cal. yr BP and 7800 cal. yr BP. *D. nervosus*-type decrease

386 through this zone, while *Chironomus anthracinus*-type and *Tanytarsus mendax*-type,

387 disappear entirely. *Lauterborniella* is only present in the lake between 8200 cal. yr BP and

388 8000 cal. yr BP. Collector-gatherers (67 %) reach their greatest abundance throughout this

389   zone, while collector-filterers present a trough (12 %). Predators (15 %), scrapers (< 1 %),

390   and shredders (3 %) all show minor decreases in percentage abundance.

391   4.3.4 CAZ4 ca. 7690 – 6000 cal. yr BP (297 – 238 cm)

392   *H. marcidus*-type, *Thienemannimyia*, *Pseudochironomus* and *M. insignilobus*-type are

393   abundant at the beginning of CAZ4 between 7700 to 7550 cal. yr BP, and decrease quickly

394   after 7550 cal. yr BP. *T. chinyensis*-type (18 %) is quite dominant. *D. nervosus*-type (17 %),

395   *M. pedellus*-type (~8 %), *T. glabrescens*-type (6 %), *T. mendax*-type (3 %) and *C. edwardsi*-

396   type (2 %) remain abundant. Collector-filters recover in this zone (35 %), while collector-

397   gatherers decrease (46 %). Between 6150 and 6000 cal. yr BP, at the end of this zone, there

398   is a sharp shift in the abundance of both guilds, with collector-filterers increasing (32 - 45 %)

399   and collector-gatherers decreasing (53 – 33 %). Predators are variable throughout the zone

400   (max = 17 %, min = 0 %, average = 12 %). Scrapers (2 %) and shredders (3 %) show a

401   relatively stable low abundance apart from a notable shift at the end of the zone, where the

402   former falls by 6 % and the latter increases by 6 %.

403   4.3.5 CAZ5 ca. 5900 – 1500 cal. yr BP (236 – 50 cm)

404   Overall, CAZ5 is dominated by *T. chinyensis*-type (19%), *T. mendax*-type (10%) and *T.*

405   *glabrescens*-type (8 %), together comprising around one third of the chironomid

406   community. *Heterotanytarsus* (14 %) is also quite prominent. The zone comprises the sub-

407   section of core A, with the notable decrease in *D. nervosus*-type taking place towards the

408   bottom of the core. *H. marcidus*-type (2-14 %), *T. chinyensis*-type (23-34 %) and

409   *Thienemannimyia* (4-11 %) increase in numbers between 6050 cal. yr BP and 5700 cal. yr BP.

410   While, *D. nervosus*-type (15-0 %), *P. nubifer*-type (7-0 %), *M. pedellus*-type (7-4 %), *T.*

411   *mendax*-type (2-0 %) and *T. glabrescens*-type (11-6.5 %) all decrease. Two shifts in

412   chironomid community structure are evident in the Late Holocene; the first is between 4150

413   and 3700 cal. yr BP, and the second more abrupt shift occurs between 1750 and 1700 cal. yr

414   BP. The former phase shows a decline in *M. pedellus*-type, *Procladius* and *T. glabrescens*-

415   type after 4150 cal. yr BP. The latter abrupt decline shows a brief but rapid increase in

416   *Thienemannimyia*, *M. insignilobus*-type and *H. marcidus*-type.

417   Collector-gatherers and collector-filterers show an opposing and variable trend in

418   this zone. This is particularly evident between 1750 and 1700 cal. yr BP, when collector-

419   filterers decrease from 49 % to 33 %, and collector-gatherers replace them with a notable

420   rise from 28 % to 45 %. Predators notably increase by 1790 cal. yr BP to 24%, remaining

421   relatively high (~ 17-18 %) until 1660 cal. yr BP. Shredders and scrapers stay relatively stable

422   at this time but show minor variability throughout the zone.

423   4.3.6 Non-metric multidimensional scaling

424   The non-metric multidimensional scaling (NMDS) applied to the chironomid

425   stratigraphy shows an overview of community change through time. CAZ1 is spaced further

426   from all other zones in the ordination space and is driven by cool adapted taxa such as *T.*

427   *lugens*, *M. insignilobus*-type, and *Protanypus*. CAZ2-CAZ3 overlap, with CAZ3 located further

428   to the right of the bottom quantrant, which is driven by *Lauterborniella*, *Psectrocladius*

429   *septentrionalis*-type, and *Pseudochironomus*. The ordination space occupied by CAZ2, CAZ4

430   and CAZ5 is much larger than the other two zones, provides a general overview of lake

431   development over the Holocene along NMDS Axis 1 (Fig. 4(i) and 4(ii)). The shift towards the

432   left of the graph is driven by T. *palidicornis*-type, Polypedilum *sordens*-type, *Stempellina*,

433   *Tanytarus* undefined, and *Eukiefferiella*.

434   Figure 4 Here

435   4.3.7 Chironomid-inferred temperature model

436   The chironomid-inferred July air temperature model (C-IT) for Lough Nakeeroge

437   ranged from 11.4 ^{o}C to 14.5 ^{o}C (Fig. 3). Potito et al (2014) states that the root-mean square

438   error of prediction (RMSEP) of 0.56 ^{o}C is considerably smaller than errors reported from

439   other regional training sets. Thus, the model has greater applicability for reconstructing

440   Ireland's relatively subdued Holocene temperature fluctuations. The lowest C-IT estimates

441   occur at > 10,000 cal. yr BP and the highest at 1990 cal. yr BP. The period < 10,000 cal. yr BP,

442   is composed of three samples, which fall slightly outside the ordination space of the

443   Western Ireland training set, but were still statistically calculated to be a good 'fit-to-

444   temperature' (Fig 5). C-IT estimates increase from > 10,000 cal. yr BP, with sustained high

445   values between 10,000 and 6000 cal. yr BP. Within this inferred warmer period, C-ITs show a

446   decline 7800 and 7500 cal. yr BP (12.5 ^{o}C). Between 6030 and 5800 cal. yr BP the model

447   shows a notable decline in C-IT over a 230-year period. By 5200 cal. yr BP inferred

448   temperatures increase gradually, with a decline in values inferred between 4050 and 3400

449   cal. yr BP, and a marked abrupt decline between 1730 and 1690 cal. yr BP. A subsequent

450   increase in C-IT is evident for the rest of the core with inferred values reaching an average of

451   13.8 ^{o}C, with the highest inferred temperature recorded at 1990 cal. yr BP (14.5 ^{o}C). The

452   chironomid taxa identified in the Irish training set (Potito et al. 2014) are well represented

453   throughout the Lough Nakeeroge core. The CCA shows that the downcore chironomid

454   assemblage are located within the ordination space captured by the Western Ireland

455   training set (Fig. 5) (Potito et al. 2014).

456   Figure 5 Here

457   4.4 Pollen Stratigraphy

458   The pollen profile was divided into four significant pollen assemblage zones (PAZs),

459   with zone boundaries occurring at 9750 cal. yr BP, 7850 cal. yr BP, and 3125 cal. yr BP (Fig.

460   6). In total 48 different taxa were identified. Pollen concentrations ranged from 735,811 to

461   19,349 grains per ml^{-1} of wet sediment, with grains more densely concentrated in the

462   bottom section of the core and decreasing towards the top.

463   4.4.1 PAZ1 ca. > 10,000 – 9750 cal. yr BP (404 – 377 cm)

464   In PAZ1, > 10,000 cal. yr BP, *Poaceae*, *Salix*, *Juniperus* and a range of ericaceous taxa

465   dominated the landscape, comprising around 70 % of the pollen record. This open

466   herbaceous landscape with dwarf shrubs declined by 9850 cal. yr BP and a *Betula*-dominant

467   woodland began to establish. Unfortunately, due to the lack of pollen in the sediment,

468   notable gaps in the pollen record exists between 9650 cal. yr BP and 8800 cal. yr BP, and

469   again between 8725 cal. yr BP and 8100 cal. yr BP.

470   4.4.2 PAZ2 ca. 9650 – 7890 cal. yr BP (373 – 305 cm)

471   In PAZ2, *Betula* becomes more dominant and by 8700 cal. yr BP *Pinus* and *Corylus*

472   increase in abundance. *Ulmus* and *Quercus* also appear at the end of PAZ2 and all Ericales

473   decrease to 2 %. By 7800 cal. yr BP mixed woodland is well established with *Corylus* (9 %),

474   *Pinus* (23 %), *Betula* (21 %). *Isoetes* also increases towards the end of the Zone from 2 % to

475   17 %. Ferns decrease throughout PAZ 2 (24 % to 2 %).

476   Figure 6 Here

477   4.4.3 PAZ3 ca. 7790 – 3220 cal. yr BP (301 – 130 cm)

478   Throughout PAZ3 mixed woodland continues to dominate and *Isoetes* becomes

479   more common. Total Ericales, most notably *Calluna*, was recorded relatively continuously

480   throughout the zone with evident increases at times of notably lower woodland cover,

481   which punctuate the record between 5550 cal. yr BP and 5450 cal. yr BP, and again at 4850

482   cal. yr BP. Between 5900 cal. yr BP and 5450 cal. yr BP, *Betula, Pinus, Ulmus, Quercus, Alnus*

483   and *Corylus* decrease from 64 % to 20 % of the total landscape cover. *Calluna* increases from

484   15 % to 30 %, while *Isoetes* increases from 21 % to 57 %. By 5350 cal. yr BP, woodland

485   recovers to 76 %, while *Calluna* and *Isoetes* decrease. A more abrupt decline in woodland

486   (74 – 39 %) and increase in *Calluna* (13 – 34 %) is evident between 5000 cal. yr BP and 4850

487   cal. yr BP. PCA axis 1 for pollen shows two notable shifts at 5450 cal. yr BP and 4850 cal. yr

488   BP, in a rather featureless record. Towards the end of the zone, between 4000 cal. yr BP and

489   3700 cal. yr BP, there is a fall in the abundance of most tree species once more (81 – 44 %)

490   and *Calluna* becomes more dominant (4 – 19 %).

491   4.4.4 PAZ 4 ca. 3130 – 1500 cal. yr BP (126 – 50 cm)

492   Throughout PAZ 4 (3125 cal. yr BP to 1500 cal. yr BP) all trees decrease, most notably

493   *Pinus* (15 – 2 %), *Betula* (11 – 2 %), *Quercus* (14 – 1 %) and *Ulmus* (1.5 – 0 %). There is also an

494   increase in *Isoetes* between 3000 and 2600 cal. yr BP (6 – 56 %). By 1500 cal. yr BP, the

495   landscape shifts from one dominated by woodland to one reflecting dwarf shrub

496   colonisation.

497   **5. Interpretation and discussion**

498   5.1 Early Holocene

499   The early Holocene marks the period with the greatest taxa turnover and change in

500   C-IT (Fig. 3). It must be noted that the dates for these samples are beyond the basal ^{14}C date

501   (9830 cal. yr BP), and estimates have been attained through extrapolation of the Bayesian

502   age-depth model (Blaauw and Christen, 2011). It is suspected that these sediments are older

503   than the age-depth model implies. Taking this into consideration, a low C-IT of 11.4 °C is

504   observed in this portion of the record (Fig 3). Taxa associated with cool, oligotrophic lake

505   conditions dominate the earliest portion of the record before 10,000 cal. yr BP; taxa include

506   *M. insignilobus*-type, *T. lugens*-type, *T. chinyensis*-type and *Protanypus*. Species diversity is

507   low in this portion of the stratigraphy. Here, the chironomid collector-filterer feeding guild

508   dominates. This group filters small-sized organic particles from the water column, and are

509   commonly found in tubes extending above the surface of the substrate (Cummins, 1973).

510   Collector-filterers tend to thrive in cooler, less productive lakes, which are typically

511   structured by benthic-food webs, and intermediate water depth (Cummins, 1973). A similar

512   pattern is observed in Finland, where Luoto and Nevalainen (2015b) show that the collector-

513   filterer guild is most abundant in the cold early Holocene (< 10,000 cal. yr BP). There is also a

514   high concentration of chironomid head capsules and pollen grains, corresponding with a

515   minimum in sediment organic carbon, likely indicating a slow rate of sedimentation, a

516   typical feature of early lake ontology in an adjusting climate (Fig. 3 and Fig. 8). *Salix*,

517   *Juniperus*, and a range of ericaceous taxa, are dominant reflecting dwarf shrub colonisation

518   of the landscape during this phase.

519   At c. 10,000 cal. yr BP, the chironomid community appears to shift to an alternative

520   'stable state'. There is an evident rise in taxa associated with warmer, more productive lake

521   conditions, such as *M. pedellus*-type and *P. sordidellus/psilopterus*-type. Collector-filterers

522   decline over the time, while collector-gatherers, predators, and shredders, notably increase.

523   Collector-gatherers tends to be the most dominant feeding guild in contemporary,

524   temperature, mid-latitude lakes; they are deposit feeders and consume organic detritus that

525   accumulate on lake sediments (Cummins, 1973). Chironomid larvae with predatory feeding

526   patterns tend to feed on small rotifers and cladocerans, which are more abundant in

527   productive lakes (Vodopich and Cowell, 1984). Luoto and Nevalainen (2015a) suggest that

528   predators and collector-gatherers may be indicators of climate-trophic coupling, as these

529   feeding guilds tend to thrive in warmer, nutrient-rich lakes. Shredders are known to feed on

530   course particles of organic matter, such as submerged wood, leaf litter, and algae; they are

531   also associated with living vascular plants. These feeding guilds suggest an increase in lake

532   productivity in a potentially warmer climate. At this time, frequencies of *Betula* rise (c. 9950

533   cal. yr BP), followed by *Juniperus* and *Poaceae*. Ericales notably decrease, indicating the

534   growth of early forest. C-IT shows a marked increase from c. 10,000 - 8950 cal. yr BP. Thus,

535   the chironomid community is responding indirectly to changes in trophic conditions, which

536   is likely driven by a shift towards a warmer climate.

537   Between 8950 and 8000 cal. yr BP, the C-IT shows an overall decline, while taxa

538   associated with warmer and more productive conditions continue to increase. Collector-

539   filterers remain low, while collector-gatherers and predators continue to rise. By 8100 cal. yr

540   BP, the Lough Nakeeroge pollen reconstruction shows an increase in *Pinus*, *Quercus* and

541   *Corylus*, along with the colonisation of *Ulmus*, indicating a mature mixed tree canopy.

542   *Lauterborniella* appears for the first time in the stratigraphy at c. 8200 cal. yr BP, and aligns

543   with a notable increase in *Isoetes*. This chironomid taxon is well-known to be indicative of

544   well-developed macrophytes stands (Merritt and Cummins, 1996; Heino, 2008; Kowalewski

545   et al., 2016). Shredders and scrapers also show a minor, but notable, increase. As

546   mentioned above, these guilds tend to be associated with diverse macrophyte communities

547   (Alahuhta et al., 2011), and it is suggested that an increase in their abundance is linked to

548   the availability of plant material (Luoto and Nevalainen, 2015a). At 8200 cal. yr BP, the

549   chironomid assemblage, and functional traits of the community, are probably responding to

550   altered macrophyte abundance, indirectly driving the community into an alternative 'stable

551   state'.

552   By 7000 cal. yr BP, trees show an overall decline, and *Calluna* increases, indicating

553   peat expansion across the landscape. *Isoetes* follow a similar pattern to *Calluna*. Shredders

554   and scrapers also increase. This may indicate a rise in lake level, driven by a shift in

555   hydrogeological conditions associated with decreased tree cover and expansion of bog,

556   allowing water-tables to rise, and lake shelves to flood, where *Isoetes* can further expand

557   and thrive (Fig. 7). The shift in chironomid functional traits likely indicates a transition

558   towards higher organic production through littoral aquatic vegetation expansion (*Isoetes*)

559   and pelagic productivity. As mentioned above, shredders and scrapers are associated with

560   diverse macrophyte communities (Alahuhta et al., 2011), and collector-gatherers consume

561   organic detritus that accumulate on lake sediments (Cummins, 1973). Between 7800 and

562   6030 cal. yr BP, the collector-filterers increase once again, while the collector-gatherers

563   decrease slightly but remain dominant. Shredders, scrapers, and predators, stay relatively

564   stable. This likely indicates active pelagic, benthic, and littoral production in Lough

565   Nakeeroge. However, the C-IT increases over this time, which seems counter-intuitive to the

566   functional trait argument.

567   Figure 7 Here

568   5.2 Mid-Holocene

569   While the presence of megalithic tombs in northern Achill Island does suggest

570   human habitation in the region (archaeology.ie, 2018), the Lough Nakeeroge pollen record

571   only shows evidence of some small-scale human activity; traditional indicators, such as

572   *Plantago* and *Rumex* are present albeit in only very low abundances. Charcoal evidence

573   from the region shows levels too high to reflect solely domestic fires (Caseldine et al., 2005).

574   As human activity is present, albeit only likely to be minor, caution is exerted with C-IT

575   interpretation and there is the potential for human activity to influence the lake system and

576   thus the chironomid community. It is difficult to determine a decline in Elm for the region as

577   *Ulmus* abundance is relatively low and variable between 5500 and 4500 cal. yr BP; however,

578   two notable periods where *Ulmus* declines occur at c. 5450 and 4850 cal. yr BP.

579   Lough Nakeeroge C-IT shows a notable decline between 6050 cal. yr BP and 5800 cal.

580   yr BP, with continued low values until 5350 cal. yr BP. This is being driven by an increase in

581   *H. marcidus*-type and *Thienemannimyia*, along with an increase in *Heterotanytarsus*. There

582   is also a notable decrease in *D. nervosus*-type over this period; the taxon is well represented

583   (15% of the chironomid assemblage) at 240 cm (6030 cal. yr BP), which is located at the

584   bottom of the sub-section of core A (Sup. Fig. 2) and then decreases throughout the rest of

585   the core. This species has been identified as a keystone indicator for identifying critical

586   transitions to alternative stable states in lakes (Doncaster et al., 2016), and it clearly defines

587   a shift in the chironomid community in Lough Nakeeroge. There is also a decrease in LOI_{550}

588   around this time. Collector-gatherers decline and are briefly replaced by collector-filterers;

589   this indicates a decrease in lake productivity, potentially forcing the lake, once again, into an

590   alternative 'stable state'.

591   *Heterotanytarus* is inferred as a cooler-adapted species in the chironomid inference

592   model. However, in the 50-lake training set from Western Ireland the higher elevation lakes

593   were in catchments covered with blanket peat and contained a higher abundance of

594   *Heterotanytarus*. As elevation decreases and temperatures rise, along with bogs becoming

595   less dominant across the landscape due to drainage and conversion of peatland to pastoral

596   land from human activities, *Heterotanytarus* may not be indicative of cooler temperatures

597   but may be more related to acidic, peaty conditions, which occur in cool, higher elevation

598   sites in western Ireland. In a catchment where peat is expanding, *Heterotanytarsus* will

599   become more dominant but will also drive the model to infer cooler conditions. It is possible

600   that the C-IT model may be 1) decoupled from temperature and responding to a changing

601   landscape in the mid-Holocene or, 2) overestimating potential cooling. It is not clear that

602   temperature is the main driver of chironomid community turnover and the C-IT should be

603   interpreted with caution here.

604   The C-IT shows an increase between 5800 and 4150 cal. yr BP, with a notable lull

605   between 5600 and 5200 cal. yr BP. Peatland was now well established in the catchment, as

606   identified by the dominance of *Calluna*, *Cyperaceae*, and the chironomid taxon

607   *Heterotanytarsus*. There is a notable abrupt decline in all trees and increase in *Calluna* and

608   *Poaceae* between c. 5600 and 5400 cal. yr BP, with a parallel marked decrease in pollen

609   concentration. The chironomid feeding guilds also show variability over this period, which is

610   particularly evident in the collector-filterers and scrapers, with an overall increase in both

611   guilds. As scrappers shave material from submerged objects, such as rocks and wood

612   (Cummins, 1973), an expansion of this feeding guild may indicate an increase in the input of

613   terrestrial material to the lake. Caseldine et al. (2005) suggest an extreme in-wash event

614   from two peatlands on Achill island through humification and palynological data, which was

615   associated with increased storminess between c. 5300 and 5050 cal. yr BP. Roland et al.

616   (2015) suggests that the increase in storminess at 5200 cal. yr BP is an island-wide

617   phenomenon, and wetter conditions have been largely reported across the Northern Europe

618   at this time (Starkel, 1991; Haas et al., 1998; Magny, 1999; Hughes et al., 2000; Langdon et

619   al., 2003; Blaauw et al., 2004; Magny et al., 2006). As Lough Nakeeroge is a coastal lake in a

620   high-energy environment, in-wash events from stormier conditions c. 5600 and 5400 cal. yr

621   BP may be responsible for the suggested decrease in lake productivity (increase in collector-

622 filterers) in parallel with the increase in scrappers, which favour larger submerged material.

623 Evidence for a stormy phase at the time could be further supported by the brief decrease in

624 trees and the decline in LOI_{550}, where a marine in-wash event may have increased the

625 percentage of terrigenous fractionation, thus, leading to a decrease in the percentage of

626 organic carbon. However, as the resolution of our data is coarse and our dating model is

627 composed of only 5 radiocarbon dates, we can only speculate about a 5.2 ka event.

628 However, the timing of the suggested period of short-term environmental variability aligns

629 well with lake level variability across Europe (Magny et al., 2006), but appears to be earlier

630 then that recorded in Ireland (Caseldine et al., 2005; Roland et al., 2015).

631 5.3 Late Holocene

632 By the late Holocene, the chironomid community appears more stable. The C-IT

633 shows a broad decline between 4150 and 3800 cal. yr BP. This change is mainly due to the

634 replacement of *T. mendax*-type by the more cold-adapted *M. insignilobus*-type. Collector-

635 filterers increase at the expense of collector-gatherers over this time, while shredders show

636 a minor but stable increase. The is accompanied by a marked change in the pollen record

637 with a rise in *Salix* and a fall in the abundance of most tree species. This may suggest a

638 phase of cooler and wetter conditions in the region. Across Ireland and Britain evidence for

639 wetter conditions is suggested in peat-based palaeoecological records c. 4250 – 3750 cal. yr

640 BP (Hughes et al., 2000; Barber et al., 2003; Mauquoy et al., 2008; Daley and Barber, 2012;

641 Roland et al., 2014). It has been suggested by Roland et al. (2014) that the manifestation of

642 this '4.2 kyr event' is unclear in Ireland. Caution is, once again, exercised with this

643 interpretation of the Lough Nakeeroge reconstruction, as the resolution of the record is too

644 coarse to confidently interpret short-term events/rapid climate shifts. More research is

645 needed at a higher resolution to fully determine if the 4.2 and 5.2 ka events occur in Ireland.

646   Between 3000 and 2600 cal. yr BP, the Lough Nakeeroge C-IT increases. Here, the

647   model is being driven by an increase in *T. mendax*-type and *T. glabrescens*-type. We also see

648   a decrease in *Pinus*. Over this time there is a decline in predators, and an increase in

649   collector-filterers, while collector-gatherers stay relatively stable. Luoto and Nevalainen

650   (2015b) demonstrate that predators are associated with warmer lakes, while collector-

651   filterers were largely found in cooler, less productive waters. The C-IT and chironomid guilds

652   show conflicting inferences, with the former indicating warmer conditions and the latter

653   suggesting a cooler climate. However, numerous palaeoecological studies from Ireland and

654   Britain provide clear evidence for cooler and wetter conditions c. 2800 cal. yrs BP (Charman

655   et al., 2006; Swindles et al., 2013; Roland et al., 2014). Thus, it is likely the C-IT is decoupled

656   from temperature at this time and chironomid functional traits are more aligned with the

657   evidence from Ireland and Britain.

658   For the rest of the record, there is a general replacement of trees with shrubs and

659   grasses, and a minor decrease in the abundance of *Isoetes*. A final brief and notable fall in

660   the Lough Nakeeroge C-IT and shift in functional traits occurs between 1750 and 1700 cal. yr

661   BP. The resolution of the record is ~ 50 years in this later portion. During this time, collector-

662   filterers decrease by 15 % and collector-gatherers increase by 18 %, and LOI_{550} notably

663   declines. Predators markedly increase to 24 % by 1780, with a continued decrease for the

664   rest of the record. No pollen was extracted over this brief period. It is not clear what is

665   driving this change in the Lough Nakeeroge records at this time.

666   5.4 Comparison of Holocene proxy records and down-scaled climate simulations

667   The chironomid-inferred temperature and functional trait records were compared

668   with existing palaeoclimate reconstructions from Ireland to decipher climate signals from

669   autogenic processes. Peat-based records represent the most abundant paleoclimate data in

670   Ireland. These records are based on testate amoebae, plant macrofossils and humification

671   values from ombrotrophic raised bogs and blanket peatlands (Swindles et al., 2013). Climate

672   inferences are based on proxies of effective moisture (precipitation minus evaporation),

673   reflecting periods of summer water deficit (Charman et al., 2009; Booth et al., 2010). These

674   peatland records have been compiled from multiple sites across Ireland to decipher a

675   climate signal from 'noisy' localised autogenic processes (Swindles et al., 2013), and provide

676   quantitative curves of effective moisture at a centennial to multi-decadal scale from the

677   mid- to late Holocene. The speleothem record from Crag Cave is a high-resolution

678   temperature-sensitive proxy record from the south west of Ireland (Co. Kerry) spanning the

679   full Holocene (McDermott et al., 1999; McDermott et al., 2001). It is inferred to be reflecting

680   changes in isotopic values of the source moisture (McDermott et al., 2001). As air mass

681   history and atmospheric circulation appear to influence the $\delta^{18}O$ signature in precipitation,

682   palaeo-$\delta^{18}O$ reconstructions sourced from Irish proxy records are best interpreted as

683   reflecting a combination of parameters, and not solely palaeoprecipitation or

684   palaeotemperature (Baldini et al., 2010). While this speleothem record is a valuable climate

685   archive, the interpretation of the $\delta^{18}O$ signature can at times be ambiguous.

686   Climate model hindcasts were used to simulate various climate parameters (with the

687   annual and summer season output focused on here) to further explore climate change in

688   Ireland. Although chironomid assemblages can be inferred climatically, there are other

689   factors that can decouple the chironomid-temperature relationship. The simulated

690   conditions provide another method to assess broader (500-yr) changes in climate

691   throughout the Holocene in Ireland, which was then compared with the chironomid records

692   from Lough Nakeeroge. This was carried out to assess if there was seasonal bias in the

693   chironomid data and to decipher if this method could be used to determine time periods

694   where the chironomid community may not be driven by temperature. This comparison was

695   also carried out with the other Irish palaeoenvironmental records to gain a better

696   understanding of climate fluctuations for Ireland.

697   Our results show that there is variable correspondence between the proxy

698   reconstructions and the simulated climate variables (Fig. 8). There are some visible

699   similarities, which we tested statistically. The results of the Pearson correlations show that

700   simulated annual temperature (r^2 = 0.56, p < 0.05), annual potential evaporation (r^2 = 0.58, p

701   < 0.05), and annual precipitation (r^2 = 0.54, p < 0.05), are all significantly negatively related

702   to the Lough Nakeeroge C-IT (Table 2). Interestingly, simulated July temperature shows a

703   much weaker relationship. This may imply that the chironomid-July air temperature

704   inference model is being driven by changes in lake level throughout the Holocene as

705   potential evaporation shows a strong negative relationship with the data. This suggests that

706   increases in C-IT occurs when there is a fall in annual air temperature, annual precipitation,

707   and annual potential evaporation, and vice versa. Thus, the Lough Nakeeroge C-IT

708   represents a complicated signal driven by these three climate variables, which draws into

709   question the chironomid-climate relationship and the validity of temperature

710   reconstructions using the transfer function at this site.

711   Table 2 Here

712   The Lough Nakeeroge C-IT show little correspondence with the chironomid

713   collector-filterer guild, apart from early Holocene warming (Fig 3 and Table 2). As collector-

714   filterers tend to thrive in cooler, more oligotrophic lakes (Luoto and Nevalainen, 2015), they

715   were selected as the best guild to explore alongside the chironomid-temperature inference

716   model. When we explore the relationship between the simulated climate models and

717   chironomid collector-filterer guild, which are typically structured by benthic-food webs

718   (Luoto and Nevalainen, 2015), annual temperature shows the strongest positive relationship

719   to this guild (r^2 = 0.51, p < 0.05), and the relationship is less significant for modelled July

720   temperature (r^2 = 0.32, p = 0.23). However, the positive relationship indicates that the

721   collector-filterer guild increases when annual and July temperatures rise. As this guild is

722   associated with cooler, less productive lakes, the relationship appears to actually be

723   negative. When we interrogate the statistical relationship between the collector-filterer

724   guild and simulated annual temperature using running correlations through time, the

725   percentage of collector-filterers is low (indicating possible warmer conditions) when

726   modelled annual temperature is low but rising from c. 9500 to 7500 cal. yr BP (Sup Fig 5 (ii)).

727   As modelled annual temperature rises throughout the rest of the Holocene (6000 cal. yr BP

728   to 2000 cal. yr BP), the collector-filterers rise, indicating a cooler, late Holocene (Sup Fig 5

729   (ii)).

730   The isotope record from Crag Cave was significantly negatively correlated to annual

731   precipitation and annual temperature (both have r^2 = 0.52, p < 0.05). The relationship

732   between the $\delta^{18}O$ of meteoric precipitation and precipitation amount at both modern event

733   and daily timescales has been identified as negative in numerous observational and

734   modelling studies (Noone and Simmonds, 2002; Celle-Jeanton et al., 2004; Treble et al.,

735   2005; Lee and Fung, 2008). The negative correlation between the Crag Cave $\delta^{18}O$ record and

736   the precipitation amount simulated by the GCM could be due to the "amount effect" in the

737   former record, whereby heavier rainfall is more ^{18}O depleted (Dansgaard, 1964). Baldini et

738   al. (2010) attributes 20 % of the $\delta^{18}O$ variability in Irish meteoric precipitation to the

739   "amount effect". Thus, precipitation amount, inferred from the depletion of $\delta^{18}O$, may be a

740   useful indicator of heavy rainfall phases, and shifts in these values may reflect shifts in air

741   mass history and atmospheric circulation.

742   Both Lough Nakeeroge C-IT and Crag Cave records show a strong negative

743   relationship with modelled annual precipitation and temperature, and show a strong

744   positive relationship to each other (r^2 = 0.43, p = 0.1). It is possible, and we speculate, that

745   the C-IT may be complicated by changes in lake level, possibly through periods of heavy

746   rainfall, where littoral shelves become flooded. However, more research is needed on lakes

747   with a well constrained lake-level record to determine if any link exists.

748   When we interrogate the statistical relationship between the proxy records and

749   GCM hindcasts through running correlations the relationships are highly variable. However,

750   the Monte Carlo significance test further suggests that the relationship between each proxy

751   and/or climate variable is mostly non-significant through time (Sup Fig. 3-12). While the

752   climate model hindcasts can provide another method of exploring Holocene climate change

753   alongside palaeoclimate proxies, it is important to remember the data-model disparity for

754   global surface temperature during the late Holocene, with proxies recording overall cooling

755   (Marcott et al., 2013), and climate models consistently simulating warming (Liu et al., 2014).

756   This disparity is evident in our dataset. Marcott and Shakun (2014) argue that this Holocene

757   climate "conundrum" relates to incomplete forcings and/or insufficient sensitivity to

758   feedbacks in the models. However, Marsicek et al. (2018) and Baker et al. (2017) suggest

759   that the contradiction may be due to palaeoclimate reconstructions primarily being carried

760   out in the Northern Hemisphere mid-latitudes, where pronounced late Holocene cooling is

761   largely inferred from maritime proximal sites using multiple approaches, while continental

762   regions are largely underrepresented. Carbon and oxygen isotopes from two stalagmites in

763   the Ural mountains, suggest that continental Eurasian warming over the Holocene, not only

764   contradicts the widely recognised inferred-warmth between ~ 10,000 to 5000 cal. yr BP,

765   followed by late Holocene cooling (Marcott and Shakun, 2015), but instead match the late

766 Holocene warming trend captured by the transient model simulations (Baker et al., 2017).

767 More recent evidence shows that temperatures reconstructed from sub-fossil pollen across

768 642 sites, extending from Europe to North America, closely match climate model

769 simulations, indicating the long-term warming defined the late Holocene up to ~ 2000 cal. yr

770 BP, and that reconstructions demonstrating long-term cooling are confined to the North

771 Atlantic Region (Marsicek et al., 2018). Our analysis shows that there is a link between

772 specific simulated climate models and Lough Nakeeroge C-IT, chironomid collector-filter

773 guild, and Crag Cave δ^{18}O records. As both sites are located in western Ireland and at the

774 fringe of the Atlantic Ocean, the disparity between the proxy reconstructions and climate

775 models is not surprising, and even supports the assumptions of Marsicek et al. (2018) and

776 Baker et al. (2017).

777 5.5 Climate drivers

778   The palaeoclimate proxy records and model simulations were compared with δ^{18}O

779 record from the NGRIP ice core (North Greenland Ice Core Project members, 2004), along

780 with the TSI (Steinhilber et al., 2009) IRD records (Bond et al., 2001). It is evident that there

781 is a high degree of variability between all three records and the Irish proxy and simulated

782 climate records (Table 2); however, some patterns of coherence are evident.

783   Figure 8 Here

784   In the early Holocene, the Lough Nakeeroge FT, C-IT and Crag Cave δ^{18}O records

785 indicate warming conditions c. 10,000 to 8000 cal. yr BP. The NGRIP δ^{18}O record also

786 suggests overall warming during this early Holocene period. As the C-IT appears to be

787 statistically related to modelled annual air temperature, precipitation and potential

788 evaporation, caution is exercised with the interpretation of this transfer function solely as a

34

789 July air temperature reconstruction. TSI is high at the start of the record to 8000 cal. yr BP,

790 which suggests that the early Holocene warming may be related to orbital-induced

791 insolation. However, short lived cooler phases punctuate this overall warmer early Holocene

792 climate. A 150-yr short lived decline in $\delta^{18}O$ is evident from the Crag Cave record between

793 9350 and 9200 cal. yr BP, and a more subtle change is also evident in the Lough Nakeeroge

794 C-IT, FT, and NGRIP $\delta^{18}O$ records. However, the coarser resolution of the chironomid

795 reconstructions makes it difficult to confidently interpret such short-lived fluctuations.

796 Numerous studies have attributed these fluctuations to the interaction between solar

797 insolation, ice-sheets dynamics and heat transport of the North Atlantic (Kaufman et al.,

798 2004; Kim et al., 2004; Hald et al., 2007; Renssen et al., 2012; Blaschek and Renssen, 2013;

799 Marcott et al., 2013).

800 Between 8700 and 7800 cal. yr BP, the FT record suggest peak annual warmth. The

801 C-IT signal is not clear; however, it may suggest increased fluctuations in lake levels, possibly

802 through the close relationship between C-IT and annual temperature, precipitation and

803 potential evaporation. The collector-gatherer, shredder, and scraper, feeding guilds increase

804 at the expense of the collector-filterers. This likely indicates greater organic production in

805 the littoral aquatic vegetation and pelagic zones. An increase in *Isoetes* in the pollen record

806 supports the change in chironomid functionality. It suggests that the lake's water column

807 deepened so that it flooded the littoral shelves, which may have been the result of

808 increased precipitation. The $\delta^{18}O$ record from Crag Cave shows variability over this time

809 period, where the record fluctuates between low and high $\delta^{18}O$ values. Although the precise

810 nature of what is driving the variability in chironomids is unclear and more research is

811 needed at a higher temporal resolution.

812   Apart from the NGRIP δ¹⁸O record, there is no clear evidence of the short lived 8.2

813   kyr event. This event was not detected in the conventional stalagmite (CC3) from Crag Cave

814   δ¹⁸O record; the large (∼8 %) decrease in δ¹⁸O is now known to be an analytical artefact

815   (McDermott et al., 2001; Fairchild et al., 2006). The lack of an 8.2 ka event signal may be due

816   to the coarse temporal resolution of the palaeoclimate records, as this event has been

817   observed in other Irish lakes (Holmes et al., 2016). A cooler phase with variable precipitation

818   from c. 7700 to 6800 is suggested from the Crag Cave δ¹⁸O, Lough Nakeeroge FT and CIT

819   records. TSI is low over this period and the NGRIP δ¹⁸O record shows variability similar to

820   Crag Cave.

821   The Lough Nakeeroge FT, Crag Cave δ¹⁸O record, and standardised water table

822   compilation, show similar trends between 6500 and 5200 cal. yr BP, which suggests

823   warmer/drier conditions before 5800 cal. yr BP with a shift to cooler/wetter conditions.

824   Figure 8 demonstrates that these cooler/wetter conditions between c. 5800 and 5200 cal. yr

825   BP occurred during a peak in IRD (Bond et al., 2001), along with reduced TSI. There is also

826   evidence for cooler conditions across Greenland in the NGRIP δ¹⁸O record (Fig. 8), and from

827   the GISP2 δ¹⁸O record (Stuiver et al., 1995; Alley, 2000). Modelling techniques have shown

828   that the expansion of sea-ice led to cooler conditions across the North Atlantic at this time

829   (Renssen et al., 2006). These conditions are perceived to be modulated by a persistent

830   North Atlantic Oscillation-like system, most likely induced by changes in the strength and

831   position of the Azores High pressure system, equivalent to the North Atlantic Oscillation

832   (Goslin et al., 2018). Although the resolution of the Lough Nakeeroge chironomid record is

833   not at a high temporal resolution to capture short-time climate fluctuations, it is suggested

834   that a period of intense storminess coined the '5.2 ka event' occurred during this cool/wet

835   phase, which was characterised by the increased intensity of westerly winds over Ireland,

836   with prevailing cyclonic activity and an associated increase in precipitation (Roland et al.,

837   2015).

838   By 4150 and 3800 cal. yr BP, the standardised water table compilation indicates

839   wetter conditions (Swindles et al., 2013). The collector-filterers display a subtle increase

840   between 4150 and 3700 cal. yr BP, while the C-IT declines. This is accompanied by a marked

841   change in the pollen record, with a rise in *Salix* and a fall in the abundance of Pinus, and

842   most tree species, between 3900 and 3700 cal. yr BP. This may indicate cooler and wetter

843   conditions between 4150 and 3800 cal. yr BP. However, Crag Cave $\delta^{18}O$ record shows a

844   much earlier short-lived decline from 4500 to 4200 cal. yr BP. Peat-based palaeoecological

845   records from Ireland and Britain indicate wetter conditions c. 4250 – 3750 cal. yr BP (Hughes

846   et al., 2000; Barber et al., 2003; Mauquoy et al., 2008; Daley and Barber, 2012; Roland et al.,

847   2014). TSI and IRD are stable at this time, suggesting that they are not driving this shift to

848   cooler/wetter conditions.

849   The wet/cool phase in the late Holocene (c. 2700 to 2400 cal. yr BP) is well-

850   documented across Ireland and Britain (Charman et al., 2006; Swindles et al., 2013; Roland

851   et al., 2014) and is registered in the Lough Nakeeroge FT record, with an increase in the

852   collector-filterer guild (Fig. 8). This climate phase is suggested to be widespread in the North

853   Atlantic region and occurs when TSI and IRD are low (Fig. 8). Hereafter, the standardised

854   water table record, Crag Cave $\delta^{18}O$ record, and the Lough Nakeeroge FT reconstruction

855   suggests a shift to cooler/drier conditions between 2000 and 1700 cal. yr BP. This brief

856   event has no clear connection to the IRD; however, it coincides with a subtle decline in TSI.

857   **6. Conclusions**

858   Our study is a contribution to the advancement of our understanding of Holocene

859   climate variability in Ireland. We present a new chironomid-inferred July air temperature

860   model, chironomid functional trait reconstruction, and palynological record, from a lake in

861   western Ireland that spans the early to late Holocene (c. < 10,000 to 1500 cal. yr BP). While

862   this study demonstrates the complexities of chironomid transfer functions in Irish lakes, it

863   makes a valuable contribution to 1) our understanding of chironomids as palaeoindicators of

864   climate and, 2) improves our knowledge of long-term Holocene climate variability in Ireland.

865   We can draw several conclusions from this study:

866   1. Our results show a connection between the collector-filterer feeding guild and

867   simulated annual air temperature. As chironomids play a pivotal role in the biogeochemical

868   cycling behind food-web structure in lakes, their feeding functions reflect the state of

869   trophic levels. Functional traits expressed through chironomid feeding guilds may be

870   sufficient for reconstructing past trends in temperature. However, other factors such as

871   fluctuating lake level should also be considered. More research is needed to determine the

872   strength of the relationship between chironomid feeding guilds, climate, and lake level. We

873   suggest the development of a transfer function based on functional traits, which can be

874   used alongside and complementary to the chironomid-inferred temperature models. This

875   may help decipher autogenic and allogenic factors. The link between chironomid functional

876   traits and palaeoclimate is only emerging, and more research is needed at a higher temporal

877   resolution to determine if this relationship is evident in other regions of Ireland.

878   2. The chironomid-record from Lough Nakeeroge reflects a complicated range of

879   driving factors. The Pearson's correlations between the C-IT reconstruction and the five

880   variables simulated from the climate models, suggest that the record is being driven by a

881 combination of annual air temperature, annual precipitation, and annual potential

882 evaporation. Although the running correlations and Monte Carlo test show that this

883 relationship is weak and, often, non-significant through time. Improvements can be made to

884 the transfer function method by increasing the geographic scope of training sets to capture

885 larger gradients in geographic zones, lake types and climate boundaries.

886   3. Although the palaeoclimate data is highly variable, several important phases and

887 events can be identified from the records, and tied to recent studies from the Ireland,

888 Britain, and North Atlantic region. Although, more research is needed in the early Holocene

889 from terrestrial archives to fully understand climate variability and drivers at this time.

890   4. There is a clear contradiction between the proxy records and climate model

891 hindcasts over the mid- to late Holocene. The discrepancy between late Holocene cooling

892 inferred from proxy records and warming evident in the simulated climate models reflects

893 the well-known Holocene temperature conundrum. Our data supports recent evidence,

894 which suggests that the North Atlantic may be responsible for the 'conundrum'. More

895 research is needed comparing simulated climate models to proxy reconstructions from

896 continental regions.

897   5. There is no clear evidence to link the terrestrial palaeoclimate records with

898 changes in IRD, apart from one phase 5800 and 5200 cal. ye BP. There are times when

899 changes in solar activity appear to be related to fluctuations in the proxy records. However,

900 running correlation analysis shows that this relationship is generally weak and variable

901 through time.

902 **Acknowledgements**

909   **Reference List**

910   AHLBERG, K., ALMGREN, E., WRIGHT JR, H. & ITO, E. 2001. Holocene stable-isotope stratigraphy at

911   Lough Gur, County Limerick, Western Ireland. *The Holocene*, 11**,** 367-372.

912   ALAHUHTA, J., VUORI, K.-M. & LUOTO, M. 2011. Land use, geomorphology and climate as

913   environmental determinants of emergent aquatic macrophytes in boreal catchments.

914   ALLEY, R. B. 2000. Ice-core evidence of abrupt climate changes. *Proceedings of the National Academy*

915   *of Sciences*, 97**,** 1331-1334.

916   AMESBURY, M. J., BOOTH, R. K., ROLAND, T. P., BUNBURY, J., CLIFFORD, M. J., CHARMAN, D. J.,

917   ELLIOT, S., FINKELSTEIN, S., GARNEAU, M. & HUGHES, P. D. 2018. Towards a Holarctic

918   synthesis of peatland testate amoeba ecology: Development of a new continental-scale

919   palaeohydrological transfer function for North America and comparison to European data.

920   *Quaternary Science Reviews*, 201**,** 483-500.

921   AMESBURY, M. J., SWINDLES, G. T., BOBROV, A., CHARMAN, D. J., HOLDEN, J., LAMENTOWICZ, M.,

922   MALLON, G., MAZEI, Y., MITCHELL, E. A. & PAYNE, R. J. 2016. Development of a new pan-

923   European testate amoeba transfer function for reconstructing peatland palaeohydrology.

924   *Quaternary Science Reviews*, 152**,** 132-151.

925   ARCHAEOLOGY.IE. 2018. Archaeology Survey Database

926   www.archaeology.ie [Online], Assessed on the 5th April 2018.

927 ÁRVA, D., TÓTH, M., MOZSÁR, A. & SPECZIÁR, A. 2017. The roles of environment, site position, and

928   seasonality in taxonomic and functional organization of chironomid assemblages in a

929   heterogeneous wetland, Kis-Balaton (Hungary). *Hydrobiologia*, 787**,** 353-373.

930 BAKER, J. L., LACHNIET, M. S., CHERVYATSOVA, O., ASMEROM, Y. & POLYAK, V. J. 2017. Holocene

931   warming in western continental Eurasia driven by glacial retreat and greenhouse forcing.

932   *Nature Geoscience*, 10**,** 430.

933 BALDINI, L. M., MCDERMOTT, F., BALDINI, J. U., FISCHER, M. J. & MÖLLHOFF, M. 2010. An

934   investigation of the controls on Irish precipitation δ 18 O values on monthly and event

935   timescales. *Climate dynamics*, 35**,** 977-993.

936 BARBER, K. E., CHAMBERS, F. M. & MADDY, D. 2003. Holocene palaeoclimates from peat

937   stratigraphy: macrofossil proxy climate records from three oceanic raised bogs in England

938   and Ireland. *Quaternary Science Reviews*, 22**,** 521-539.

939 BEHRE, K.-E. 1981. The interpretation of anthropogenic indicators in pollen diagrams. *Pollen et*

940   *spores*, 23**,** 225-245.

941 BENNETT, K. 2009. psimpoll'and 'pscomb': C programs for analysing pollen data and plotting pollen

942   diagrams (version 4.27) Available online from Queen's University Quaternary Geology

943   program at URL.

944 BIRKS, H. 1998. DG Frey and ES Deevey Review 1: Numerical tools in palaeolimnology–Progress,

945   potentialities, and problems. *Journal of paleolimnology*, 20**,** 307-332.

946 BLAAUW, M. & CHRISTEN, J. A. 2011. Flexible paleoclimate age-depth models using an

947   autoregressive gamma process. *Bayesian analysis*, 6**,** 457-474.

948 BLAAUW, M. & CHRISTEN, J. A. 2013. Bacon Manual e v2. 2. *Blaauw, M., Wohlfarth, B., Christen, JA,*

949   *Ampel, L., Veres, D., Hughen, KA, Preusser, F., et al.(2010),—Were Last Glacial Climate Events*

950   *Simultaneous between Greenland and France***,** 387-394.

951 BLAAUW, M., VAN GEEL, B. & VAN DER PLICHT, J. 2004. Solar forcing of climatic change during the

952   mid-Holocene: indications from raised bogs in The Netherlands. *The Holocene,* 14**,** 35-44.

953 BLASCHEK, M. & RENSSEN, H. 2013. The Holocene thermal maximum in the Nordic Seas: the impact

954 of Greenland Ice Sheet melt and other forcings in a coupled atmosphere-sea ice-ocean

955 model.

956 BOND, G., KROMER, B., BEER, J., MUSCHELER, R., EVANS, M. N., SHOWERS, W., HOFFMANN, S.,

957 LOTTI-BOND, R., HAJDAS, I. & BONANI, G. 2001. Persistent solar influence on North Atlantic

958 climate during the Holocene. *Science*, 294**,** 2130-2136.

959 BOOTH, R., LAMENTOWICZ, M. & CHARMAN, D. 2010. Preparation and analysis of testate amoebae

960 in peatland palaeoenvironmental studies. *Mires & Peat*, 7.

961 BROOKS, S. J., AXFORD, Y., HEIRI, O., LANGDON, P. G. & LAROCQUE-TOBLER, I. 2012. Chironomids

962 can be reliable proxies for Holocene temperatures. A comment on Velle et al.(2010). *The*

963 *Holocene*, 22**,** 1495-1500.

964 BROOKS, S. J. & LANGDON, P. G. 2014. Summer temperature gradients in northwest Europe during

965 the Lateglacial to early Holocene transition (15–8 ka BP) inferred from chironomid

966 assemblages. *Quaternary International*, 341**,** 80-90.

967 BROOKS, S. J., LANGDON, P. G. & HEIRI, O. 2007. *The identification and use of Palaearctic*

968 *Chironomidae larvae in palaeoecology*, Quaternary Research Association.

969 CASELDINE, C. & FYFE, R. 2006. A modelling approach to locating and characterising elm

970 decline/landnam landscapes. *Quaternary science reviews*, 25**,** 632-644.

971 CASELDINE, C., FYFE, R., LANGDON, C. & THOMPSON, G. 2007. Simulating the nature of vegetation

972 communities at the opening of the Neolithic on Achill Island, Co. Mayo, Ireland—the

973 potential role of models of pollen dispersal and deposition. *Review of Palaeobotany and*

974 *Palynology*, 144**,** 135-144.

975 CASELDINE, C., THOMPSON, G., LANGDON, C. & HENDON, D. 2005. Evidence for an extreme climatic

976 event on Achill Island, Co. Mayo, Ireland around 5200–5100 cal. yr BP. *Journal of Quaternary*

977 *Science: Published for the Quaternary Research Association*, 20**,** 169-178.

978   CELLE-JEANTON, H., GONFIANTINI, R., TRAVI, Y. & SOL, B. 2004. Oxygen-18 variations of rainwater

979   during precipitation: application of the Rayleigh model to selected rainfalls in Southern

980   France. *Journal of Hydrology*, 289**,** 165-177.

981   CHARMAN, D. J., BARBER, K. E., BLAAUW, M., LANGDON, P. G., MAUQUOY, D., DALEY, T. J., HUGHES,

982   P. D. & KAROFELD, E. 2009. Climate drivers for peatland palaeoclimate records. *Quaternary*

983   *Science Reviews*, 28**,** 1811-1819.

984   CHARMAN, D. J., BLUNDELL, A., CHIVERRELL, R. C., HENDON, D. & LANGDON, P. G. 2006. Compilation

985   of non-annually resolved Holocene proxy climate records: stacked Holocene peatland

986   palaeo-water table reconstructions from northern Britain. *Quaternary Science Reviews*, 25**,**

987   336-350.

988   CHEW, D. M., DALY, J. S., PAGE, L. & KENNEDY, M. 2003. Grampian orogenesis and the development

989   of blueschist-facies metamorphism in western Ireland. *Journal of the Geological Society*, 160**,**

990   911-924.

991   CHIQUE, C., POTITO, A. P., MOLLOY, K. & CORNETT, J. 2018. Tracking recent human impacts on a

992   nutrient sensitive Irish lake: integrating landscape to water linkages. *Hydrobiologia*, 807**,**

993   207-231.

994   CUMMINS, K. W. 1973. Trophic relations of aquatic insects. *Annual review of entomology*, 18**,** 183-

995   206.

996   DALEY, T. & BARBER, K. 2012. Multi-proxy Holocene palaeoclimate records from Walton Moss,

997   northern England and Dosenmoor, northern Germany, assessed using three statistical

998   approaches. *Quaternary International*, 268**,** 111-127.

999   DALEY, T. J., THOMAS, E. R., HOLMES, J. A., STREET-PERROTT, F. A., CHAPMAN, M. R., TINDALL, J. C.,

1000   VALDES, P. J., LOADER, N. J., MARSHALL, J. D. & WOLFF, E. W. 2011. The 8200 yr BP cold

1001   event in stable isotope records from the North Atlantic region. *Global and Planetary Change*,

1002   79**,** 288-302.

1003   DANSGAARD, W. 1964. Stable isotopes in precipitation. *Tellus*, 16**,** 436-468.

1004   DAVIES-BARNARD, T., RIDGWELL, A., SINGARAYER, J. & VALDES, P. 2017. Quantifying the influence of

1005   the terrestrial biosphere on glacial–interglacial climate dynamics. *Climate of the Past*, 13,

1006   1381-1401.

1007   DIEFENDORF, A. F., PATTERSON, W. P., MULLINS, H. T., TIBERT, N. & MARTINI, A. 2006. Evidence for

1008   high-frequency late Glacial to mid-Holocene (16,800 to 5500 cal yr BP) climate variability

1009   from oxygen isotope values of Lough Inchiquin, Ireland. *Quaternary Research*, 65, 78-86.

1010   DINEZIO, P. N. & TIERNEY, J. E. 2013. The effect of sea level on glacial Indo-Pacific climate. *Nature*

1011   *Geoscience*, 6, 485.

1012   DONCASTER, C. P., CHÁVEZ, V. A., VIGUIER, C., WANG, R., ZHANG, E., DONG, X., DEARING, J. A.,

1013   LANGDON, P. G. & DYKE, J. G. 2016. Early warning of critical transitions in biodiversity from

1014   compositional disorder. *Ecology*, 97, 3079-3090.

1015   EGGERMONT, H. & HEIRI, O. 2012. The chironomid-temperature relationship: expression in nature

1016   and palaeoenvironmental implications. *Biological Reviews*, 87, 430-456.

1017   FAIRCHILD, I. J., SMITH, C. L., BAKER, A., FULLER, L., SPÖTL, C., MATTEY, D. & MCDERMOTT, F. 2006.

1018   Modification and preservation of environmental signals in speleothems. *Earth-Science*

1019   *Reviews*, 75, 105-153.

1020   FOURNIER, B., LARA, E., JASSEY, V. E. & MITCHELL, E. A. 2015. Functional traits as a new approach for

1021   interpreting testate amoeba palaeo-records in peatlands and assessing the causes and

1022   consequences of past changes in species composition. *The Holocene*, 25, 1375-1383.

1023   GAŁKA, M., TOBOLSKI, K., GÓRSKA, A. & LAMENTOWICZ, M. 2017. Resilience of plant and testate

1024   amoeba communities after climatic and anthropogenic disturbances in a Baltic bog in

1025   Northern Poland: implications for ecological restoration. *The Holocene*, 27, 130-141.

1026   GANDY, N., GREGOIRE, L. J., ELY, J. C., CLARK, C. D., HODGSON, D. M., LEE, V., BRADWELL, T. &

1027   IVANOVIC, R. F. 2018. Marine ice sheet instability and ice shelf buttressing of the Minch Ice

1028   Stream, northwest Scotland. *The Cryosphere*, 12, 3635-3651.

1029 GHILARDI, B. & O'CONNELL, M. 2013. Early Holocene vegetation and climate dynamics with

1030 particular reference to the 8.2 ka event: pollen and macrofossil evidence from a small lake in

1031 western Ireland. *Vegetation History and Archaeobotany*, 22**,** 99-114.

1032 GOMES, W. I. A., DA SILVA JOVEM-AZEVÊDO, D., PAIVA, F. F., MILESI, S. V. & MOLOZZI, J. 2018.

1033 Functional attributes of Chironomidae for detecting anthropogenic impacts on reservoirs: A

1034 biomonitoring approach. *Ecological Indicators*, 93**,** 404-410.

1035 GOSLIN, J., FRUERGAARD, M., SANDER, L., GAŁKA, M., MENVIEL, L., MONKENBUSCH, J., THIBAULT, N.

1036 & CLEMMENSEN, L. B. 2018. Holocene centennial to millennial shifts in North-Atlantic

1037 storminess and ocean dynamics. *Scientific reports*, 8**,** 12778.

1038 HAAS, J. N., RICHOZ, I., TINNER, W. & WICK, L. 1998. Synchronous Holocene climatic oscillations

1039 recorded on the Swiss Plateau and at timberline in the Alps. *The holocene*, 8**,** 301-309.

1040 HALD, M., ANDERSSON, C., EBBESEN, H., JANSEN, E., KLITGAARD-KRISTENSEN, D., RISEBROBAKKEN,

1041 B., SALOMONSEN, G. R., SARNTHEIN, M., SEJRUP, H. P. & TELFORD, R. J. 2007. Variations in

1042 temperature and extent of Atlantic Water in the northern North Atlantic during the

1043 Holocene. *Quaternary Science Reviews*, 26**,** 3423-3440.

1044 HEAD, K., TURNEY, C. S., PILCHER, J. R., PALMER, J. & BAILLIE, M. 2007. Problems with identifying the

1045 '8200-year cold event'in terrestrial records of the Atlantic seaboard: a case study from

1046 Dooagh, Achill Island, Ireland. *Journal of Quaternary Science*, 22**,** 65-75.

1047 HEINO, J. 2008. Patterns of functional biodiversity and function-environment relationships in lake

1048 littoral macroinvertebrates. *Limnology and Oceanography*, 53**,** 1446-1455.

1049 HEIRI, O., BROOKS, S. J., BIRKS, H. J. B. & LOTTER, A. F. 2011. A 274-lake calibration data-set and

1050 inference model for chironomid-based summer air temperature reconstruction in Europe.

1051 *Quaternary Science Reviews*, 30**,** 3445-3456.

1052 HEIRI, O. & LOTTER, A. F. 2001. Effect of low count sums on quantitative environmental

1053 reconstructions: an example using subfossil chironomids. *Journal of Paleolimnology*, 26**,** 343-

1054 350.

1055 HEIRI, O. & MILLET, L. 2005. Reconstruction of Late Glacial summer temperatures from chironomid

1056   assemblages in Lac Lautrey (Jura, France). *Journal of Quaternary Science*, 20**,** 33-44.

1057 HOLMES, J., ARROWSMITH, C., AUSTIN, W., BOYLE, J., FISHER, E., HOLME, R., MARSHALL, J.,

1058   OLDFIELD, F. & VAN DER POST, K. 2010. Climate and atmospheric circulation changes over

1059   the past 1000 years reconstructed from oxygen isotopes in lake-sediment carbonate from

1060   Ireland. *The Holocene*, 20**,** 1105-1111.

1061 HOLMES, J., JONES, R., HAAS, J. N., MCDERMOTT, F., MOLLOY, K. & O'CONNELL, M. 2007. Multi-

1062   proxy evidence for Holocene lake-level and salinity changes at An Loch Mór, a coastal lake

1063   on the Aran Islands, western Ireland. *Quaternary Science Reviews*, 26**,** 2438-2462.

1064 HOLMES, J. A., TINDALL, J., ROBERTS, N., MARSHALL, W., MARSHALL, J. D., BINGHAM, A., FEESER, I.,

1065   O'CONNELL, M., ATKINSON, T. & JOURDAN, A.-L. 2016. Lake isotope records of the 8200-

1066   year cooling event in western Ireland: comparison with model simulations. *Quaternary*

1067   *Science Reviews*, 131**,** 341-349.

1068 HOOGAKKER, B., SMITH, R. S., SINGARAYER, J. S., MARCHANT, R., PRENTICE, I., ALLEN, J., ANDERSON,

1069   R., BHAGWAT, S., BEHLING, H. & BORISOVA, O. 2016. Terrestrial biosphere changes over the

1070   last 120 kyr. *Climate of the Past*, 12**,** 51-73.

1071 HU, J., EMILE-GEAY, J. & PARTIN, J. 2017. Correlation-based interpretations of paleoclimate data–

1072   where statistics meet past climates. *Earth and Planetary Science Letters*, 459**,** 362-371.

1073 HUGHES, P. D., MAUQUOY, D., BARBER, K. & LANGDON, P. G. 2000. Mire-development pathways

1074   and palaeoclimatic records from a full Holocene peat archive at Walton Moss, Cumbria,

1075   England. *The Holocene*, 10**,** 465-479.

1076 IVANOVIC, R., GREGOIRE, L., KAGEYAMA, M., ROCHE, D., VALDES, P., BURKE, A., DRUMMOND, R.,

1077   PELTIER, W. R. & TARASOV, L. 2016. Transient climate simulations of the deglaciation 21-9

1078   thousand years before present (version 1)-PMIP4 Core experiment design and boundary

1079   conditions. *Geoscientific Model Development*.

1080   JEPPESEN, E., JENSEN, J. P., AMSINCK, S. L. & JOHANSSON, L. S. 2001. Paleoecological methods as

1081   tools in assessing the near-pristine state of lakes. *TemaNord*, 563**,** 45-49.

1082   JUGGINS, S. 2013. Quantitative reconstructions in palaeolimnology: new paradigm or sick science?

1083   *Quaternary Science Reviews*, 64**,** 20-32.

1084   KAUFMAN, D. S., AGER, T. A., ANDERSON, N. J., ANDERSON, P. M., ANDREWS, J. T., BARTLEIN, P. J.,

1085   BRUBAKER, L. B., COATS, L. L., CWYNAR, L. C. & DUVALL, M. L. 2004. Holocene thermal

1086   maximum in the western Arctic (0–180 W). *Quaternary Science Reviews*, 23**,** 529-560.

1087   KIM, J.-H., RIMBU, N., LORENZ, S. J., LOHMANN, G., NAM, S.-I., SCHOUTEN, S., RÜHLEMANN, C. &

1088   SCHNEIDER, R. R. 2004. North Pacific and North Atlantic sea-surface temperature variability

1089   during the Holocene. *Quaternary Science Reviews*, 23**,** 2141-2154.

1090   KNIGHT, J. 2015. Ductile and brittle styles of subglacial sediment deformation: an example from

1091   western Ireland. *Sedimentary Geology*, 318**,** 85-96.

1092   KOENIG, I., MULOT, M. & MITCHELL, E. A. 2018. Taxonomic and functional traits responses of

1093   Sphagnum peatland testate amoebae to experimentally manipulated water table. *Ecological*

1094   *Indicators*, 85**,** 342-351.

1095   KOWALEWSKI, G. A., KORNIJÓW, R., MCGOWAN, S., KACZOROWSKA, A., BAŁAGA, K., NAMIOTKO, T.,

1096   GĄSIOROWSKI, M. & WASIŁOWSKA, A. 2016. Disentangling natural and anthropogenic

1097   drivers of changes in a shallow lake using palaeolimnology and historical archives.

1098   *Hydrobiologia*, 767**,** 301-320.

1099   LAMENTOWICZ, M., GALKA, M., TOBOLSKI, K., LAMENTOWICZ, L., ERSEK, V., JASSEY, V. E. & VAN DER

1100   KNAAP, W. O. Functional traits of testate amoebae and multi-proxy data unveil exceptional

1101   Baltic bog ecohydrology, autogenic succession and climate change during the last 2000 years

1102   in CE Europe. EGU General Assembly Conference Abstracts, 2017. 6705.

1103   LANGDON, P., BARBER, K. & HUGHES, P. 2003. A 7500-year peat-based palaeoclimatic reconstruction

1104   and evidence for an 1100-year cyclicity in bog surface wetness from Temple Hill Moss,

1105   Pentland Hills, southeast Scotland. *Quaternary science reviews*, 22**,** 259-274.

1106   LANGDON, P., BROWN, A., CASELDINE, C., BLOCKLEY, S. & STUIJTS, I. 2012. Regional climate change

1107   from peat stratigraphy for the mid-to late Holocene in central Ireland. *Quaternary*

1108   *International*, 268**,** 145-155.

1109   LEE, J. E. & FUNG, I. 2008. "Amount effect" of water isotopes and quantitative analysis of

1110   post-condensation processes. *Hydrological Processes: An International Journal*, 22**,** 1-8.

1111   LIU, Z., ZHU, J., ROSENTHAL, Y., ZHANG, X., OTTO-BLIESNER, B. L., TIMMERMANN, A., SMITH, R. S.,

1112   LOHMANN, G., ZHENG, W. & TIMM, O. E. 2014. The Holocene temperature conundrum.

1113   *Proceedings of the National Academy of Sciences*, 111**,** E3501-E3505.

1114   LUOTO, T. P., KAUKOLEHTO, M., WECKSTRÖM, J., KORHOLA, A. & VÄLIRANTA, M. 2014. New

1115   evidence of warm early-Holocene summers in subarctic Finland based on an enhanced

1116   regional chironomid-based temperature calibration model. *Quaternary Research*, 81**,** 50-62.

1117   LUOTO, T. P. & NEVALAINEN, L. 2015a. Climate-forced patterns in midge feeding guilds.

1118   *Hydrobiologia*, 742**,** 141-152.

1119   LUOTO, T. P. & NEVALAINEN, L. 2015b. Late Holocene precipitation and temperature changes in

1120   Northern Europe linked with North Atlantic forcing. *Climate Research*, 66**,** 37-48.

1121   LUOTO, T. P. & OJALA, A. E. 2018. Controls of climate, catchment erosion and biological production

1122   on long-term community and functional changes of chironomids in High Arctic lakes

1123   (Svalbard). *Palaeogeography, Palaeoclimatology, Palaeoecology*, 505**,** 63-72.

1124   LUOTO, T. P., RANTALA, M. V., GALKIN, A., RAUTIO, M. & NEVALAINEN, L. 2016. Environmental

1125   determinants of chironomid communities in remote northern lakes across the treeline–

1126   Implications for climate change assessments. *Ecological indicators*, 61**,** 991-999.

1127   MAGNY, M. 1999. Lake-level fluctuations in the Jura and french subalpine ranges associated with ice-

1128   rafting events in the north atlantic and variations in the polar atmospheric circulation

1129   [Corrélations entre les fluctuations du niveau des lacs du Jura et des Alpes françaises du

1130   Nord, les débâcles d'icebergs dam l'Atlantique Nord et la circulation atmosphérique polaire].

1131   *Quaternaire*, 10**,** 61-64.

MAGNY, M., LEUZINGER, U., BORTENSCHLAGER, S. & HAAS, J. N. 2006. Tripartite climate reversal in Central Europe 5600–5300 years ago. *Quaternary research*, 65, 3-19.

MARCISZ, K., COLOMBAROLI, D., JASSEY, V. E., TINNER, W., KOŁACZEK, P., GAŁKA, M., KARPIŃSKA-KOŁACZEK, M., SŁOWIŃSKI, M. & LAMENTOWICZ, M. 2016. A novel testate amoebae trait-based approach to infer environmental disturbance in Sphagnum peatlands. *Scientific reports*, 6, 33907.

MARCOTT, S. A. & SHAKUN, J. D. 2015. Holocene climate change and its context for the future. *PAGES*, 23, 28.

MARCOTT, S. A., SHAKUN, J. D., CLARK, P. U. & MIX, A. C. 2013. A Reconstruction of Regional and Global Temperature for the Past 11,300 Years. *Science*, 339, 1198-1201.

MARSICEK, J., SHUMAN, B. N., BARTLEIN, P. J., SHAFER, S. L. & BREWER, S. 2018. Reconciling divergent trends and millennial variations in Holocene temperatures. *Nature*, 554, 92.

MAUQUOY, D., YELOFF, D., VAN GEEL, B., CHARMAN, D. J. & BLUNDELL, A. 2008. Two decadally resolved records from north-west European peat bogs show rapid climate changes associated with solar variability during the mid–late Holocene. *Journal of Quaternary Science: Published for the Quaternary Research Association*, 23, 745-763.

MCDERMOTT, F., FRISIA, S., HUANG, Y., LONGINELLI, A., SPIRO, B., HEATON, T. H., HAWKESWORTH, C. J., BORSATO, A., KEPPENS, E. & FAIRCHILD, I. J. 1999. Holocene climate variability in Europe: evidence from δ18O, textural and extension-rate variations in three speleothems. *Quaternary Science Reviews*, 18, 1021-1038.

MCDERMOTT, F., MATTEY, D. P. & HAWKESWORTH, C. 2001. Centennial-scale Holocene climate variability revealed by a high-resolution speleothem δ18O record from SW Ireland. *Science*, 294, 1328-1331.

MCGOWAN, S., GUNN, H. V., WHITEFORD, E. J., ANDERSON, N. J., JONES, V. J. & LAW, A. C. 2018. Functional attributes of epilithic diatoms for palaeoenvironmental interpretations in South-West Greenland lakes. *Journal of paleolimnology*, 60, 273-298.

1158 MCKEOWN, M. 2013. *A Palaeolimnological Assessment of Human and Climate Influences on*

1159 *Chironomid Communities in Western Ireland.*

1160 MCKEOWN, M. & POTITO, A. P. 2016. Assessing recent climatic and human influences on chironomid

1161 communities from two moderately impacted lakes in western Ireland. *Hydrobiologia*, 765**,**

1162 245-263.

1163 MCKEOWN, M., POTITO, A. P. & HICKEY, K. R. 2012. The long-term temperature record from

1164 Markree Observatory, County Sligo, from 1842 to 2011. *Irish Geography*, 45**,** 257-282.

1165 MERRITT, R. W. & CUMMINS, K. W. 1996. *An introduction to the aquatic insects of North America*,

1166 Kendall Hunt.

1167 MET ÉIREANN. 2018. *Temperature* [Online]. [Accessed Accessed 3rd March 2018].

1168 MOORE, P. D., WEBB, J. A. & COLLISON, M. E. 1991. *Pollen analysis*, Blackwell scientific publications.

1169 MORRIS, P. J., SWINDLES, G. T., VALDES, P. J., IVANOVIC, R. F., GREGOIRE, L. J., SMITH, M. W.,

1170 TARASOV, L., HAYWOOD, A. M. & BACON, K. L. 2018. Global peatland initiation driven by

1171 regionally asynchronous warming. *Proceedings of the National Academy of Sciences*, 115**,**

1172 4851-4856.

1173 NEVALAINEN, L. & LUOTO, T. P. 2017. Relationship between cladoceran (Crustacea) functional

1174 diversity and lake trophic gradients. *Functional ecology*, 31**,** 488-498.

1175 NOONE, D. & SIMMONDS, I. 2002. Associations between δ 18O of water and climate parameters in a

1176 simulation of atmospheric circulation for 1979–95. *Journal of Climate*, 15**,** 3150-3169.

1177 NORTH GREENLAND ICE CORE PROJECT MEMBERS 2004. High resolution record of Northern

1178 Hemisphere climate extending into the last interglacial period. *Nature*, 431**,** 147-151.

1179 O'DONNELL, D. R., HAMMAN, C. R., JOHNSON, E. C., KLAUSMEIER, C. A. & LITCHMAN, E. 2017.

1180 Temperature selection drives evolution of function-valued traits in a marine diatom. *bioRxiv***,**

1181 167817.

1182   OKSANEN, J., BLANCHET, F. G., KINDT, R., LEGENDRE, P., MINCHIN, P. R., O'HARA, R., SIMPSON, G. L.,

1183   SOLYMOS, P., STEVENS, M. H. H. & WAGNER, H. 2015. Package 'vegan'. *Community ecology*

1184   *package, version*, 2.

1185   PALMER, M. A., HAKENKAMP, C. C. & NELSON-BAKER, K. 1997. Ecological heterogeneity in streams:

1186   why variance matters. *Journal of the North American Benthological Society*, 16**,** 189-202.

1187   PATTON, H., HUBBARD, A., ANDREASSEN, K., AURIAC, A., WHITEHOUSE, P. L., STROEVEN, A. P.,

1188   SHACKLETON, C., WINSBORROW, M., HEYMAN, J. & HALL, A. M. 2017. Deglaciation of the

1189   Eurasian ice sheet complex. *Quaternary Science Reviews*, 169**,** 148-172.

1190   PINDER, L. C. V. 1995. The habitats of chironomid larvae. *In:* ARMITAGE, P. D., CRANSTON, P. S. &

1191   PINDER, L. C. V. (eds.) *The Chironomidae: Biology and ecology of non-biting midges.*

1192   Dordrecht: Springer Netherlands.

1193   PLUNKETT, G. 2006. Tephra-linked peat humification records from Irish ombrotrophic bogs question

1194   nature of solar forcing at 850 cal. yr BC. *Journal of Quaternary Science: Published for the*

1195   *Quaternary Research Association*, 21**,** 9-16.

1196   POTITO, A. P., WOODWARD, C. A., MCKEOWN, M. & BEILMAN, D. W. 2014. Modern influences on

1197   chironomid distribution in western Ireland: potential for palaeoenvironmental

1198   reconstruction. *Journal of paleolimnology*, 52**,** 385-404.

1199   R CORE TEAM. 2018. R: A language and environment for statistical computing. R Foundation for

1200   Statistical Computing.

1201   RENSSEN, H., GOOSSE, H. & MUSCHELER, R. 2006. Coupled climate model simulation of Holocene

1202   cooling events: oceanic feedback amplifies solar forcing. *Climate of the Past*, 2**,** 79-90.

1203   RENSSEN, H., SEPPÄ, H., CROSTA, X., GOOSSE, H. & ROCHE, D. 2012. Global characterization of the

1204   Holocene thermal maximum. *Quaternary Science Reviews*, 48, 7-19.

1205   RIERADEVALL, M. & BROOKS, S. J. 2001. An identification guide to subfossil Tanypodinae larvae

1206   (Insecta: Diptera: Chrironomidae) based on cephalic setation. *Journal of paleolimnology*, 25**,**

1207   81-99.

1208 ROLAND, T., DALEY, T., CASELDINE, C., CHARMAN, D., TURNEY, C., AMESBURY, M., THOMPSON, G. &

1209   WOODLEY, E. 2015. The 5.2 ka climate event: Evidence from stable isotope and multi-proxy

1210   palaeoecological peatland records in Ireland. *Quaternary Science Reviews,* 124**,** 209-223.

1211 ROLAND, T. P., CASELDINE, C., CHARMAN, D., TURNEY, C. & AMESBURY, M. 2014. Was there a '4.2 ka

1212   event'in Great Britain and Ireland? Evidence from the peatland record. *Quaternary Science*

1213   *Reviews*, 83**,** 11-27.

1214 SCHETTLER, G., ROMER, R. L., O'CONNELL, M. & MOLLOY, K. 2006. Holocene climatic variations and

1215   postglacial sea-level rise geochemically recorded in the sediments of the brackish karst lake

1216   An Loch Mor, western Ireland. *Boreas*, 35**,** 674-693.

1217 SCHMERA, D., HEINO, J., PODANI, J., ERŐS, T. & DOLÉDEC, S. 2017. Functional diversity: a review of

1218   methodology and current knowledge in freshwater macroinvertebrate research.

1219   *Hydrobiologia*, 787**,** 27-44.

1220 SHENNAN, I., BRADLEY, S. L. & EDWARDS, R. 2018. Relative sea-level changes and crustal movements

1221   in Britain and Ireland since the Last Glacial Maximum. *Quaternary Science Reviews*, 188**,** 143-

1222   159.

1223 SINGARAYER, J. S., VALDES, P. J., FRIEDLINGSTEIN, P., NELSON, S. & BEERLING, D. J. 2011. Late

1224   Holocene methane rise caused by orbitally controlled increase in tropical sources. *Nature*,

1225   470**,** 82.

1226 STARKEL, L. 1991. Long-distance correlation of fluvial events in the temperate zone. *Tem-perate*

1227   *Palaeohydrology***,** 473-495.

1228 STEINHILBER, F., BEER, J. & FRÖHLICH, C. 2009. Total solar irradiance during the Holocene.

1229   *Geophysical Research Letters*, 36.

1230 STENGER-KOVÁCS, C., KÖRMENDI, K., LENGYEL, E., ABONYI, A., HAJNAL, É., SZABÓ, B., BUCZKÓ, K. &

1231   PADISÁK, J. 2018. Expanding the trait-based concept of benthic diatoms: Development of

1232   trait-and species-based indices for conductivity as the master variable of ecological status in

1233   continental saline lakes. *Ecological Indicators*, 95**,** 63-74.

1234   STUIVER, M., GROOTES, P. M. & BRAZIUNAS, T. F. 1995. The GISP2 δ18O climate record of the past

1235   16,500 years and the role of the sun, ocean, and volcanoes. *Quaternary research*, 44**,** 341-

1236   354.

1237   SWEENEY, J., SALTER-TOWNSHEND, M., EDWARDS, T., BUCK, C. E. & PARNELL, A. C. 2018. Statistical

1238   challenges in estimating past climate changes. *Wiley Interdisciplinary Reviews:*

1239   *Computational Statistics*, 10**,** e1437.

1240   SWINDLES, G., BLUNDELL, A., ROE, H. & HALL, V. 2010. A 4500-year proxy climate record from

1241   peatlands in the North of Ireland: the identification of widespread summer 'drought

1242   phases'? *Quaternary Science Reviews*, 29**,** 1577-1589.

1243   SWINDLES, G. T., LAWSON, I. T., MATTHEWS, I. P., BLAAUW, M., DALEY, T. J., CHARMAN, D. J.,

1244   ROLAND, T. P., PLUNKETT, G., SCHETTLER, G. & GEAREY, B. R. 2013. Centennial-scale climate

1245   change in Ireland during the Holocene. *Earth-Science Reviews*, 126**,** 300-320.

1246   SWINDLES, G. T., MORRIS, P. J., WHITNEY, B., GALLOWAY, J. M., GAŁKA, M., GALLEGO-SALA, A.,

1247   MACUMBER, A. L., MULLAN, D., SMITH, M. W. & AMESBURY, M. J. 2018. Ecosystem state

1248   shifts during long-term development of an Amazonian peatland. *Global change biology*, 24**,**

1249   738-757.

1250   SWINDLES, G. T., PLUNKETT, G. & ROE, H. M. 2007. A delayed climatic response to solar forcing at

1251   2800 cal. BP: multiproxy evidence from three Irish peatlands. *The Holocene*, 17, 177-182.

1252   TAYLOR, K. J., MCGINLEY, S., POTITO, A. P., MOLLOY, K. & BEILMAN, D. W. 2018. A mid to late

1253   Holocene chironomid-inferred temperature record from northwest Ireland.

1254   *Palaeogeography*, *Palaeoclimatology*, *Palaeoecology*, 505**,** 274-286.

1255   TAYLOR, K. J., STOLZE, S., BEILMAN, D. W. & POTITO, A. P. 2017. Response of chironomids to

1256   Neolithic land-use change in north-west Ireland. *The Holocene*, 27**,** 879-889.

1257   TER BRAAK, C. J. & SMILAUER, P. 2002. CANOCO reference manual and CanoDraw for Windows

1258   user's guide: software for canonical community ordination (version 4.5). www. canoco. com.

1259   TREBLE, P., BUDD, W., HOPE, P. & RUSTOMJI, P. 2005. Synoptic-scale climate patterns associated

1260   with rainfall δ18O in southern Australia. *Journal of Hydrology*, 302**,** 270-282.

1261   TURNER, T. E., SWINDLES, G. T., CHARMAN, D. J., LANGDON, P. G., MORRIS, P. J., BOOTH, R. K.,

1262   PARRY, L. E. & NICHOLS, J. E. 2016. Solar cycles or random processes? Evaluating solar

1263   variability in Holocene climate records. *Scientific reports*, 6**,** 23961.

1264   VALDES, P. J., ARMSTRONG, E., BADGER, M. P., BRADSHAW, C. D., BRAGG, F., DAVIES-BARNARD, T.,

1265   DAY, J. J., FARNSWORTH, A., HOPCROFT, P. O. & KENNEDY, A. T. 2017. The BRIDGE HadCM3

1266   family of climate models: HadCM3@ Bristol v1. 0. *Geoscientific Model Development*, 10**,**

1267   3715-3743.

1268   VAN ASCH, N., LUTZ, A. F., DUIJKERS, M. C., HEIRI, O., BROOKS, S. J. & HOEK, W. Z. 2012. Rapid

1269   climate change during the Weichselian Lateglacial in Ireland: Chironomid-inferred summer

1270   temperatures from Fiddaun, Co. Galway. *Palaeogeography*, *Palaeoclimatology*,

1271   *Palaeoecology*, 315**,** 1-11.

1272   VAN BELLEN, S., MAUQUOY, D., PAYNE, R. J., ROLAND, T. P., HUGHES, P. D., DALEY, T. J., LOADER, N.

1273   J., STREET-PERROTT, F. A., RICE, E. M. & PANCOTTO, V. A. 2017. An alternative approach to

1274   transfer functions? Testing the performance of a functional trait-based model for testate

1275   amoebae. *Palaeogeography, palaeoclimatology, palaeoecology*, 468**,** 173-183.

1276   VELLE, G., BRODERSEN, K., BIRKS, H. & WILLASSEN, E. 2010. Midges as quantitative temperature

1277   indicator species: Lessons for palaeoecology. *The Holocene*, 20**,** 989-1002.

1278   VODOPICH, D. S. & COWELL, B. C. 1984. Interaction of factors governing the distribution of a

1279   predatory aquatic insect. *Ecology*, 65**,** 39-52.

1280   WALKER, I. R. 2001. Midges: Chironomidae and related diptera. *Tracking environmental change*

1281   *using lake sediments*. Springer.

1282   WANNER, H., SOLOMINA, O., GROSJEAN, M., RITZ, S. P. & JETEL, M. 2011. Structure and origin of

1283   Holocene cold events. *Quaternary Science Reviews*, 30**,** 3109-3123.

1284   WATSON, J. E., BROOKS, S. J., WHITEHOUSE, N. J., REIMER, P. J., BIRKS, H. J. B. & TURNEY, C. 2010.

1285   Chironomid-inferred late-glacial summer air temperatures from Lough Nadourcan, Co.

1286   Donegal, Ireland. *Journal of Quaternary Science*, 25**,** 1200-1210.

1287   WIEDERHOLM, T. 1983. Chironomidae of Holarctic region: keys and diagnoses. Part 1. *Larvae*

1288   *Entomol Scand Suppl*, 19**,** 1-457.

1289   WRIGHT JR, H. E. 1980. Cores of soft lake sediments. *Boreas*, 9**,** 107-114.

1290

Fig 1. Maps showing A. location of the study area in Ireland. B. location of Lough Nakeeroge in Achill island, Co. Mayo, including elevation (contour lines of 10 m intervals), and an arrow showing the direction and orientation photograph. C. A photograph of Lough Nakeeroge on the day of coring. The white star indicates the coring location.

Fig 2. Age-depth model obtained with use of Bacon software: (i) modeled age versus depth plot, gray shaded area represents 95.4 % probability range (ii) MCMC diagnostic plot, no observed trend indicates stable solution (iii) and (iv) prior (line) and posterior (gray shape) distributions of accumulation rate (iii) and memory R (iv), confirming the reasonable choice of the parameters.

Fig 3. Chironomid stratigraphy for Lough Nakeeroge including Shannon-Wiener Diversity for each sample, chironomid head-capsule concentrations, NMDS Axis 1 and Axis 2 scores from the chironomid data, and summer air temperatures inferred using Potito et al. (2014) transfer function with LOESS smoother (span = 0.2). Chironomid accumulation zones are named CAZ.

Fig 4. NMDS bi-plot (i) of samples (ii) of common taxa. Chironomid abbreviations in (ii) are as follows: ABLA *Ablabesmyi*a, CHIRO *Chironomus anthracinus*-type, CLADO *Cladopelma*, CORY *Corynoneura edwardsi*-type, CRICI *Cricotopus intersectus*-type, CRYP *Cryptochironomus*, DICR *Dircotendipes nervosus*-type, EUK *Eukiefferiella*, HETE *Heterotanytarsus*, HETM *Heterotrissocladius marcidus*-type, LAUT Lauterborniella, LIM *Limnophyes/Paralimnophyes*

MACR *Macropelopia*, MICJ *Micropsectra junci-type*, MICI *Micropsectra insign-type*, MICR

Microtendipes pedellus-type, PAG *Pagastiella*, PARK *Parakiefferiella bathophila*-type, PARM

Paramerina, PHAE *Phaenopsectra flavipes*-type, POLN *Polypedilum nubifer*-type, POLS

Polypedilum sordens-type, PRO *Procladius*, PROT *Protanypus*, PSEC *Psectrocladius*

septentrionalis-type, PSECS *Psectrocladius sordidellus/psiloperus*-type, PSEUC

Pseudochironomus, STEM *Stempellina,* TCHI *Tanytarsus chinyensis*-type, TGLA *Tanytarsus*

glabrescens-type, THIE *Thienemannimyia*-type, TLUG *Tanytarsus lugens*-type, TMEN *Tanytarsus*

mendax-type, TPAL *Tanytarsus palidicornis*-type, TUND *Tanytarsus* undefined.

Fig 5. Conical Correspondence analysis (CCA) passively positioned the fossil samples from Lough

Nakeeroge (black dots) with assemblages present in the modern Western Ireland training set

(white dots) (Potito et al. 2014) solely constrained to July air temperature. All fossil samples had

a squared residual distance value greater than the 10th percentile of values in the modern

training set and are considered to have a good fit-to-temperature.

Fig 6. Pollen stratigraphy for Lough Nakeeroge including LOI_{550} and summer air temperatures

inferred using Potito et al. (2014) transfer function with LOESS smoother (span =0.2), and total

pollen concentration per sample. The black dots and lines indicate the depths where pollen was

extracted for analysis.

Fig 7. Lake water column illustrating high and low lake levels. The chironomid community showing all four life stages, i) egg mass, ii) larvae, iii) pupae, iv) adult. Submerged and emerged vegetation and algae are included in the image as they are a food source for the larvae collector-gatherers, scrapers, and shredders, and collector-filterers. Allogenic inputs are also represented as they can alter the chironomid community in the lake. Finally, the midge assemblage is directly and indirectly influenced by temperature, radiation, precipitation, seasonality, and evaporation. This figure has been modified from Porinchu and MacDonald (2003).

Fig 8. Composite diagram including simulated climate from a coupled atmosphere-ocean-vegetation general circulation model, the Hadley Centre Coupled Model, version 3 (HadCM3) at intervals of 500 years from 12,500 to 0 yr BP. Including total annual potential evaporation (mm), total annual precipitation (mm), total July precipitation (mm), July air temperature at 2 m above the ground surface (°C), annual air temperature at 2 m above the ground surface (°C); total solar irradiance (Steinhibler et al. 2009), a North Atlantic IRD record (Bond et al. 2001), the $\delta^{18}O$ record from the Greenland NGRIP ice core (NGRIP members, 2004); peatland water table reconstructions combined and detrended from eight sites across Ireland (Swindles et al. 2013), and $\delta^{18}O$ records from a speleothem in Crag Cave; chironomid-inferred temperature model and collector-filterer guild (representing chironomid functional traits) for Lough Nakeeroge. Grey bands indicate potential phases of climate correspondence between the records.

Sup Fig 1 (i) to (ii). The master core was corrected by aligning the LOI_{550} and LOI_{950} information from both cores A and B, along with the duplication in chironomid community structure (Sup Fig 2). Organic carbon (LOI_{550}) and inorganic carbon (LOI_{950}) for core A and core B sediment sequences for Lough Nakeeroge (i) LOI_{550} and LOI_{950} for core A and core B before realignment, and (ii) LOI_{550} and LOI_{950} for core A and core B after realignment. To realign the cores, core B was shifted down 42 cm, transferred from a depth of (i) 359-100 cm to (ii) 401-142 cm, while the bottom segment of core A was shifted down 13 cm, from (i) 352-280 cm to (ii) 365-293.

Sup Fig 1 (iii) to (iv). The portions of core A (dark grey) and core B (light grey) that were used to construct the mastercore (iii) before realignment, and (iv) after realignment. Black dots indicate the levels, and the cores, where samples were sub-sectioned for ^{14}C analysis. The areas marked with a star symbol in the (iii) core A and B are the areas where chironomid duplication was observed and (iv) shows where the core realignment corrects the duplication (see Sup. Fig 2). The realigned master core from (iv) begins at 50 cm below the sediment surface, avoiding the uppermost unconsolidated material, and reaches a depth of 401 cm (Sup Fig. 1). The master core is composed of sediment from core A taken at depths of 365-293 cm, 240-150 cm and 143-50 cm. Gaps in core A exists at 292-241 cm and 149-144 cm. Sediment from core B was taken at depths of 401-369 cm and 320-244 cm in the master core.

Sup Fig 1 (v) to (vi). Age-depth models obtained with use of Bacon software for (v) before core realignment, and (vi) after core realignment. A sixth AMS radiocarbon date was obtained for the top section of core B (120 cm); however, this date was omitted from both age-depth

models as it was decided to use the continuous section of core A from 240 – 50 cm rather than shirting back and forth between cores A and B. The ^{14}C dating model of the realigned mastercore presents an almost linear accumulation rate in the age-depth model, and the chironomid community becomes synchronous (Sup Fig 2).

Sup Fig 2. The chironomid stratigraphy showing the sections of the mastercore that are composed of core A (black filled) and core B (white with black outline). The chironomid taxa where the duplication was corrected by core re-alignment are shown between 7560 and 8300 cal. yr BP (292 – 321 cm). The taxa that show a good overlap between both cores are *Lauterborniella* (the only instances of this taxa in both cores), *Psectrocladius septentrionalis*-type, *Tanytarsus chinyensis*-type and *Heterotrissocladius marcidus*-type. Core A, core B, and the master core from Sup Fig 1 (iv) is reproduced alongside the stratigraphy so the taxa overlap and core alignment care be observed together.

Sup Fig 3 (i) to (iii). Running correlations between the proxy climate records from 2000 to 9500 cal. yr BP (time windows = 500 years). The statistical significance was calculated using a Monte Carlo simulation to determine the null hypothesis (bottom graph); coarsely dashed lines indicate significance at 95 %. Proxy records are Lough Nakeeroge chironomid-inferred temperature reconstruction (C-IT), Lough Nakeeroge chironomid collector-filterer guild (FT) (percentage compared to all other guilds), and Crag Cave δ^{18}O record.

Sup Fig 4 (i) to (iii). Running correlations between the standardized water table reconstruction for Ireland (STD WTD units) and the proxy climate records from 2000 to 6000 cal. yr BP (time windows = 500 years). The statistical significance was calculated using a Monte Carlo simulation to determine the null hypothesis (bottom graph); coarsely dashed lines indicate significance at 95 %.

Sup Fig 5 (i) to (iv). Running correlations between simulated annual surface air temperature and climate proxy records from 2000 to 9500 cal. yr BP and for STD WTD units from 2000 to 6000 cal. yr BP (time windows = 500 years). The statistical significance was calculated using a Monte Carlo simulation to determine the null hypothesis (bottom graph); coarsely dashed lines indicate significance at 95 %.

Sup Fig 6 (i) to (iv). Running correlations between simulated total annual precipitation and climate proxy records from 2000 to 9500 cal. yr BP and for STD WTD units from 2000 to 6000 cal. yr BP (time windows = 500 years). The statistical significance was calculated using a Monte Carlo simulation to determine the null hypothesis (bottom graph); coarsely dashed lines indicate significance at 95 %.

Sup Fig 7 (i) to (iv). Running correlations between simulated total annual potential evaporation and climate proxy records from 2000 to 9500 cal. yr BP and for STD WTD units from 2000 to 6000 cal. yr BP (time windows = 500 years). The statistical significance was calculated using a Monte Carlo simulation to determine the null hypothesis (bottom graph); coarsely dashed lines indicate significance at 95 %.

Sup Fig 8 (i) to (iv). Running correlations between simulated July surface air temperature and climate proxy records from 2000 to 9500 cal. yr BP and for STD WTD units from 2000 to 6000 cal. yr BP (time windows = 500 years). The statistical significance was calculated using a Monte Carlo simulation to determine the null hypothesis (bottom graph); coarsely dashed lines indicate significance at 95 %.

Sup Fig 9 (i) to (iv). Running correlations between simulated July total precipitation and climate proxy records from 2000 to 9500 cal. yr BP and for STD WTD units from 2000 to 6000 cal. yr BP (time windows = 500 years). The statistical significance was calculated using a Monte Carlo simulation to determine the null hypothesis (bottom graph); coarsely dashed lines indicate significance at 95 %.

Sup Fig 10 (i) to (iv). Running correlations between the NGRIP δ^{18}0 record (members, 2004) and proxy climate records from 2000 to 9500 cal. yr BP and for STD WTD units from 2000 to 6000

cal. yr BP (time windows = 500 years). The statistical significance was calculated using a Monte Carlo simulation to determine the null hypothesis (bottom graph); coarsely dashed lines indicate significance at 95 %.

Sup Fig 11 (i) to (iv). Running correlations between the Total Solar Irradiance (W/m^2) (TSI) record (Steinhilber et al., 2009) and proxy climate records from 2000 to 9500 cal. yr BP and for STD WTD units from 2000 to 6000 cal. yr BP (time windows = 500 years). The statistical significance was calculated using a Monte Carlo simulation to determine the null hypothesis (bottom graph); coarsely dashed lines indicate significance at 95 %.

Sup Fig 12 (i) to (iv). Running correlations between the Ice Rafted Debris (IRD) record from the North Atlantic (Bond et al., 2001). and proxy climate records from 2000 to 9500 cal. yr BP and for STD WTD units from 2000 to 6000 cal. yr BP (time windows = 500 years). The statistical significance was calculated using a Monte Carlo simulation to determine the null hypothesis (bottom graph); coarsely dashed lines indicate significance at 95 %.

(i)

Year (cal. BP)

Depth (cm)

(ii)

Log of Objective

Iteration

(iii)

acc.shape: 1.5
acc.mean: 20

Acc. rate (yr/cm)

(iv)

mem.strength: 4
mem.mean: 0.7
72 5cm sections

Memory
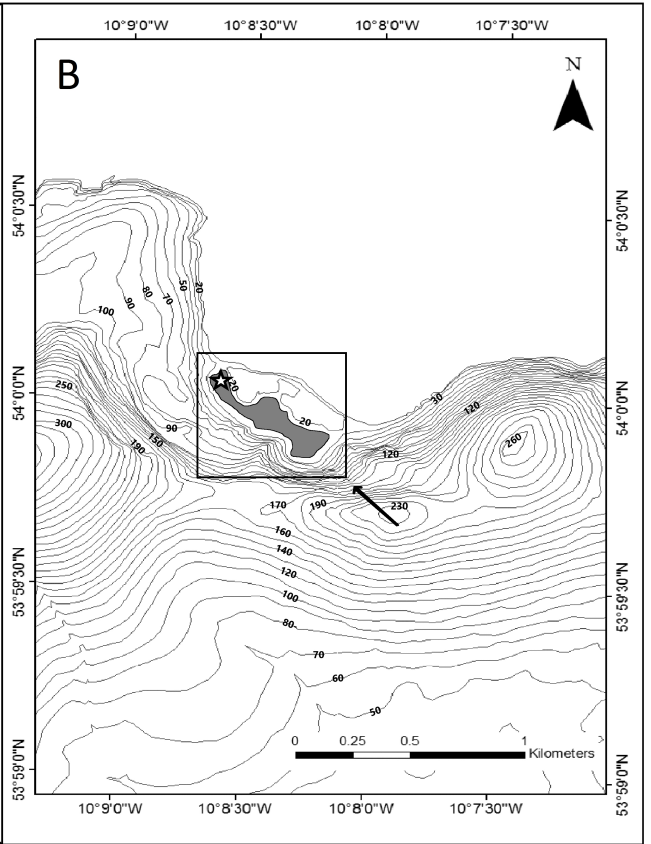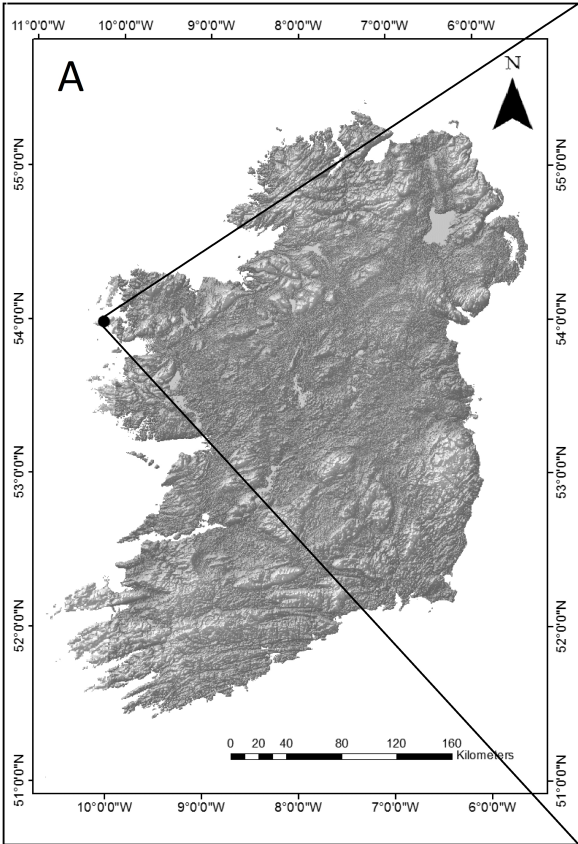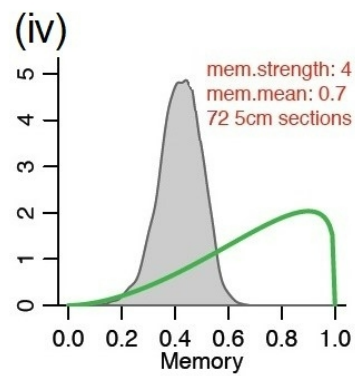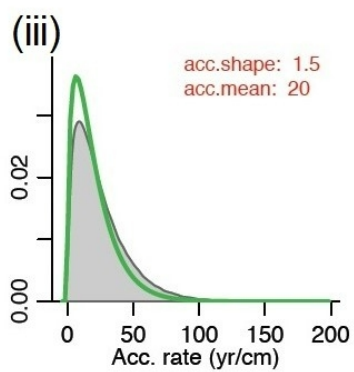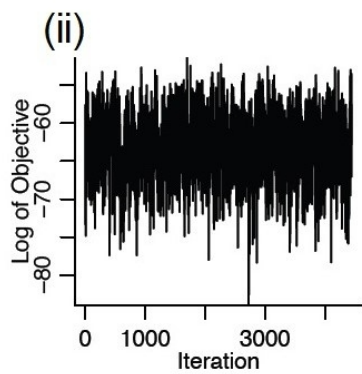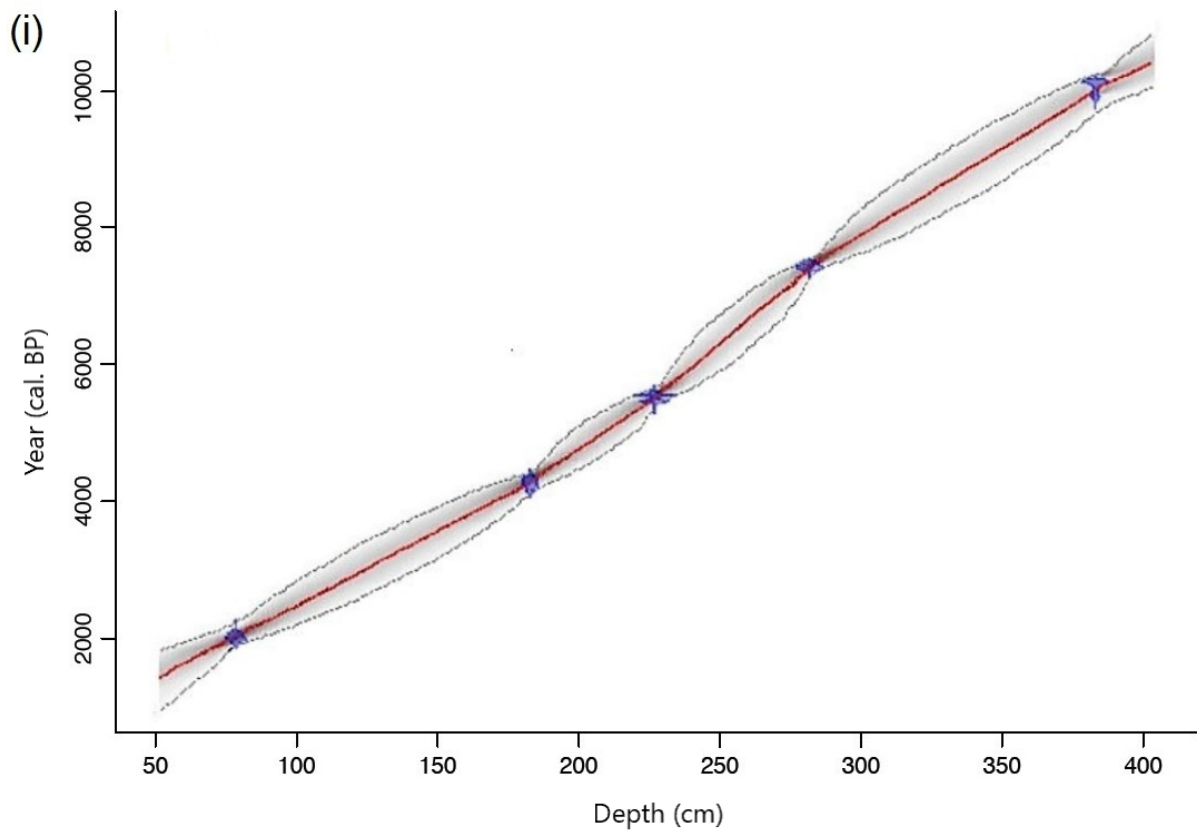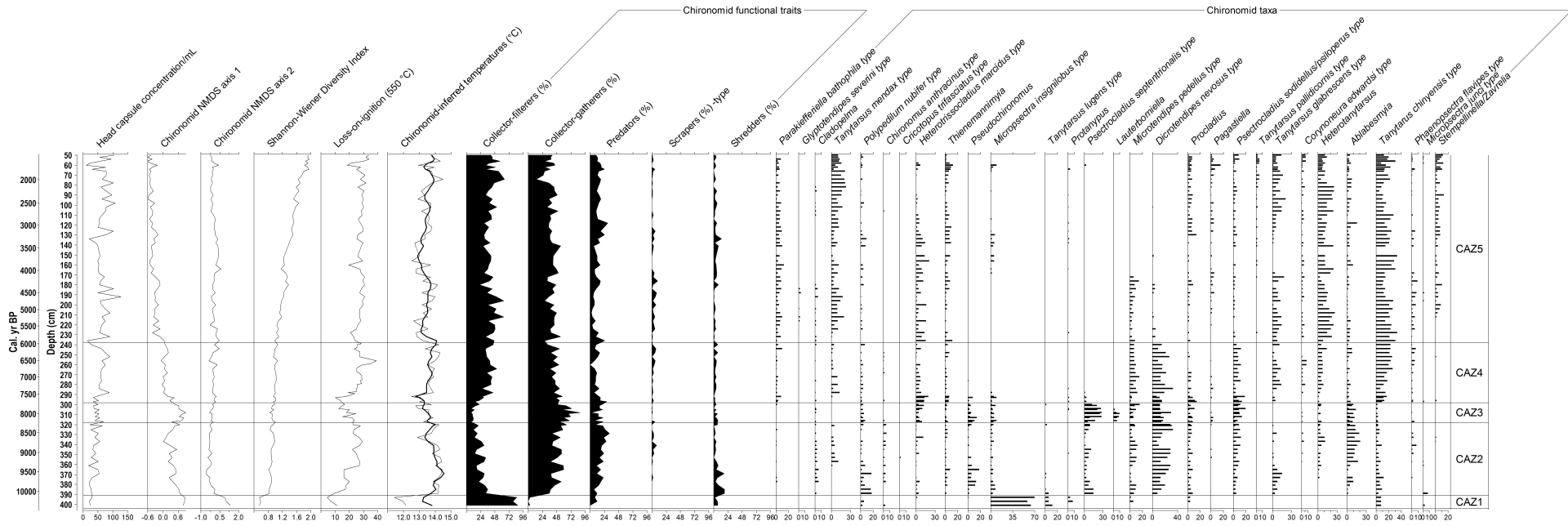
NMDS chironomid community
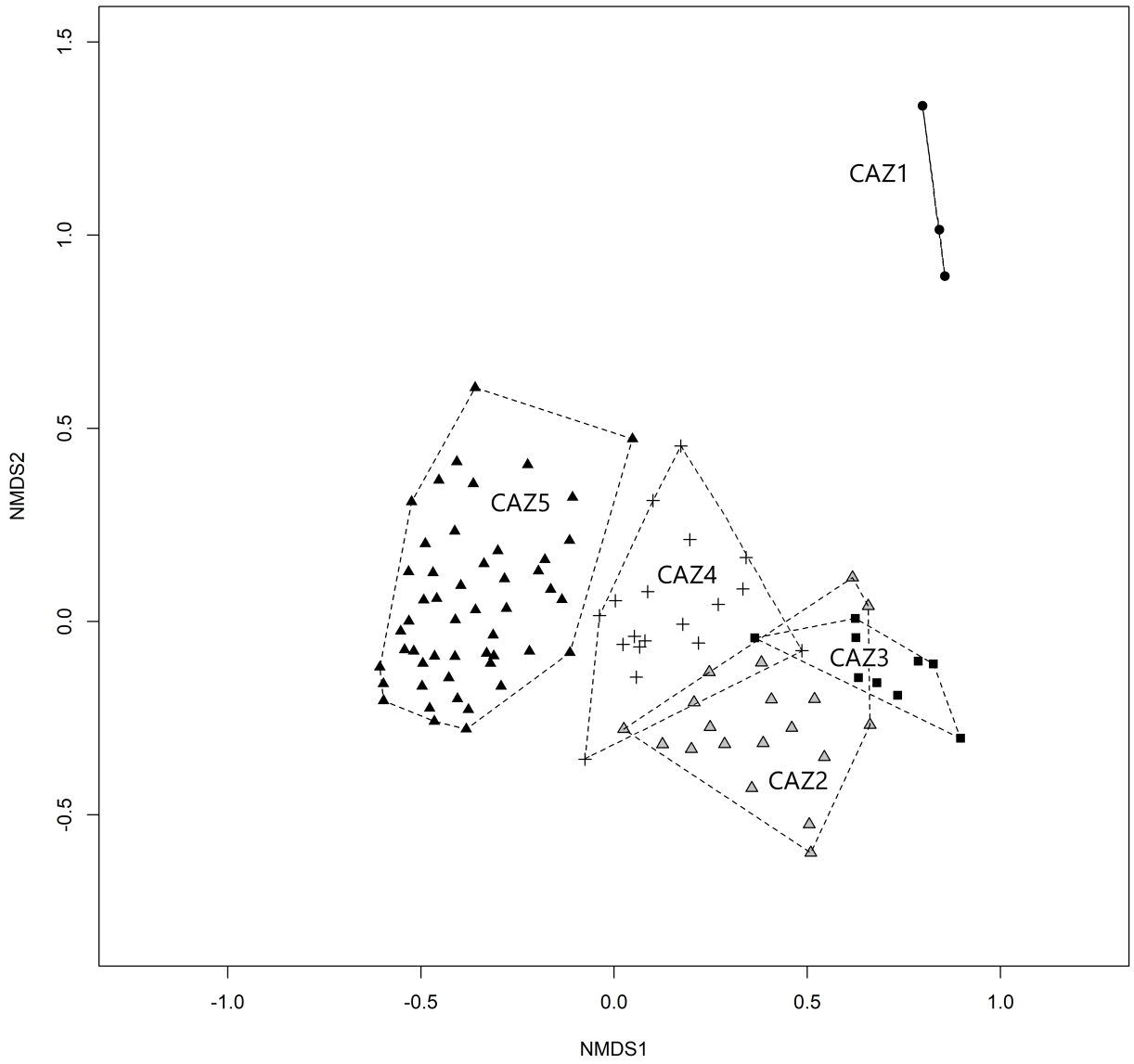
NMDS chironomid species
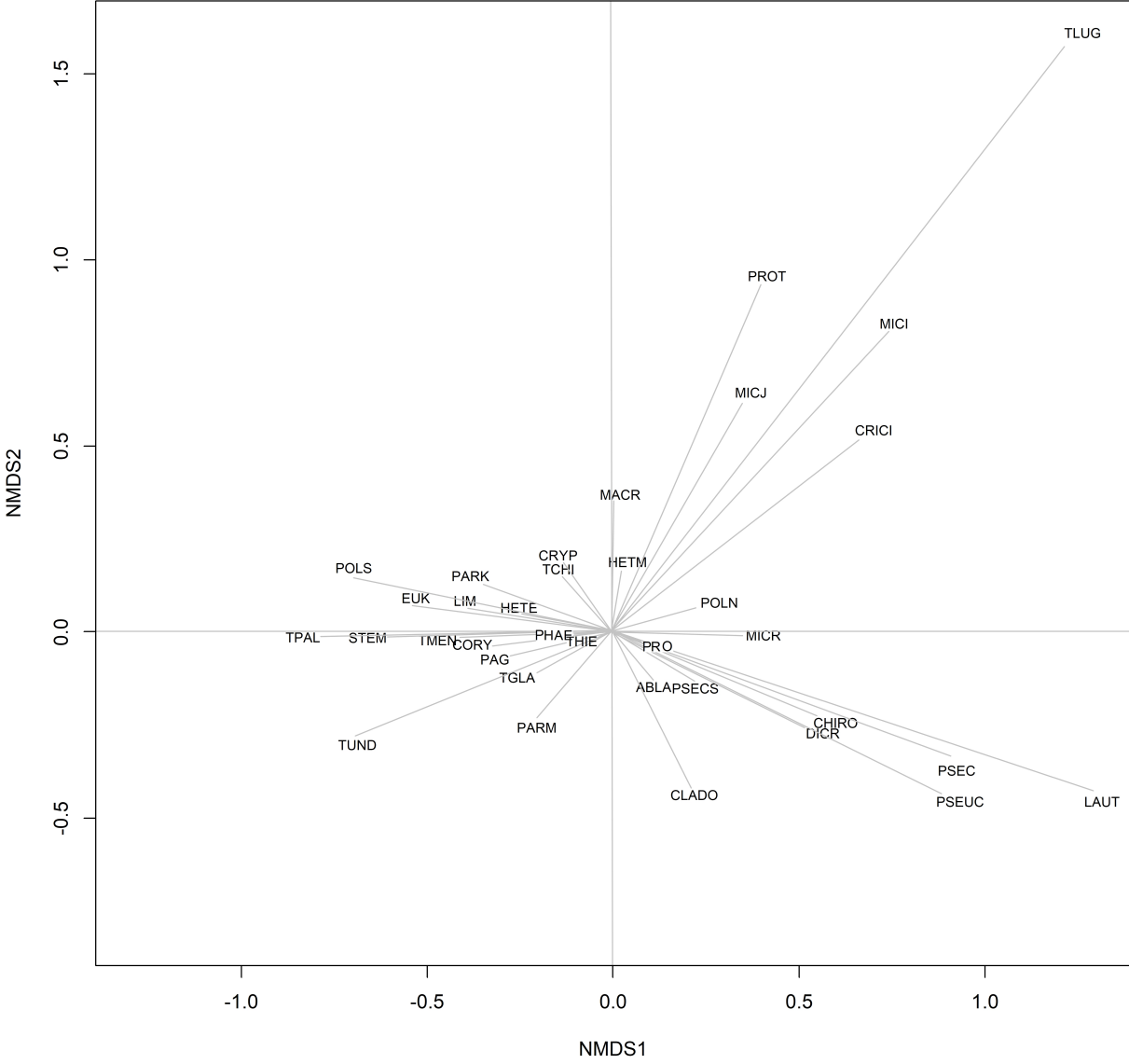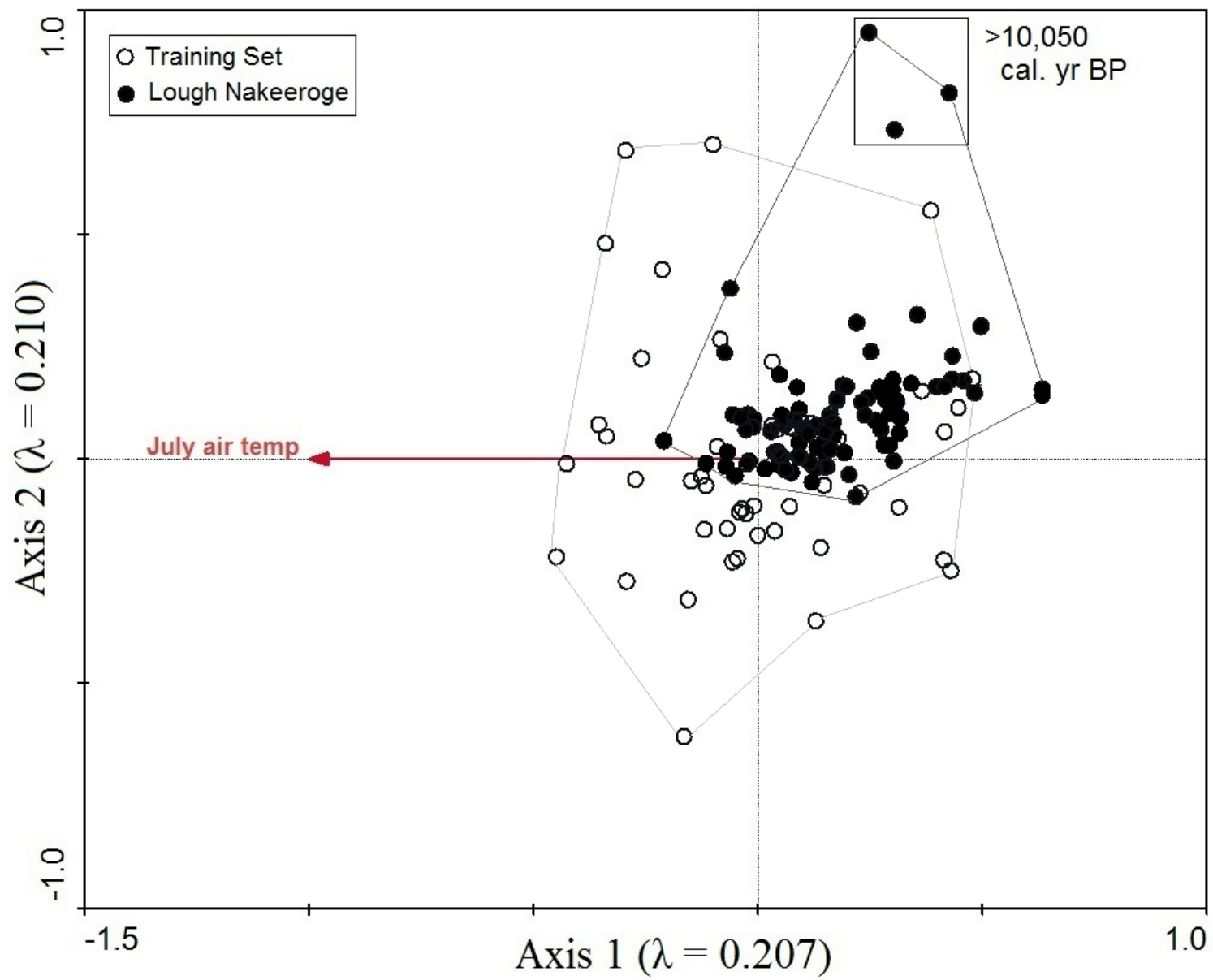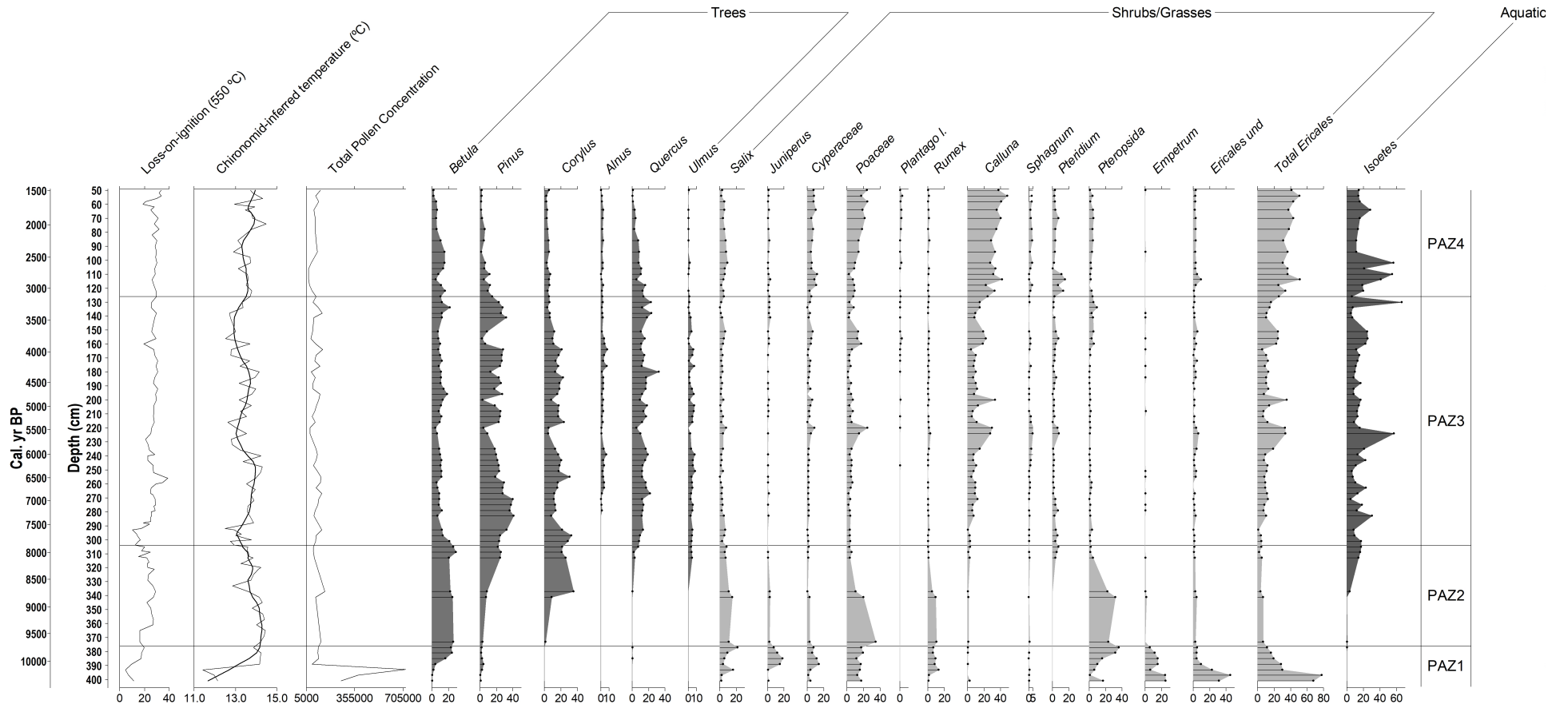
PRECIPITATION

TEMPERATURE

ADULT SWARM

SEDIMENT,
VOLCANIC ASH,
NUTRIENTS

EVAPORATION

HIGH LAKE LEVEL

EGG MASSES

LOW LAKE LEVEL

ALGAE

LARVAE

PUPAE

Sediment Core

Sediments

HEAD CAPSULE

| Climate Models | | | | | Drivers | | Greenland | | Irish palaeoclimate records | | Lough Nakeeroge chironomid records | |

(iii) Depth (cm)   CORE A   CORE B   MASTER CORE
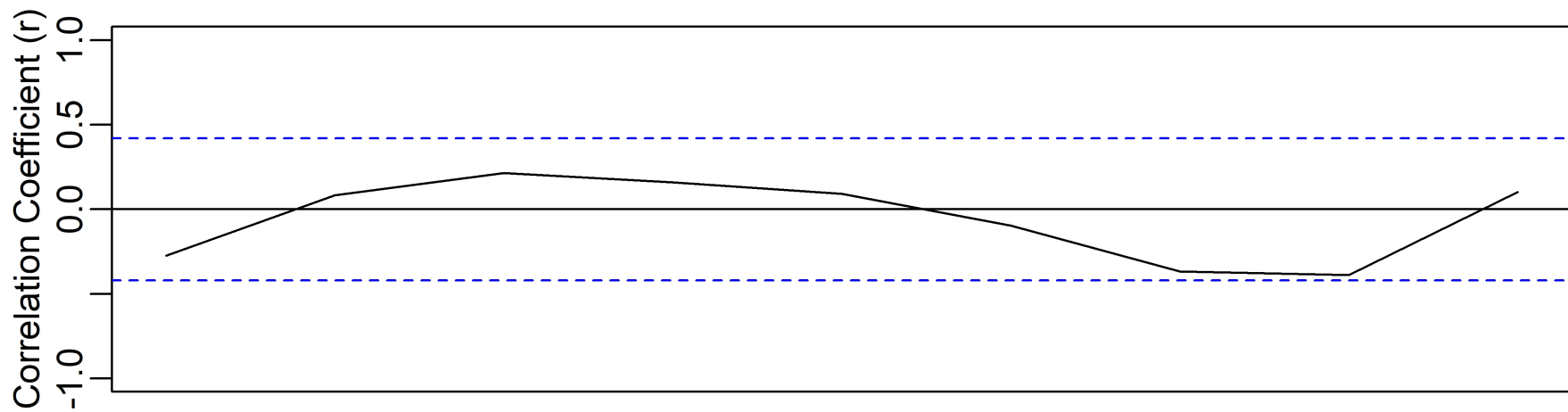
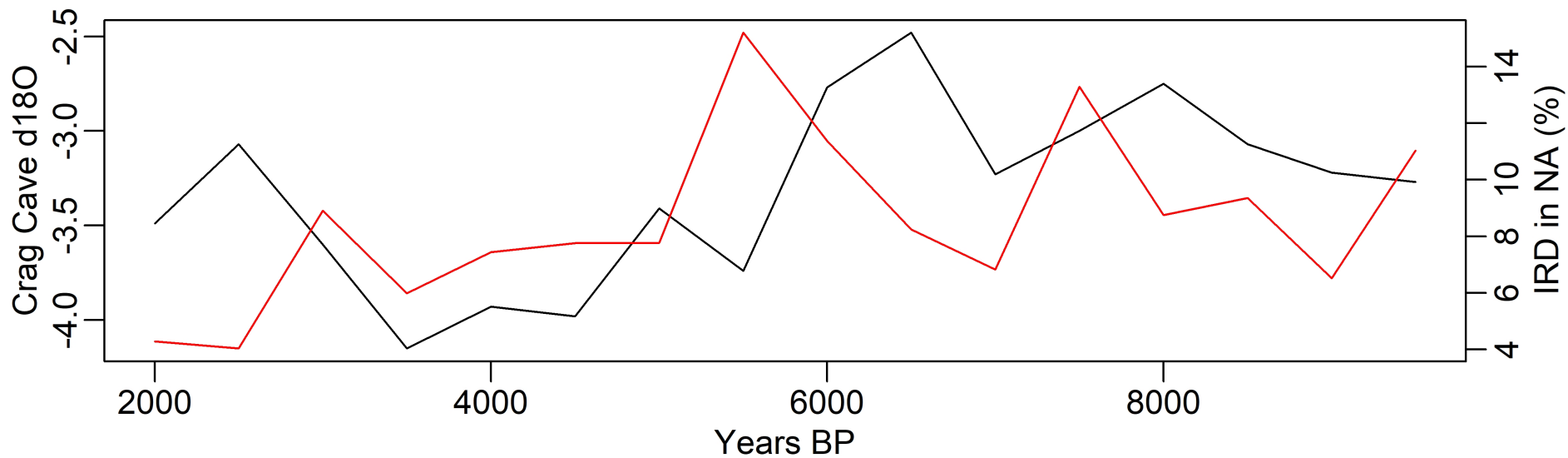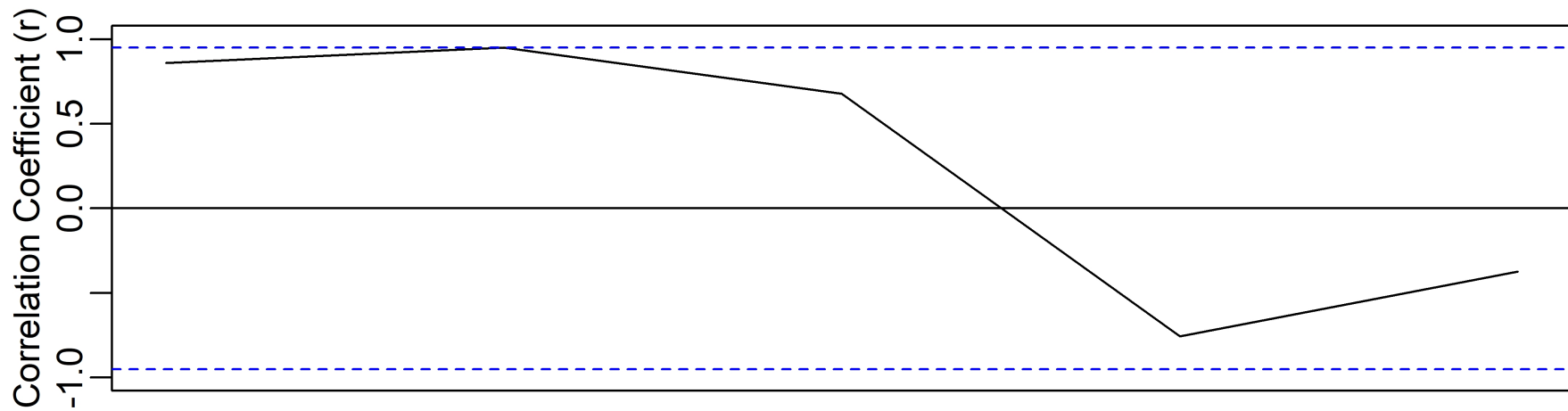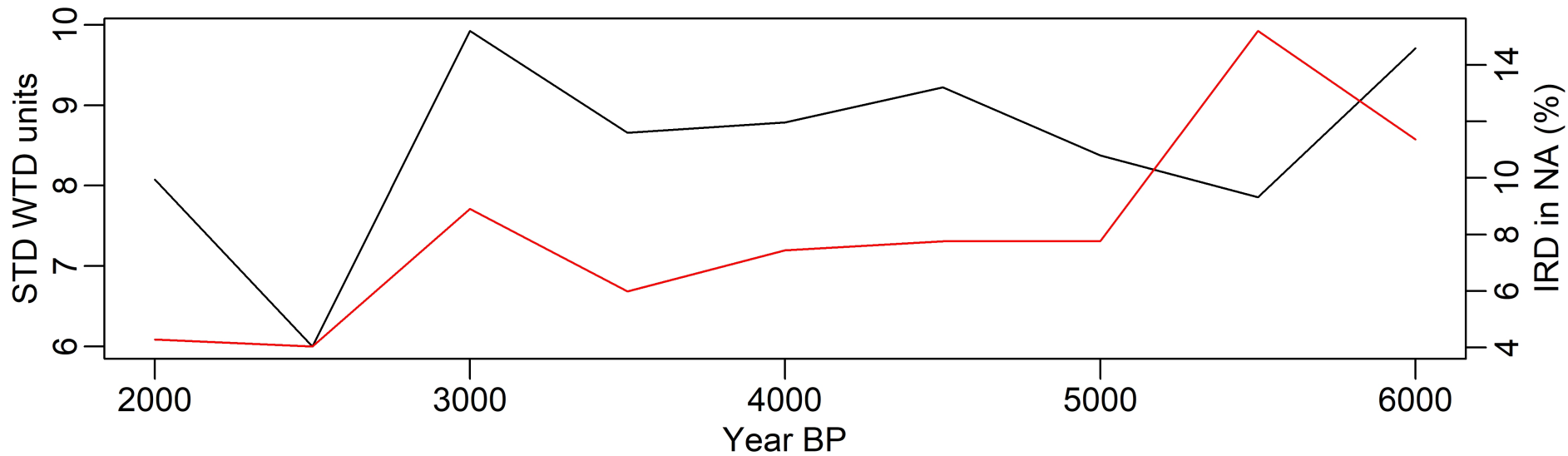(iv) Depth (cm)   CORE A   CORE B   MASTER CORE
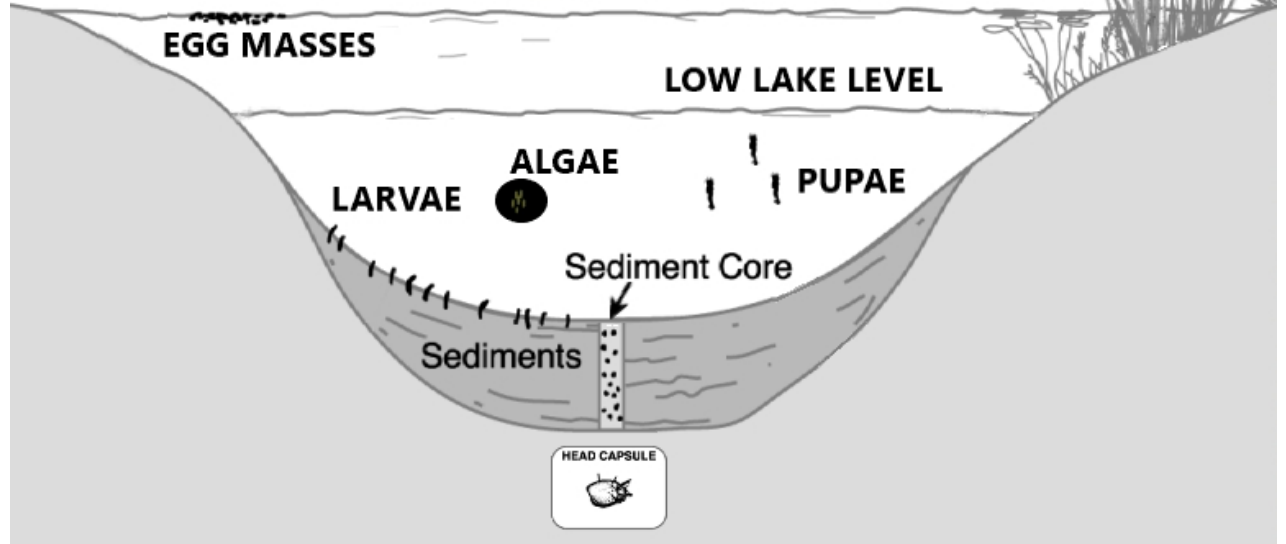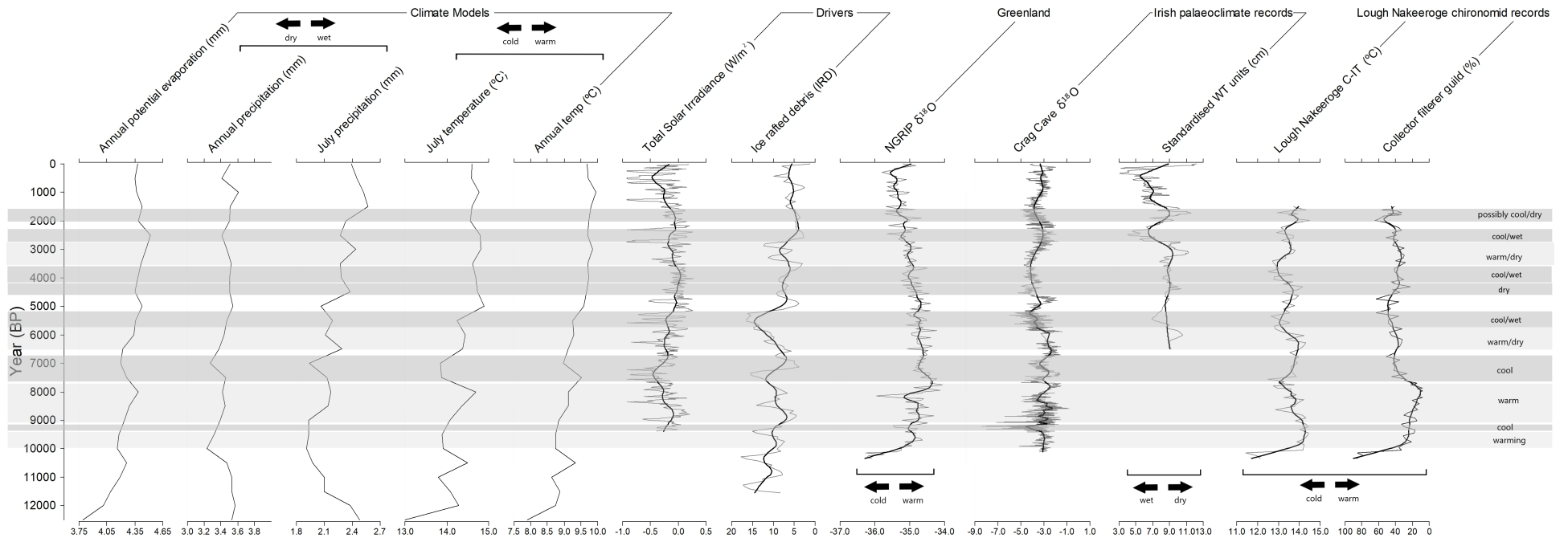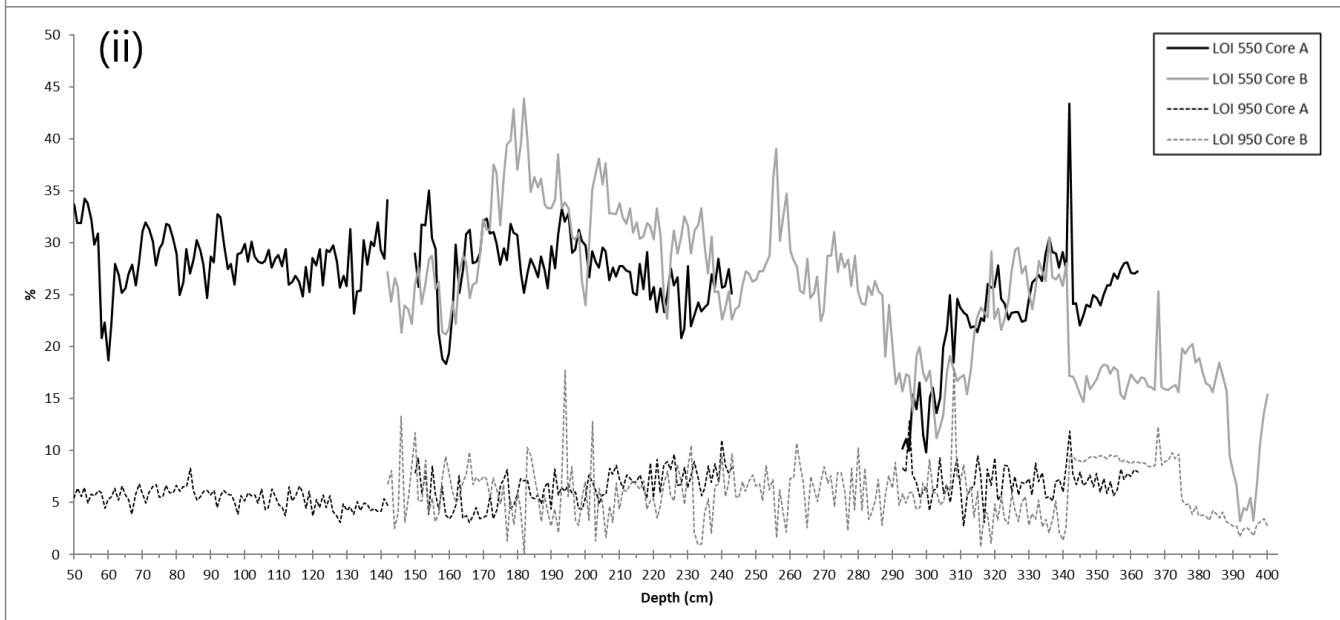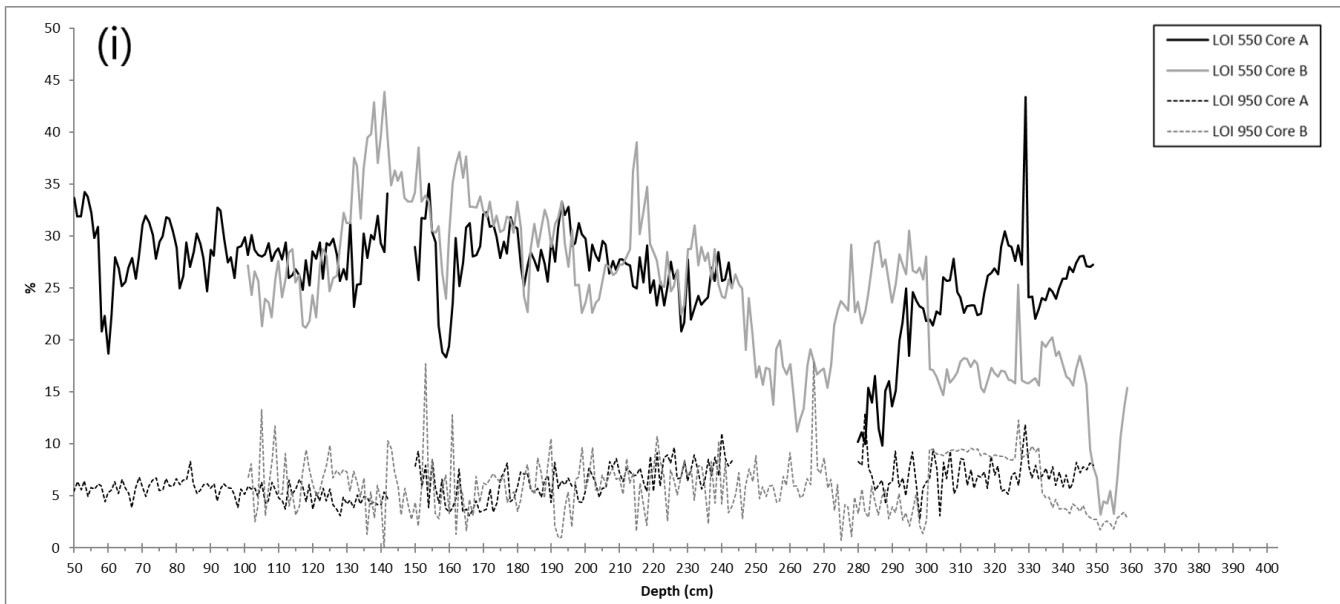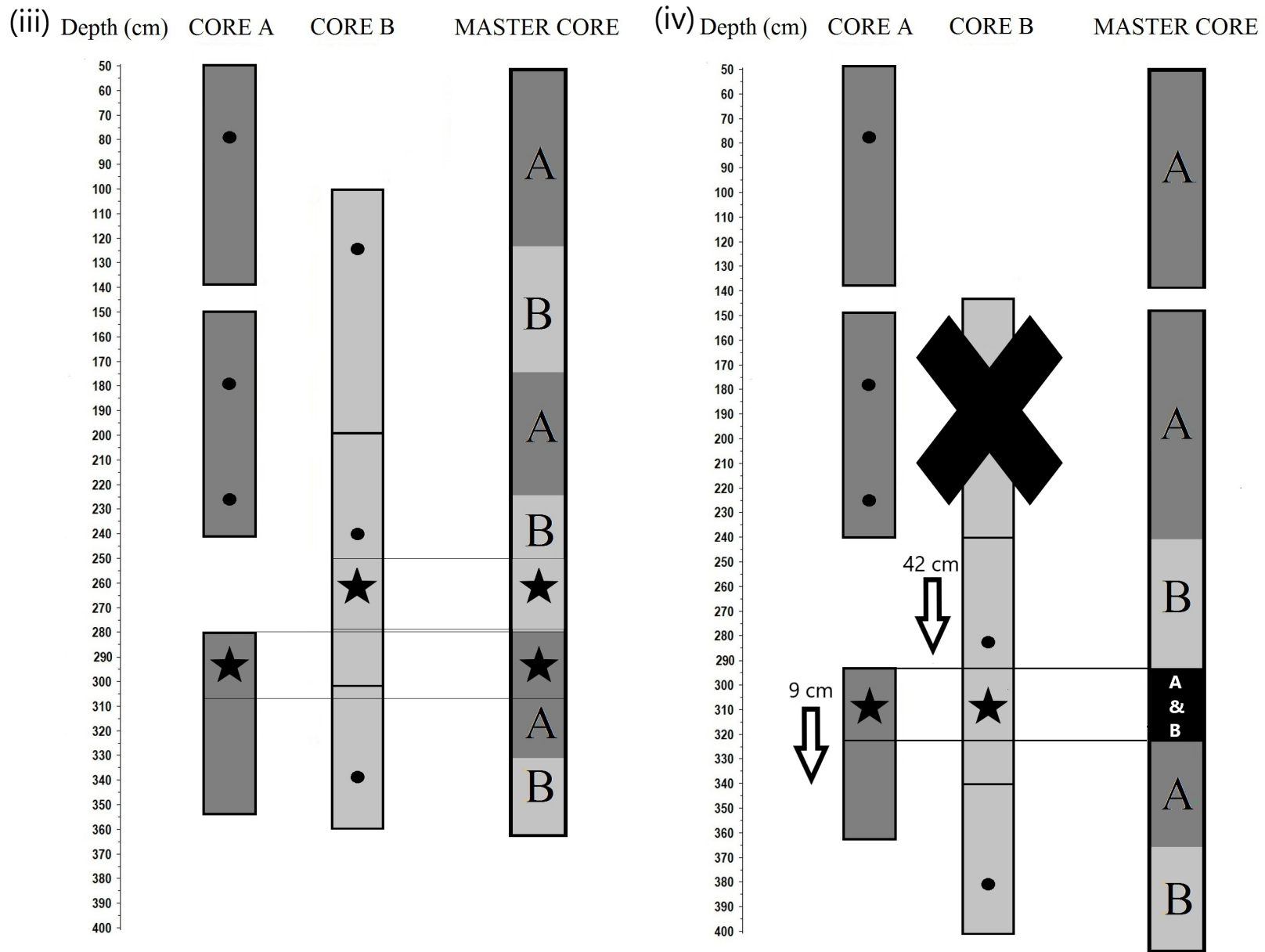
(v)
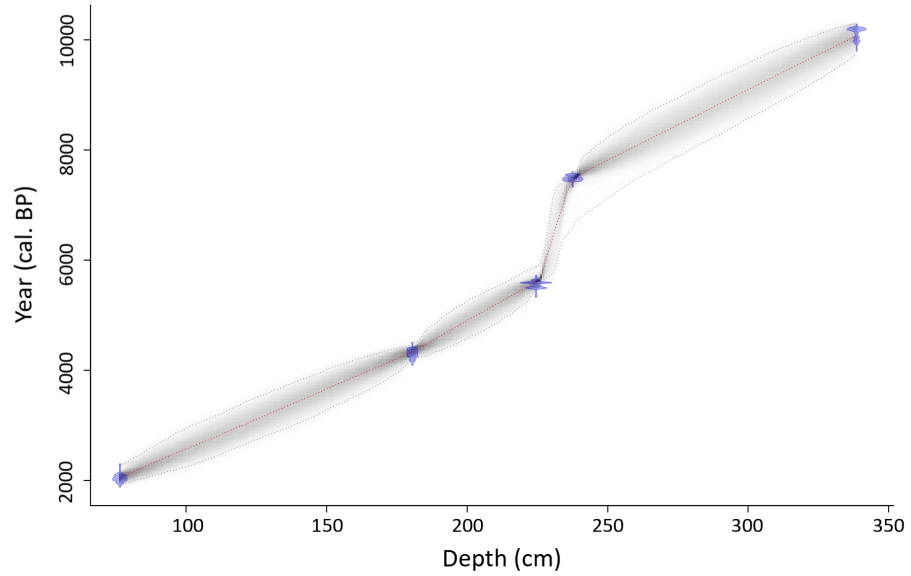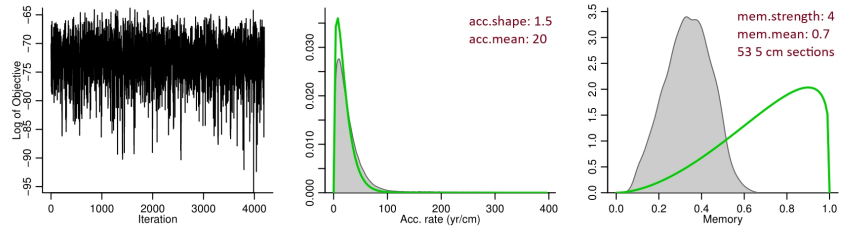
(vi)
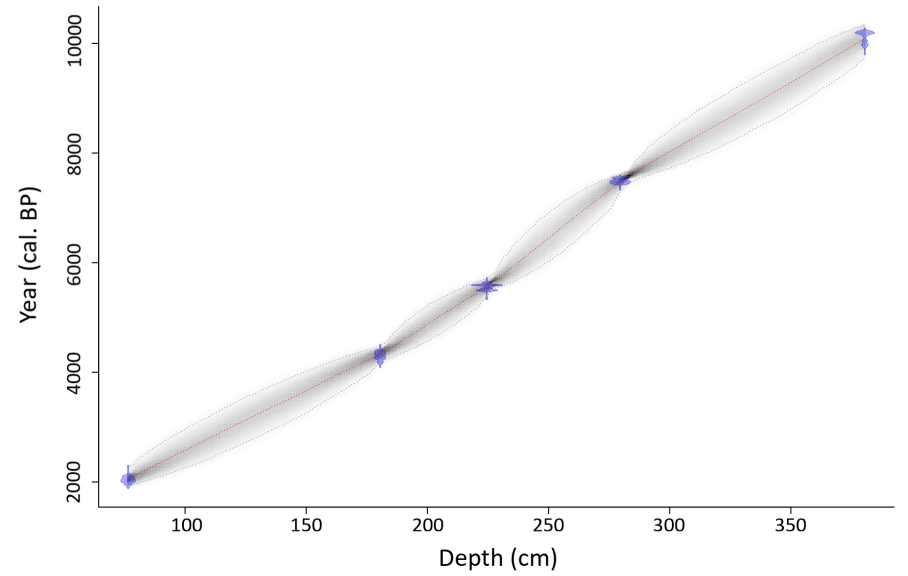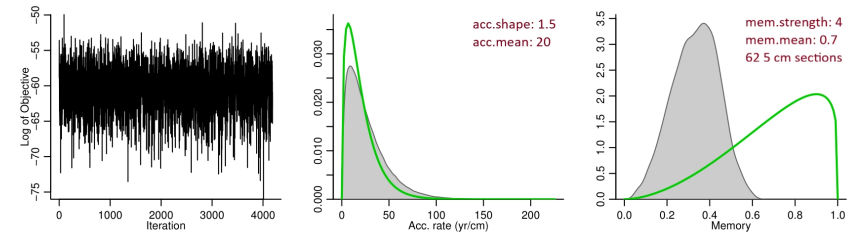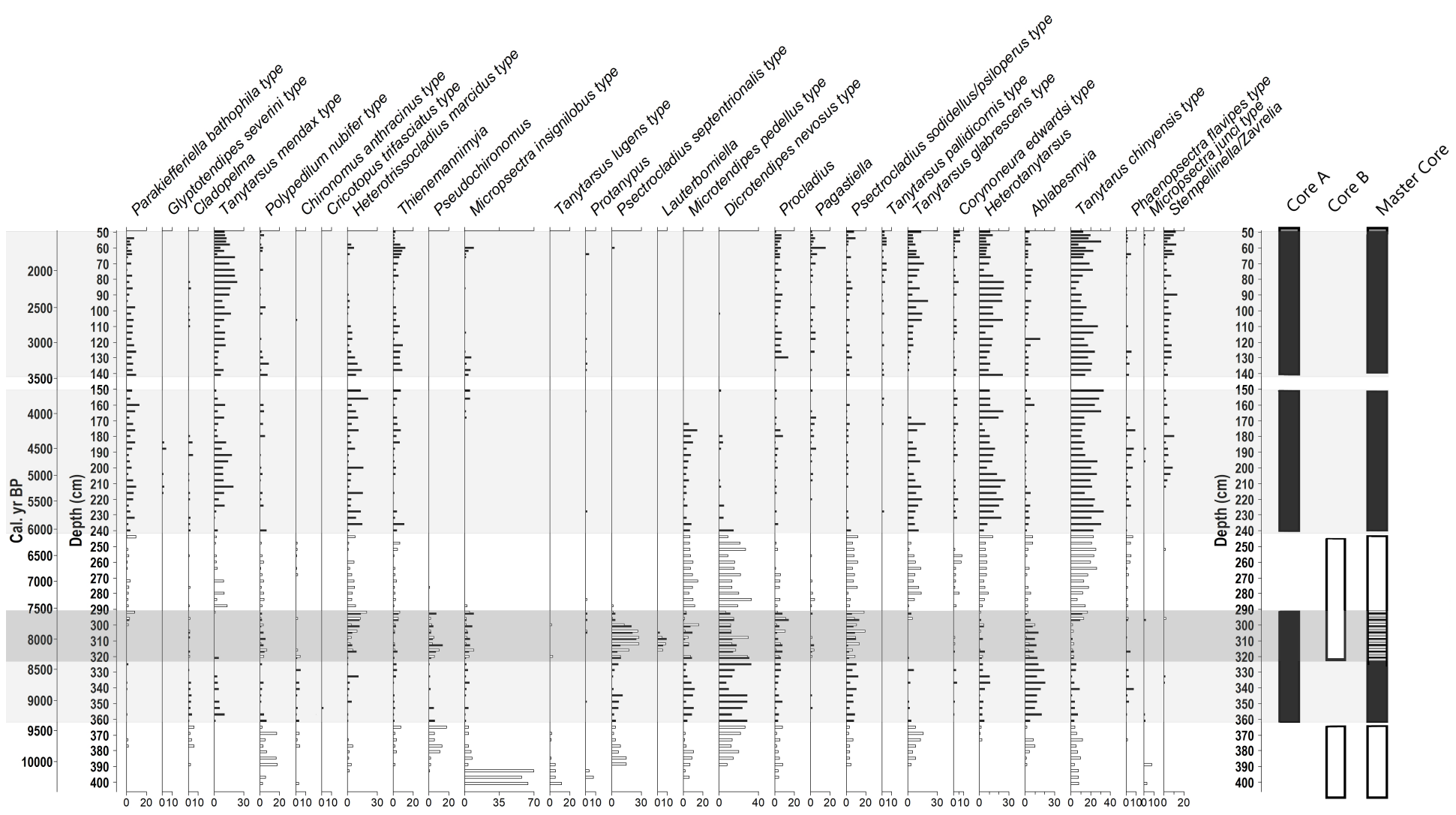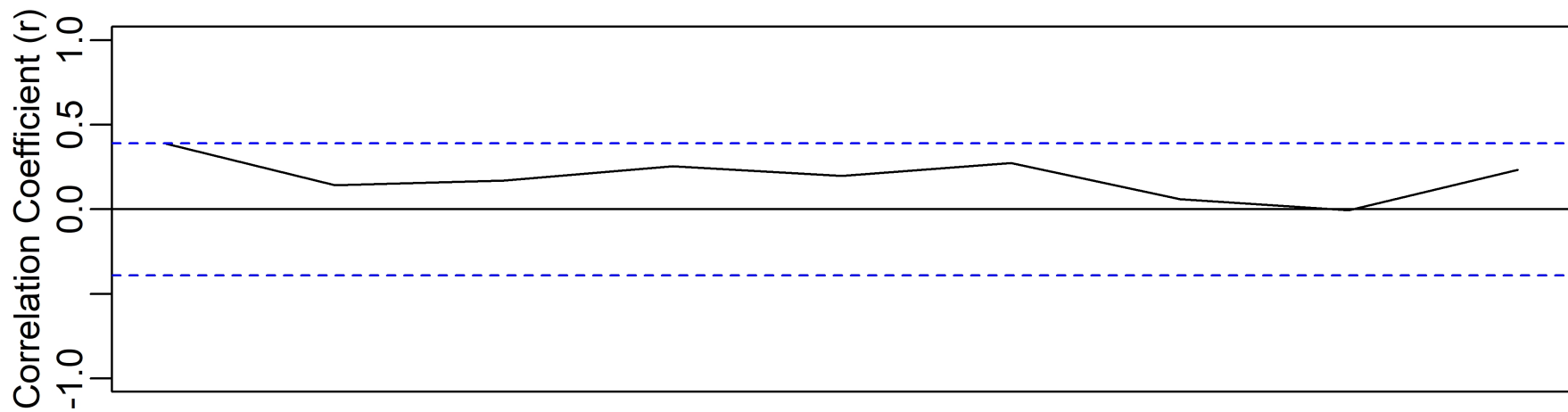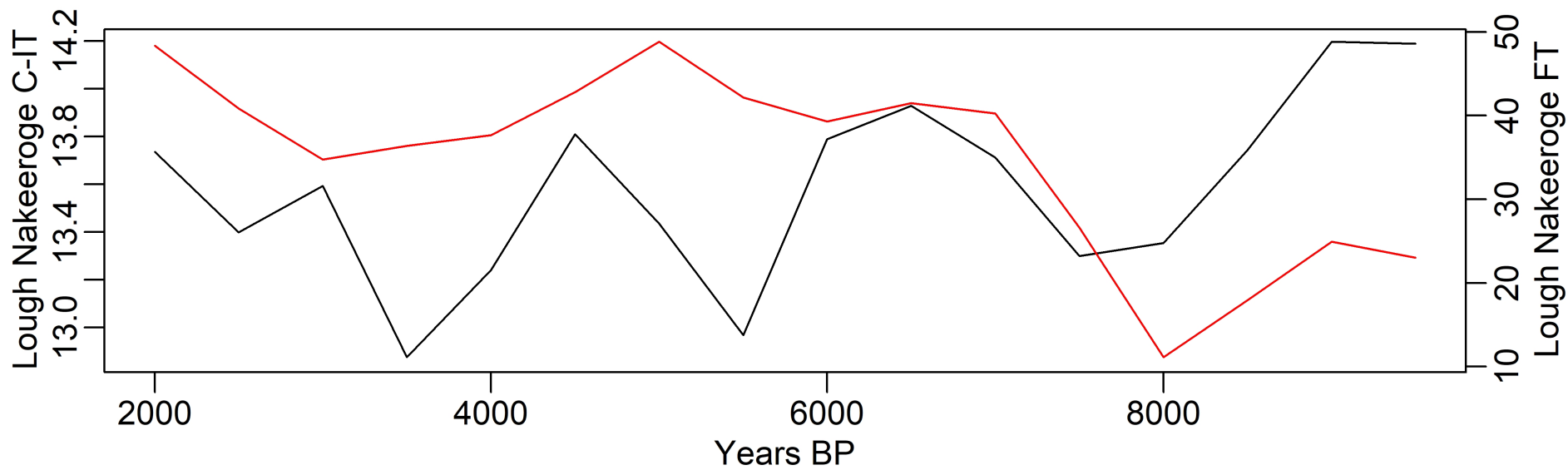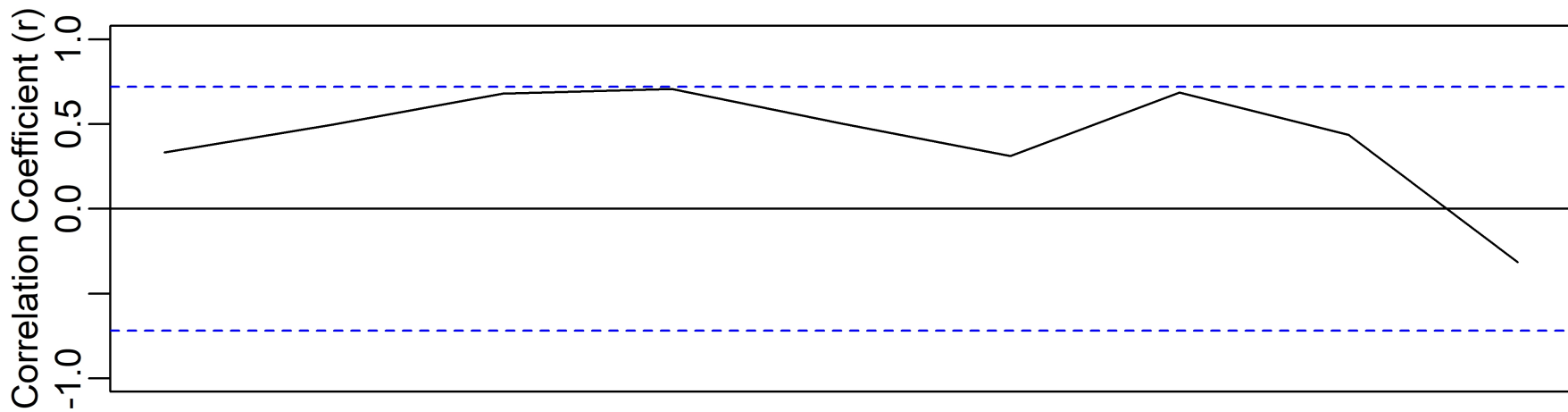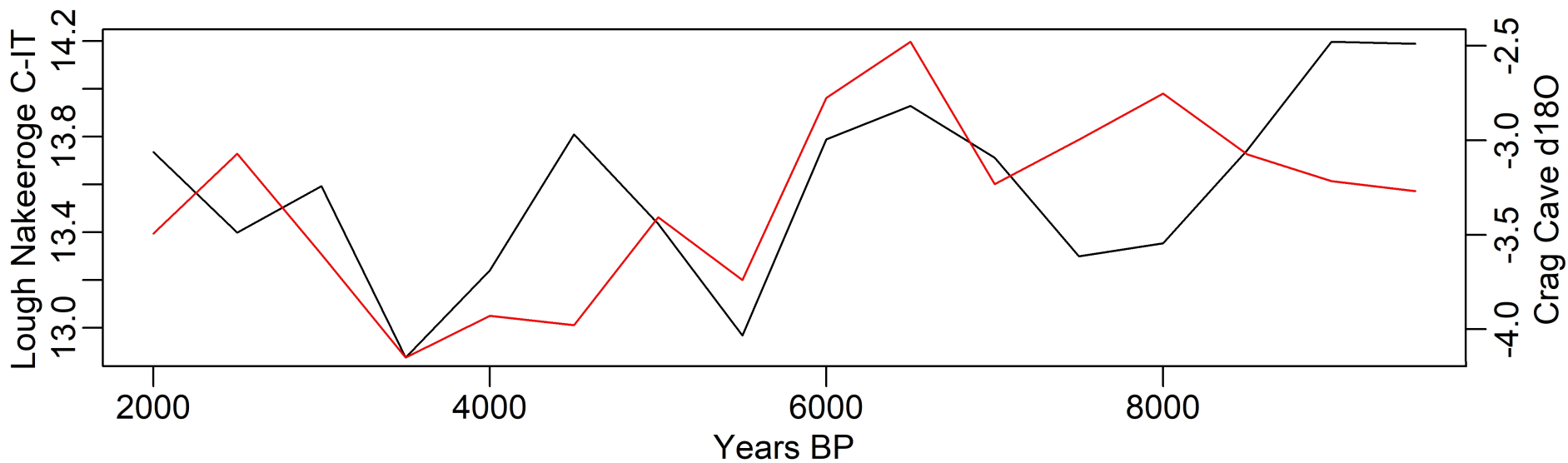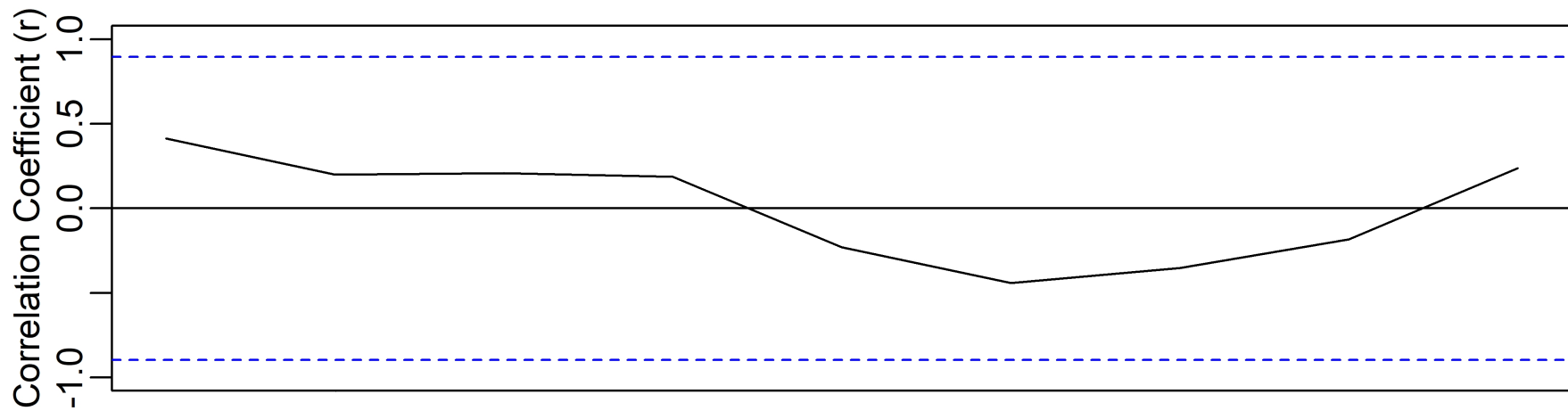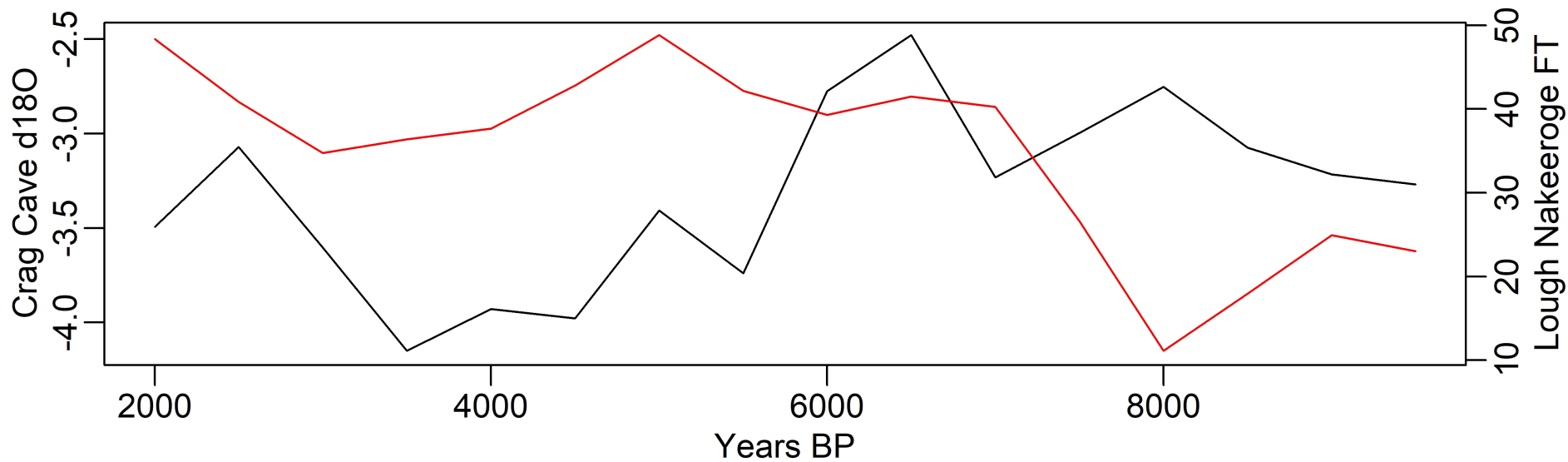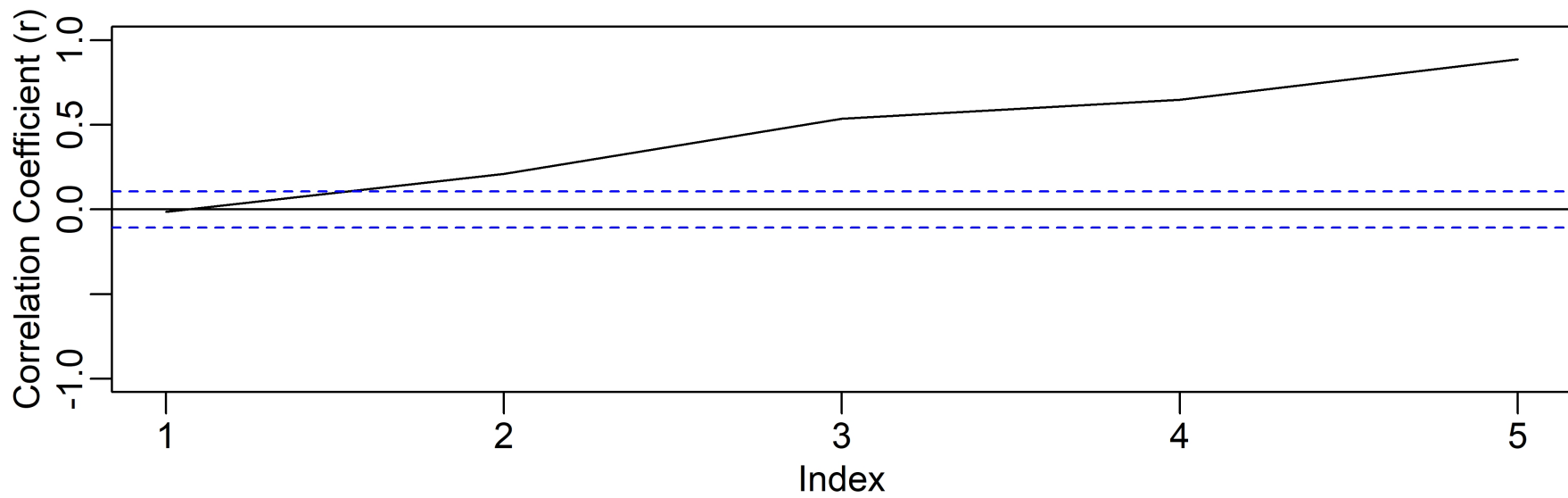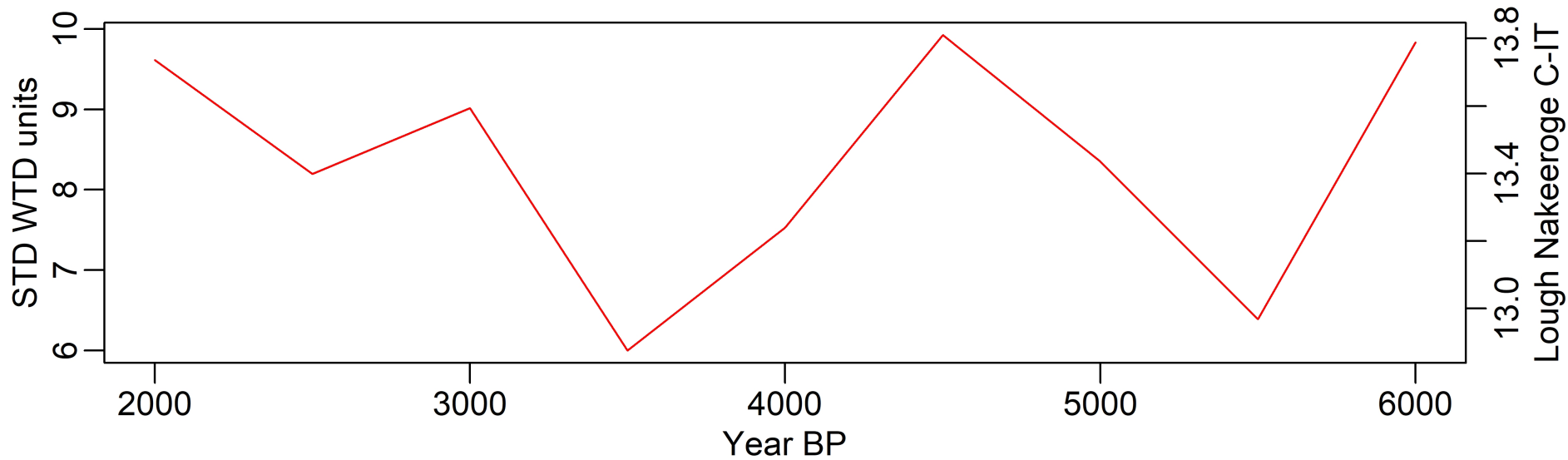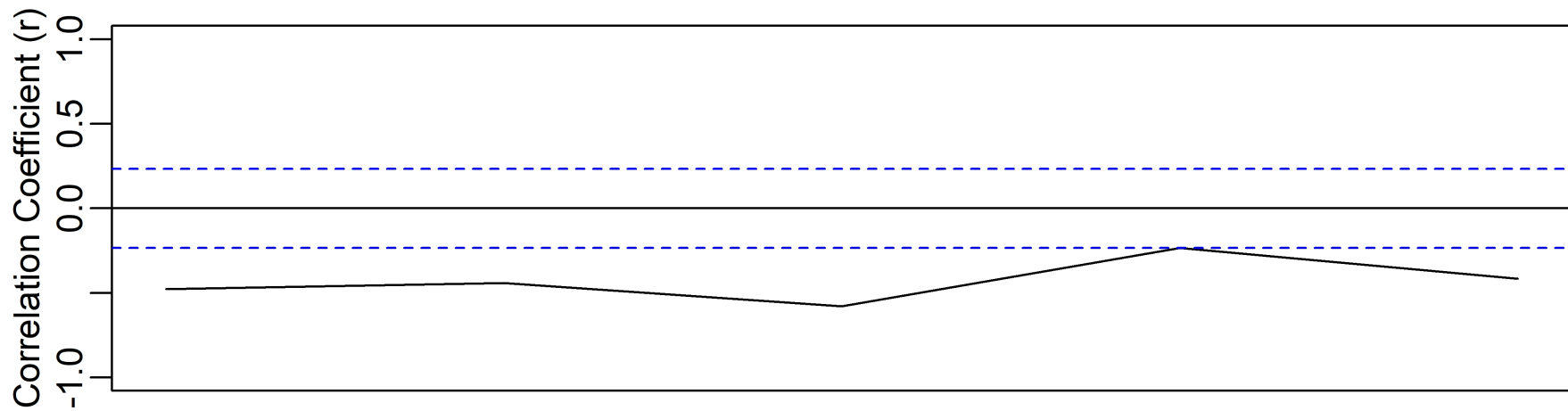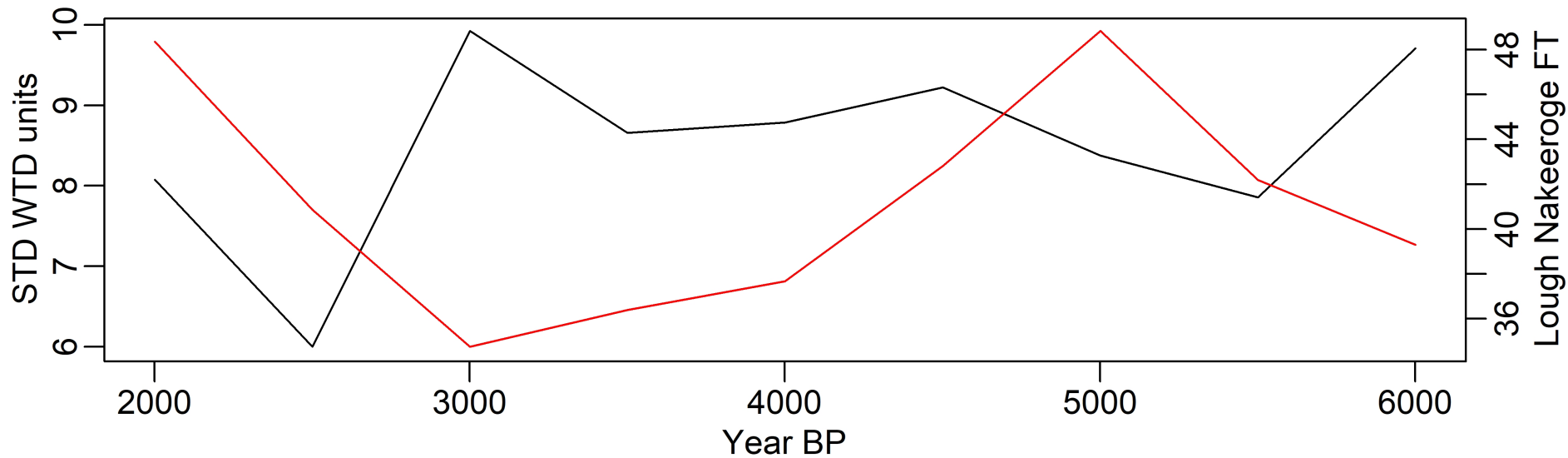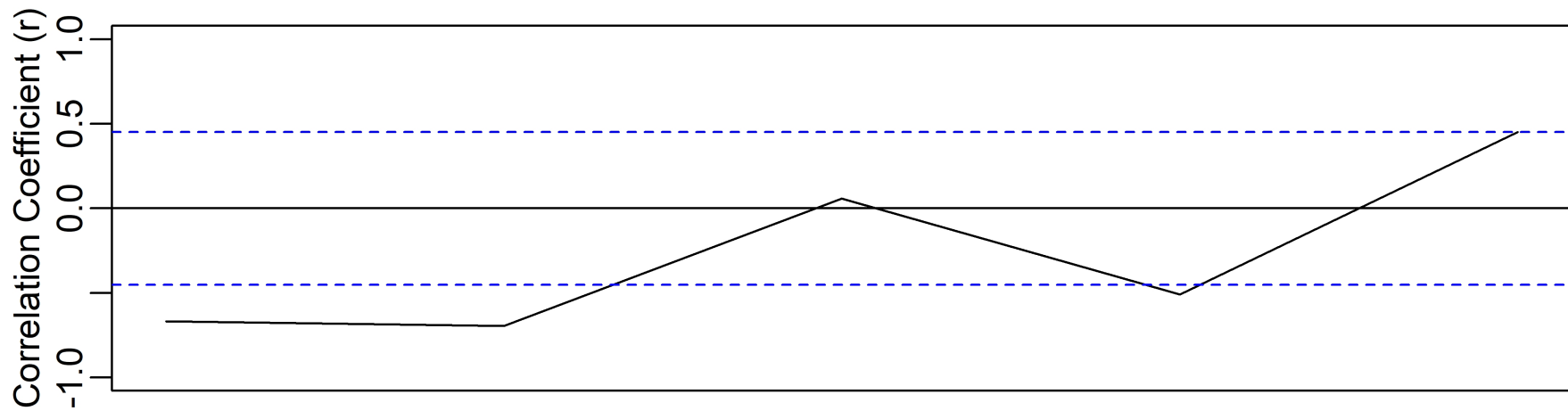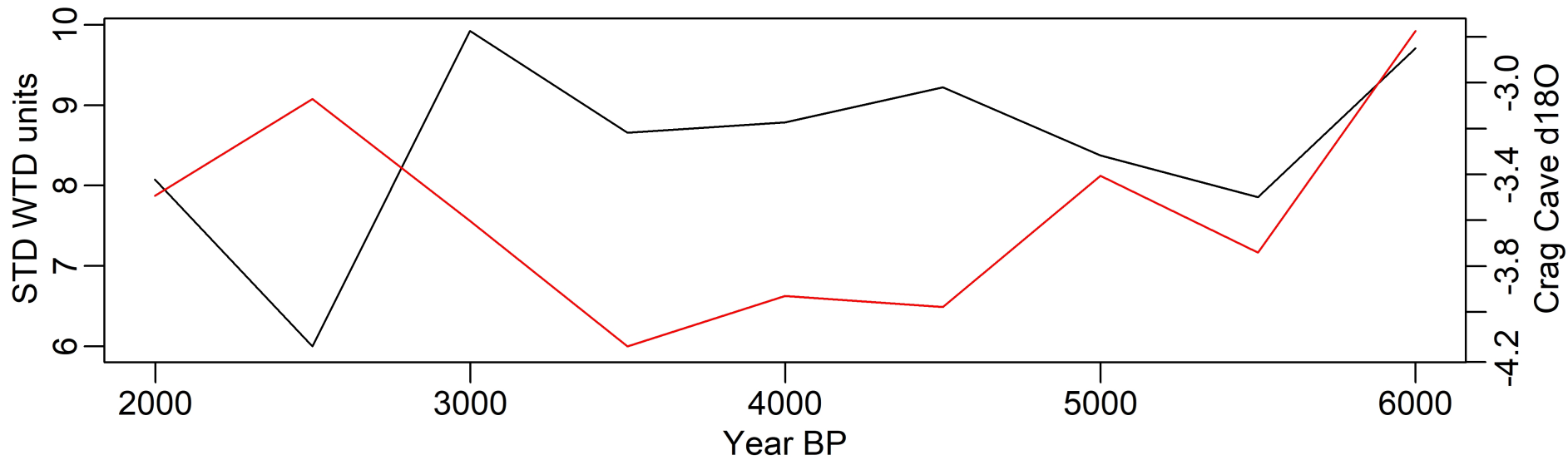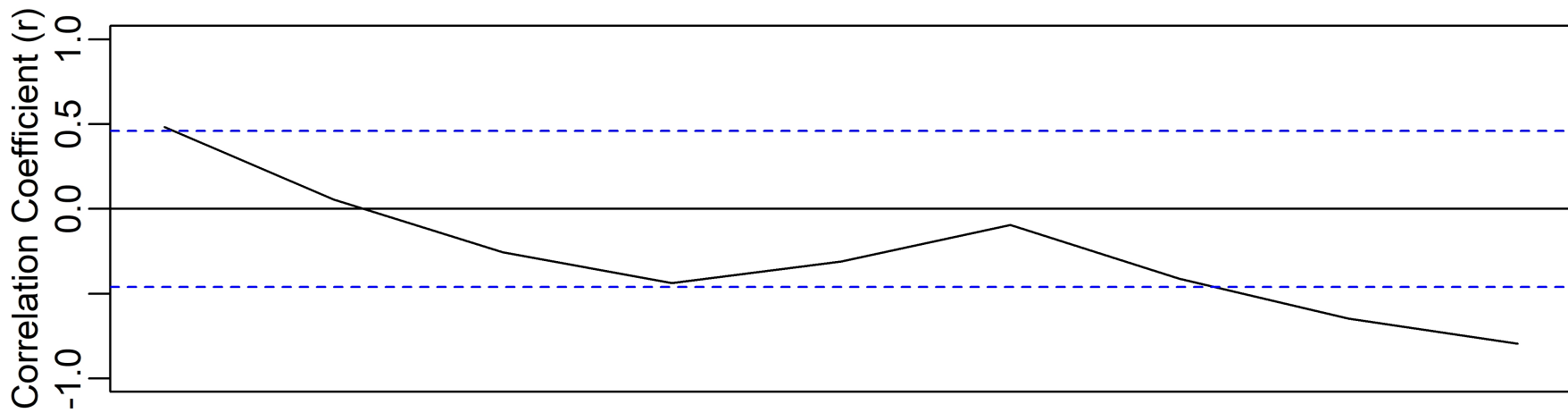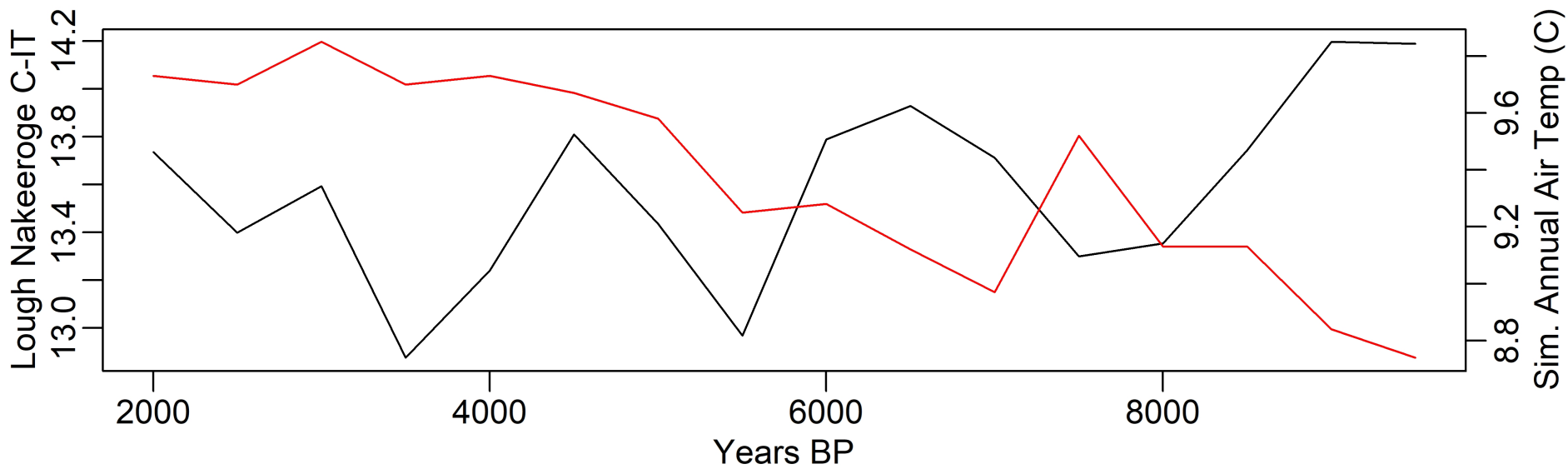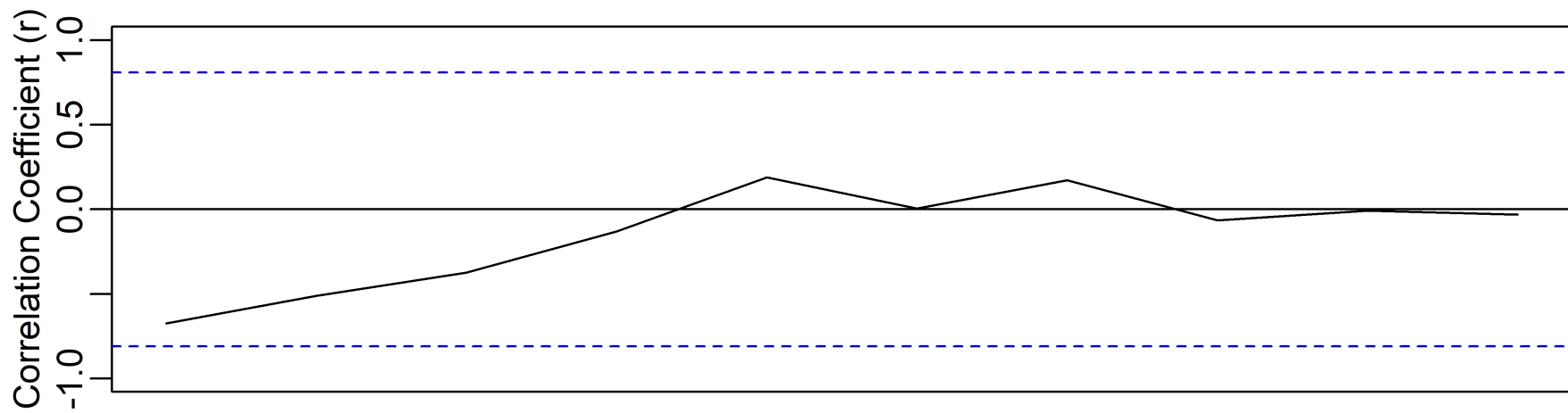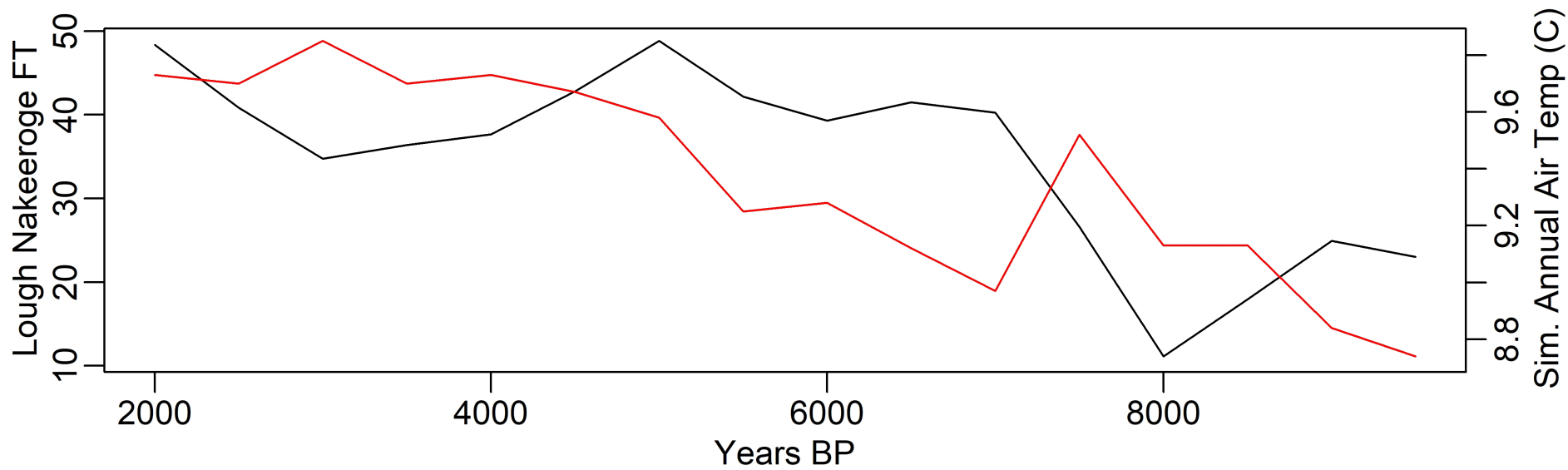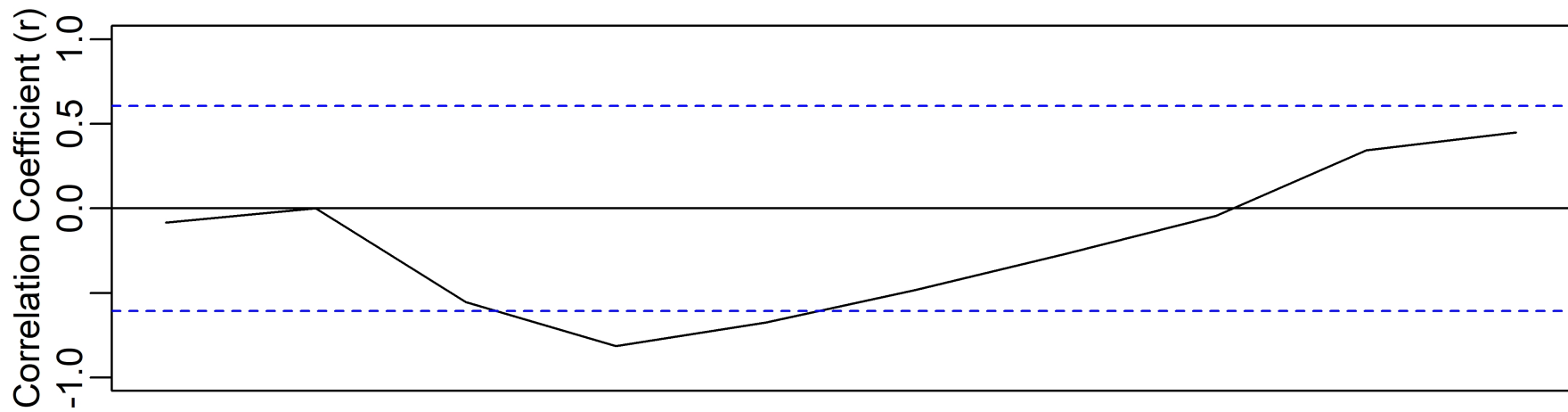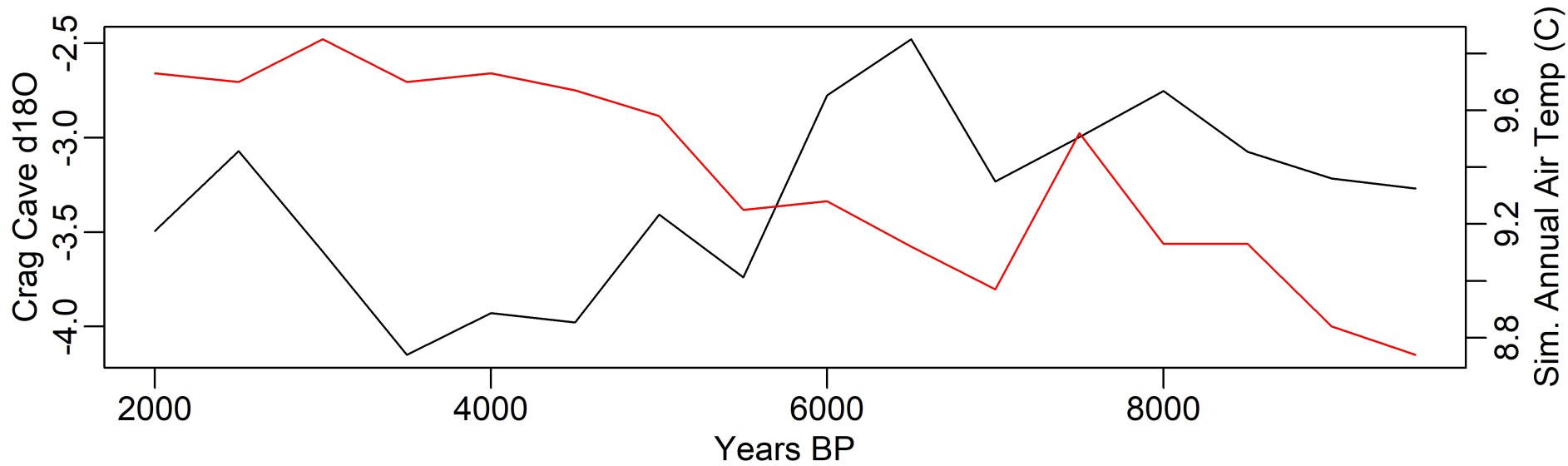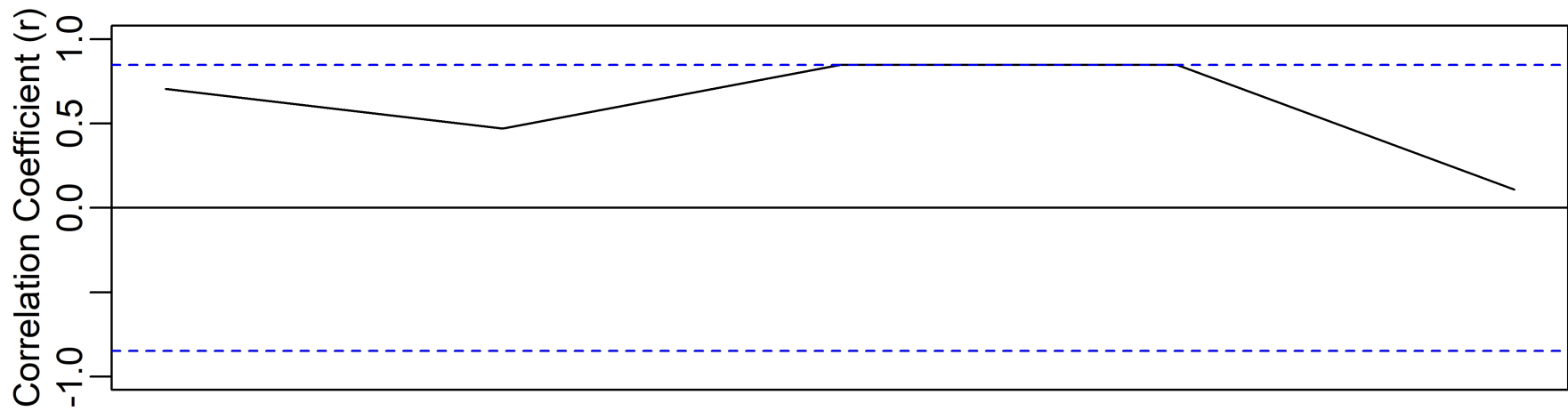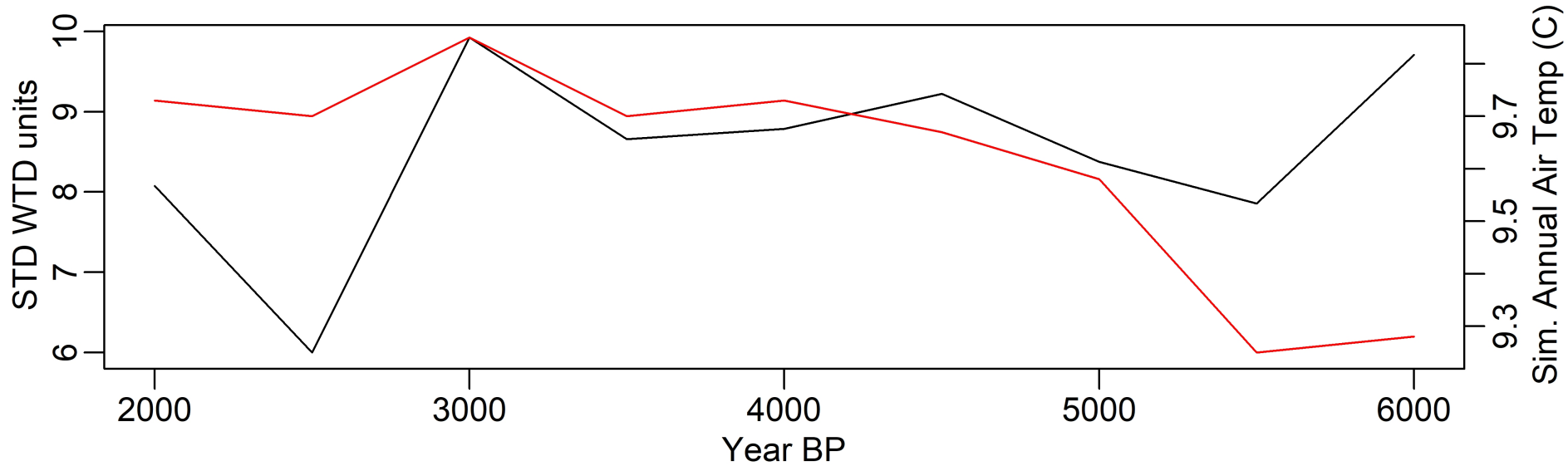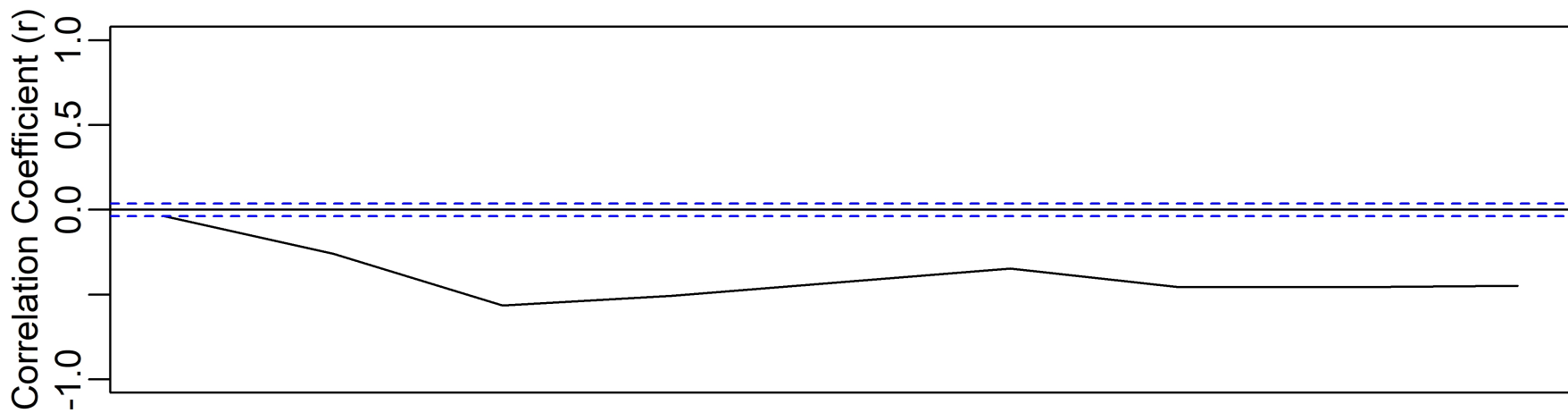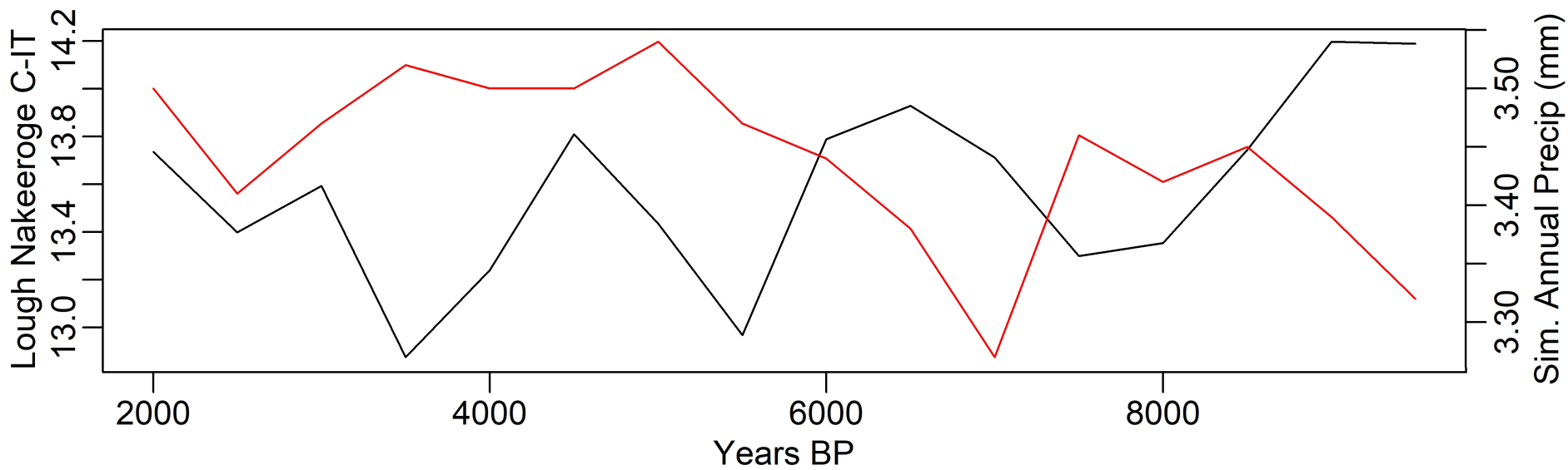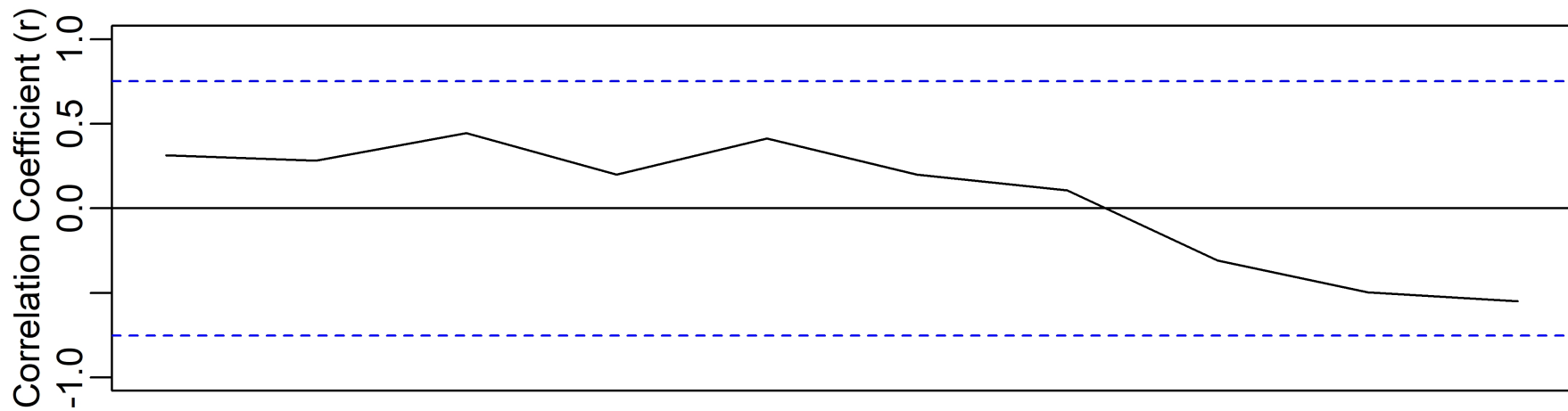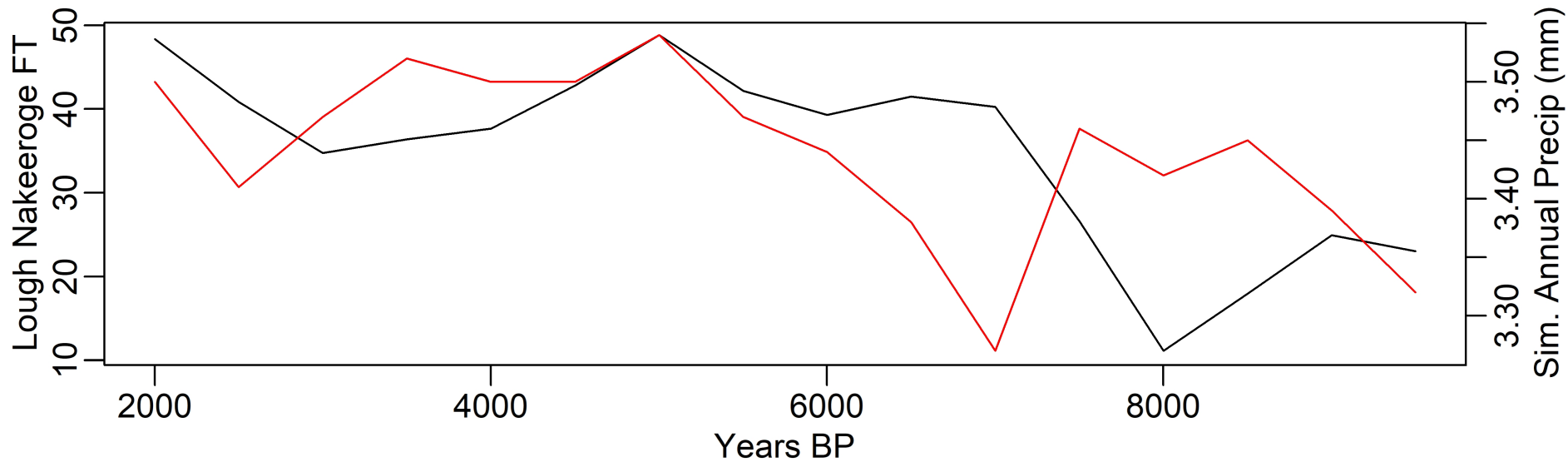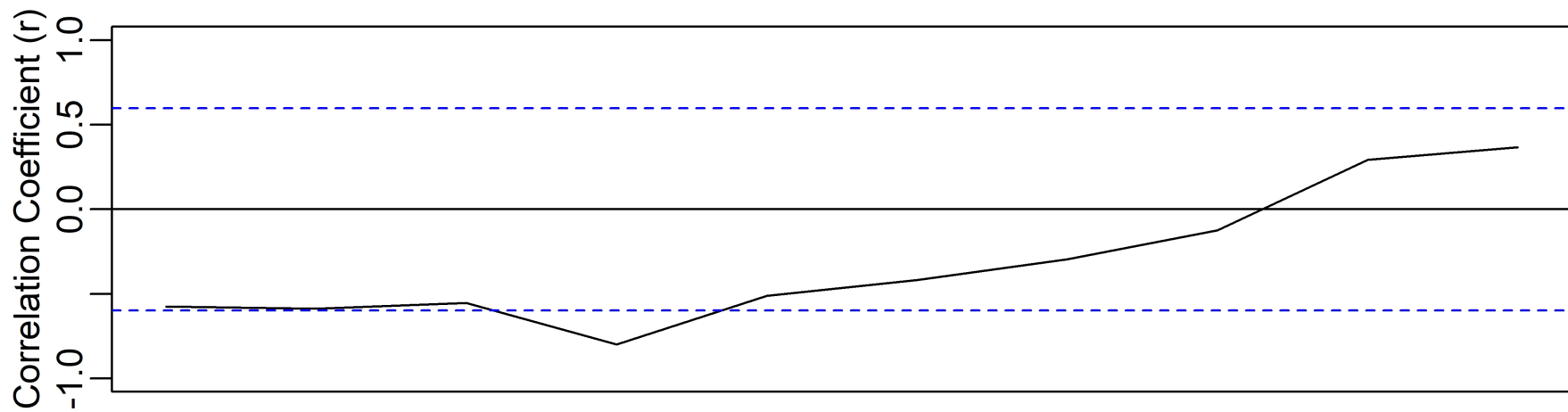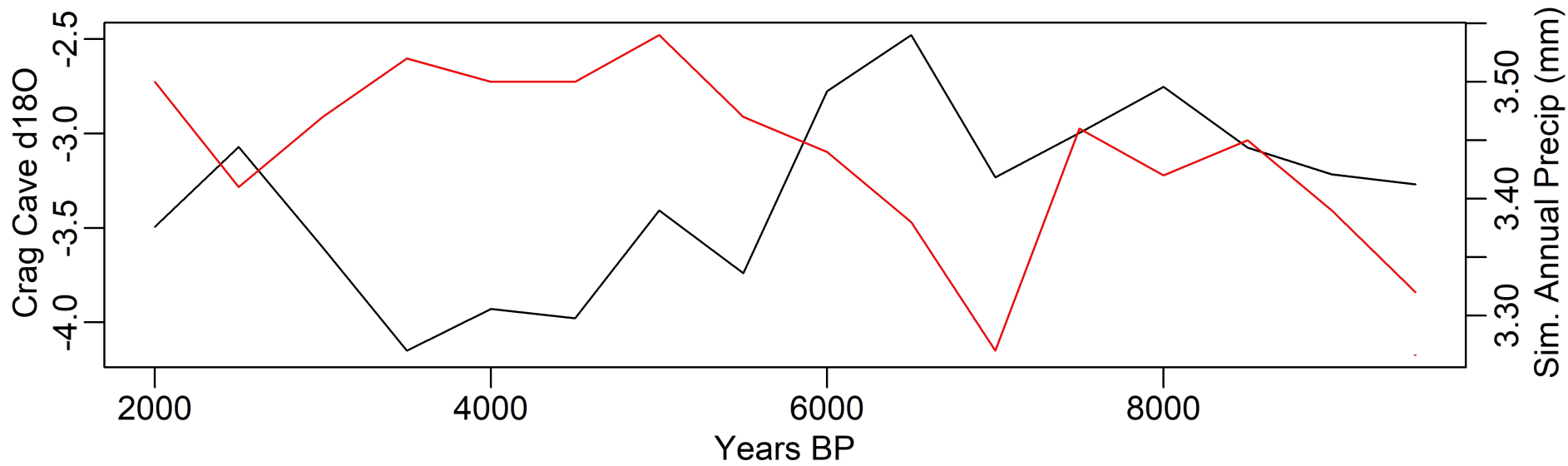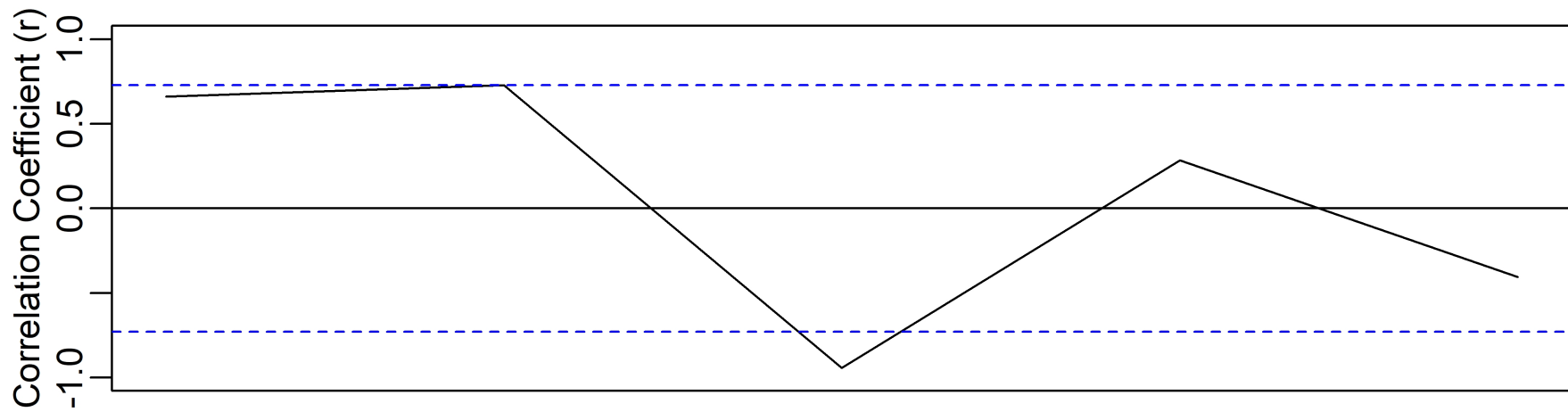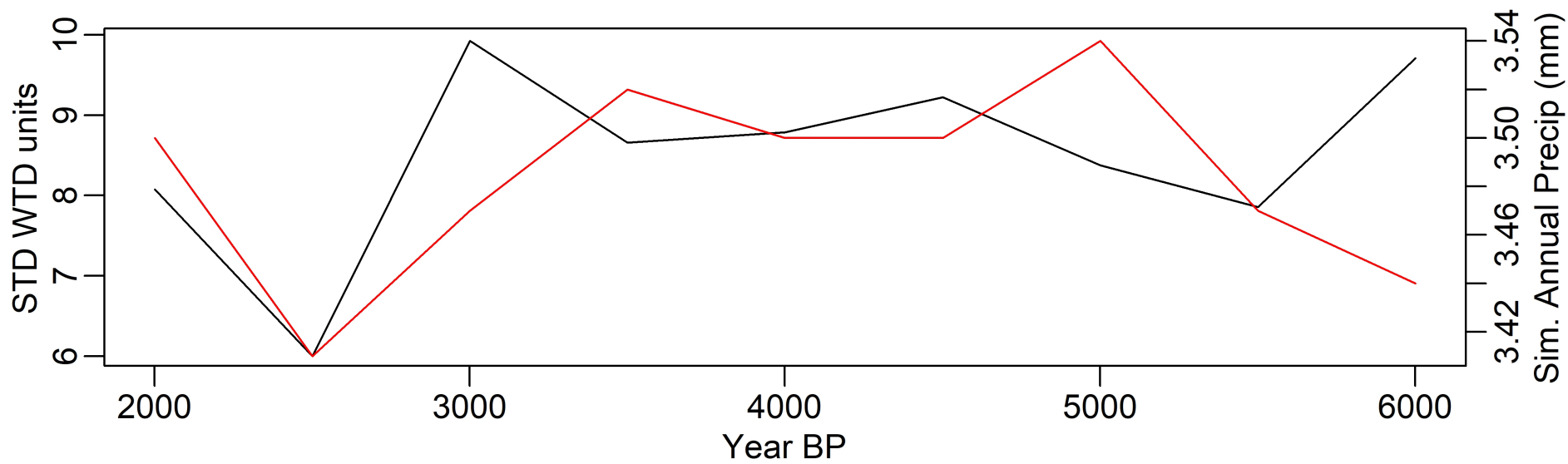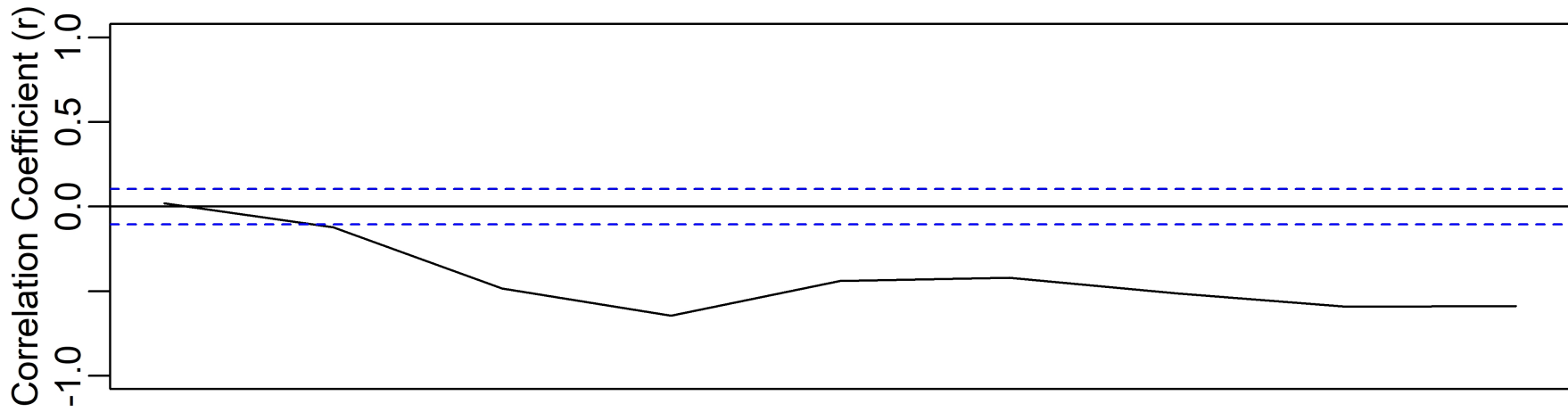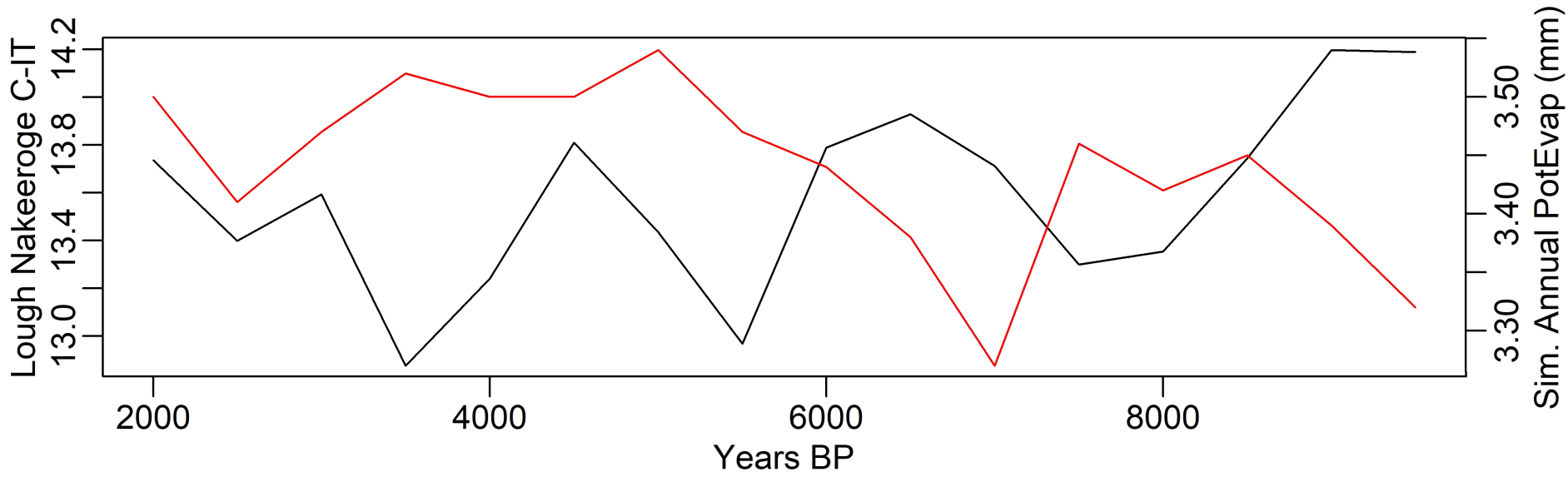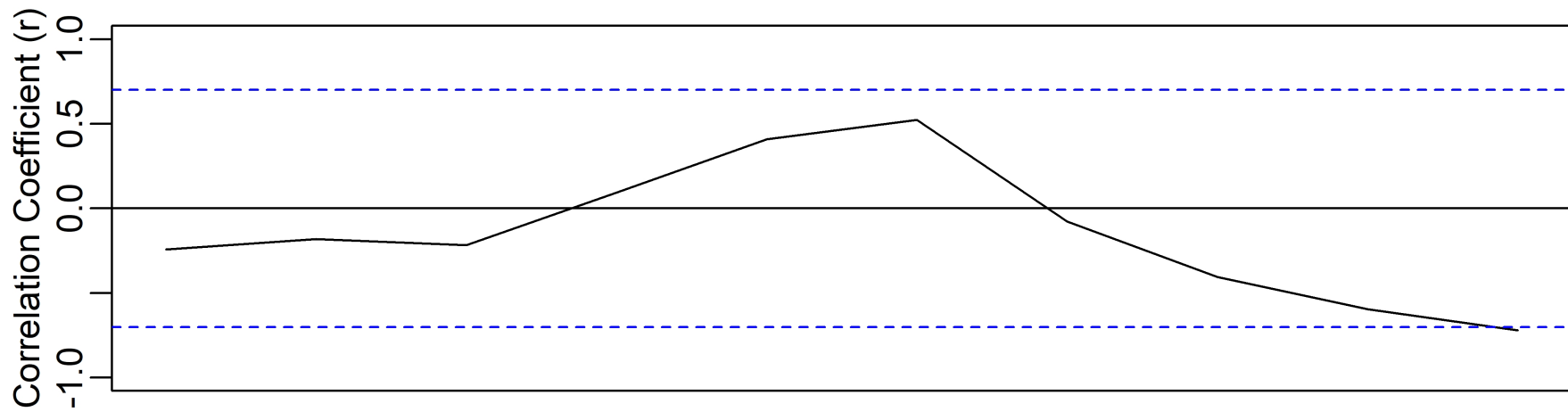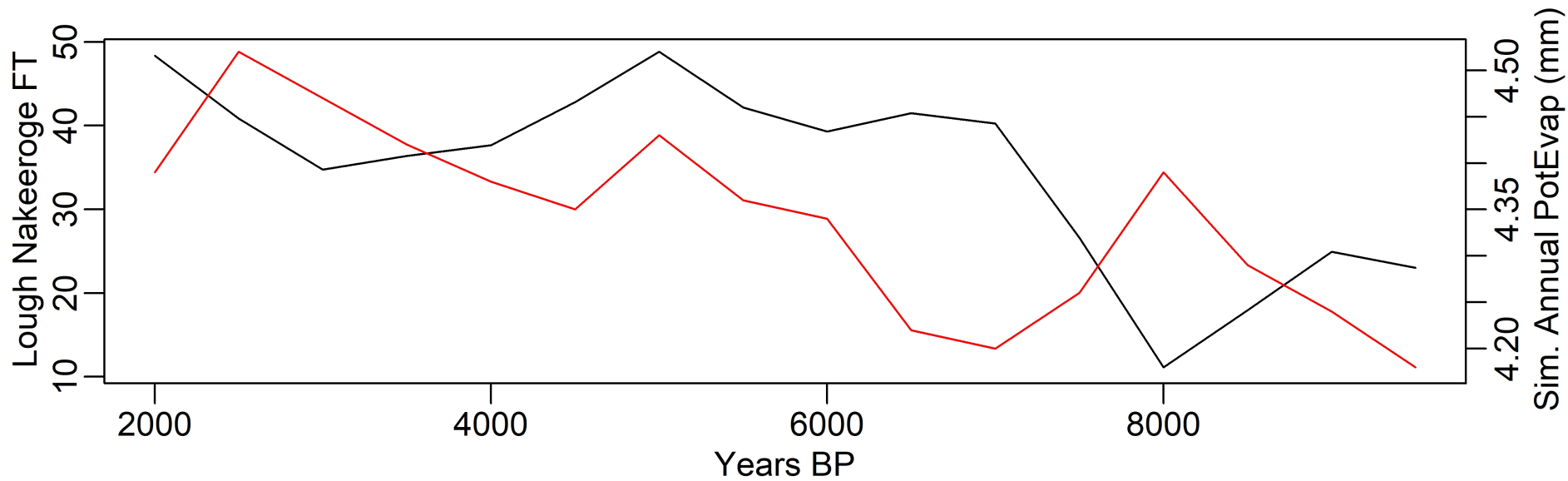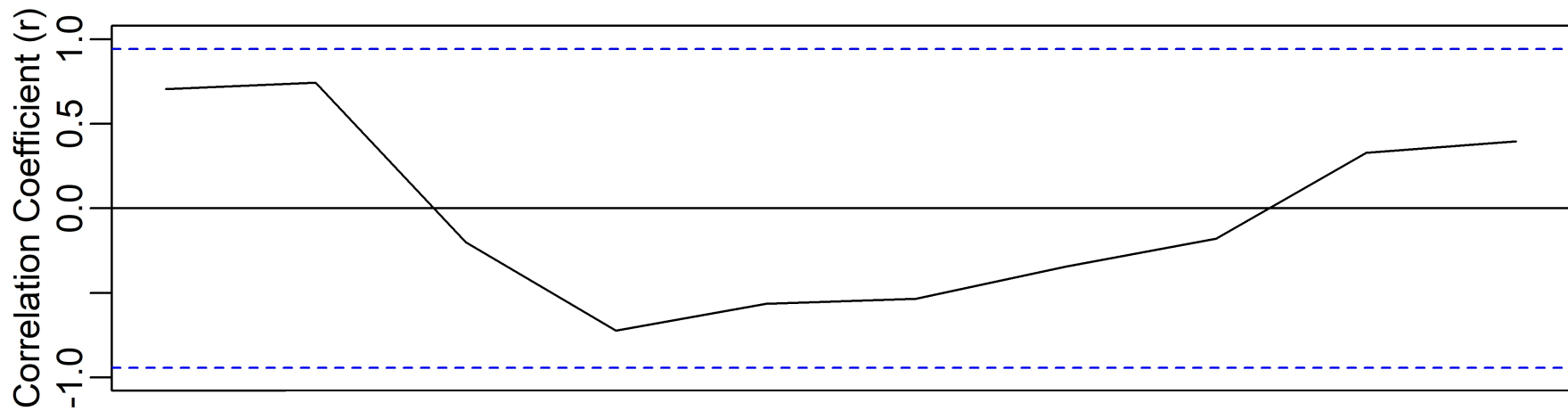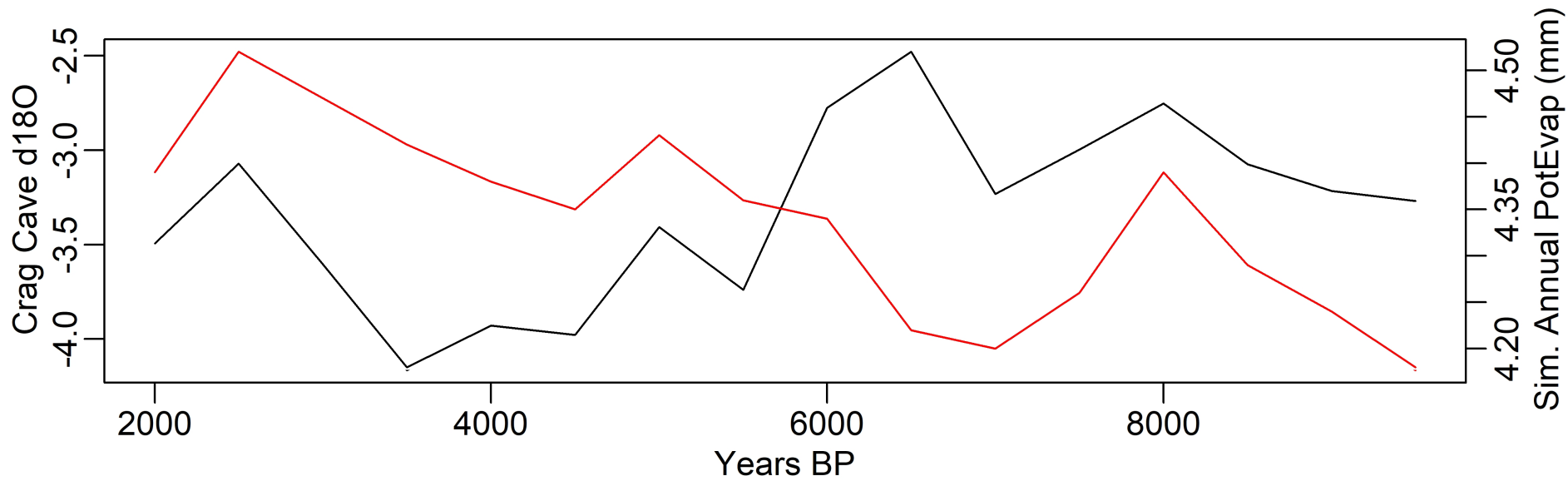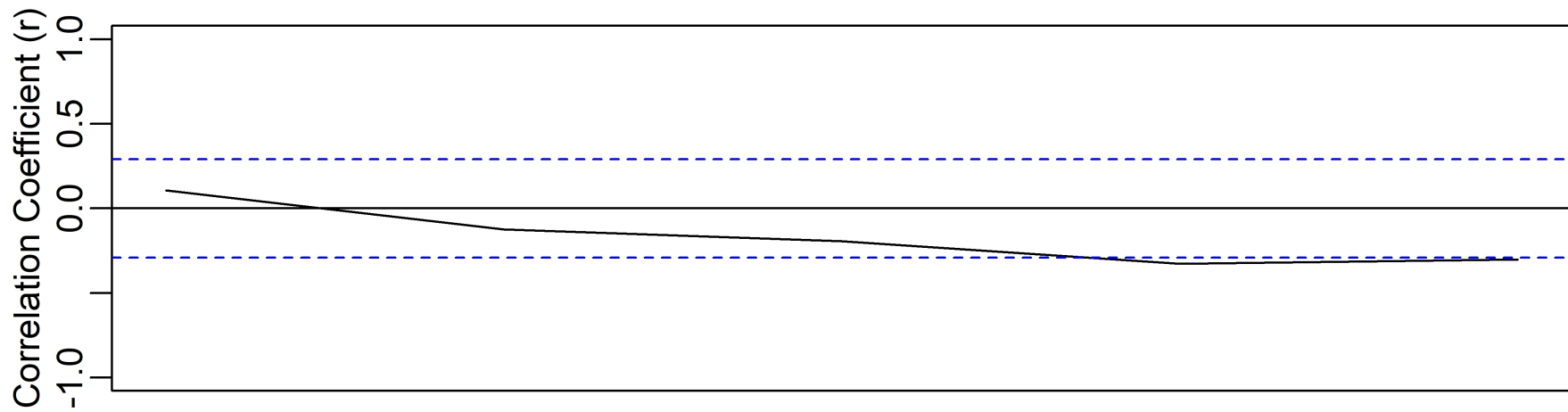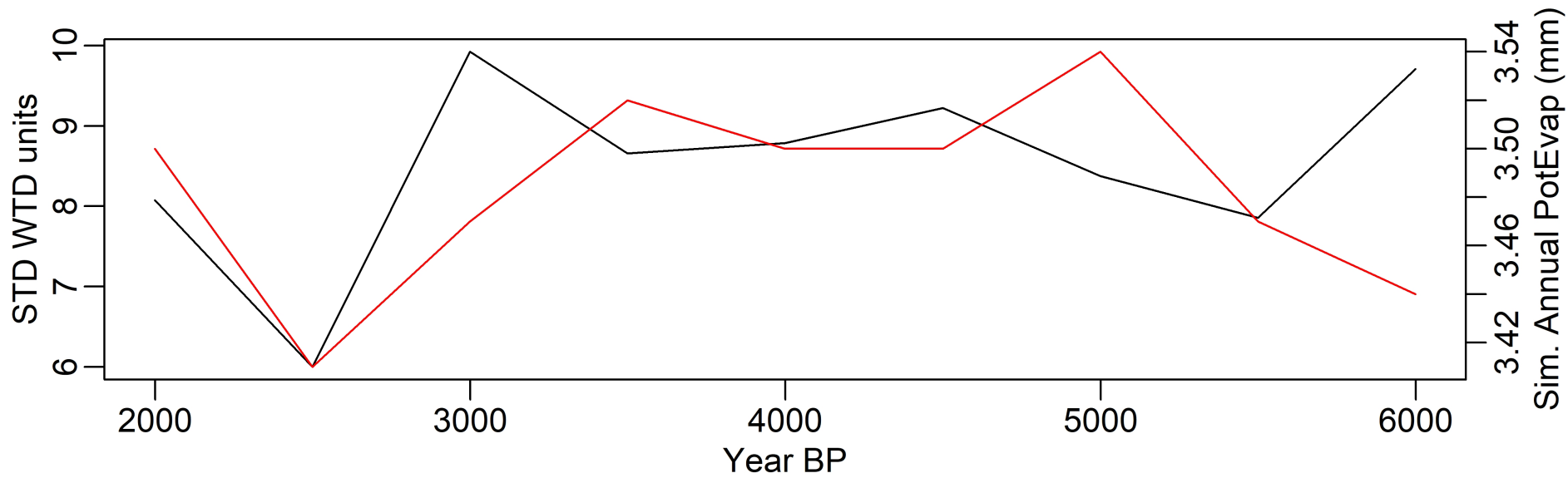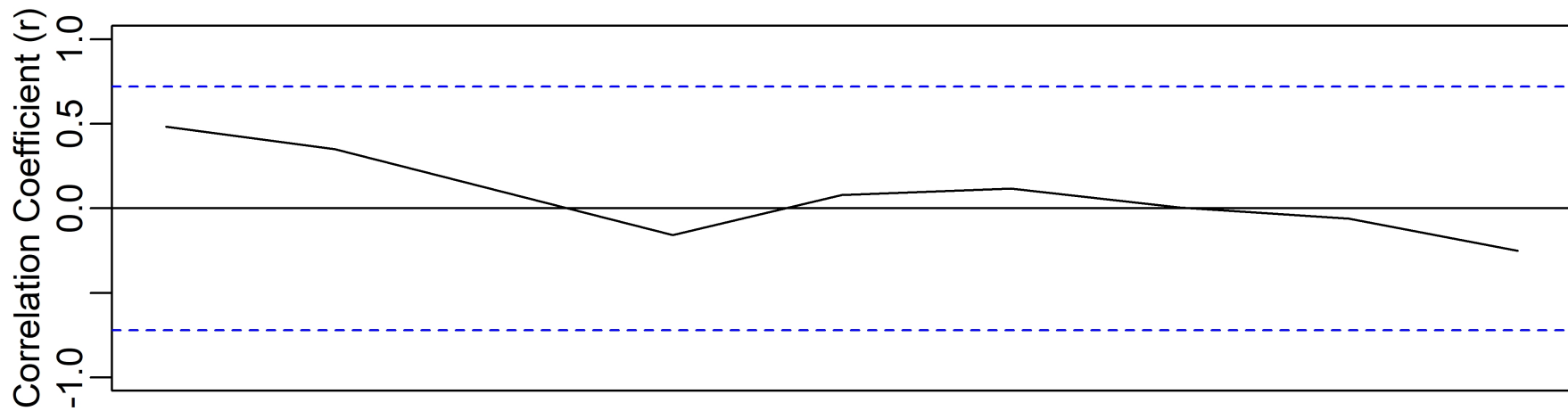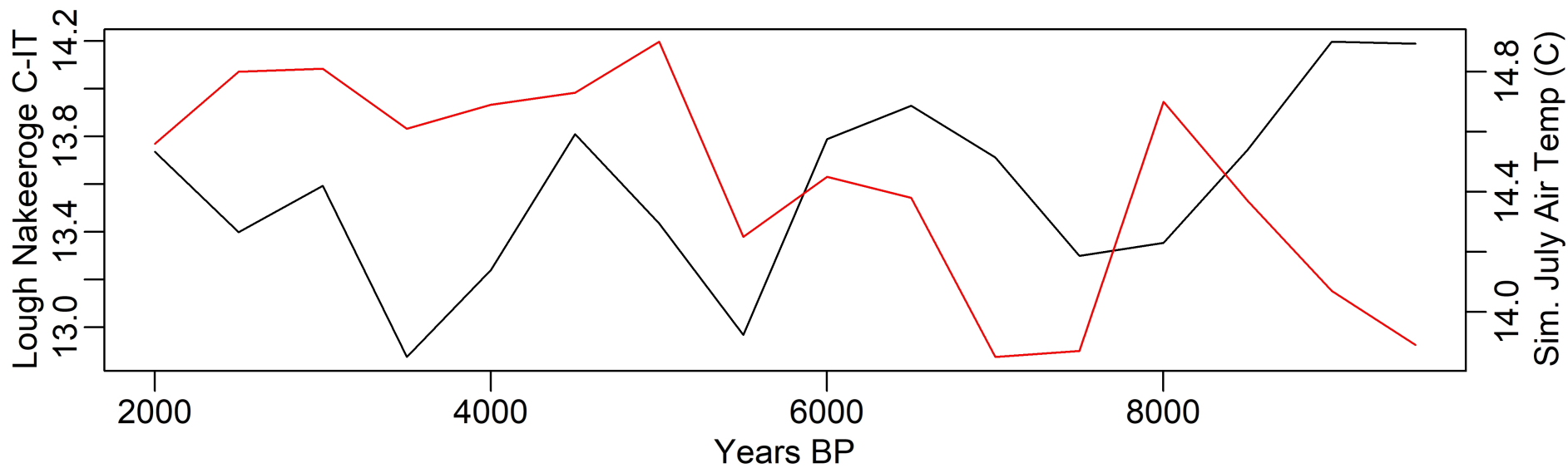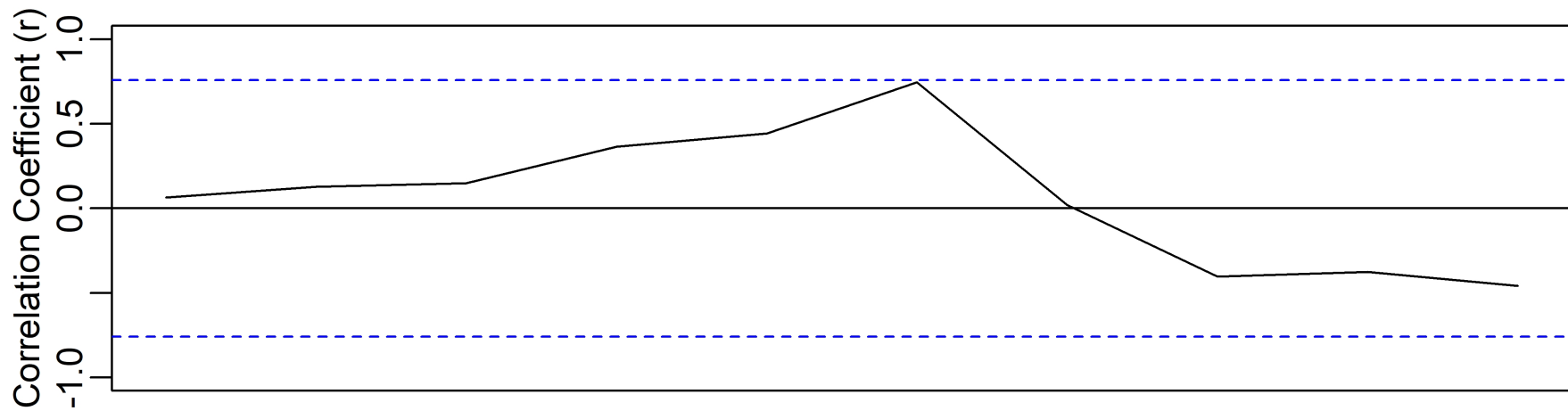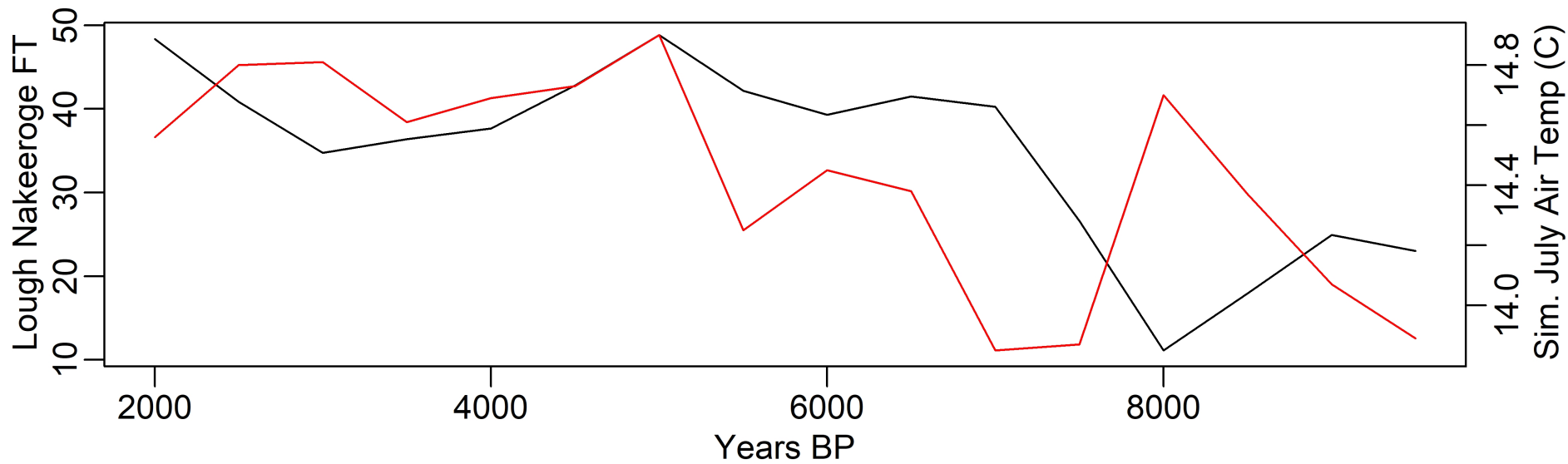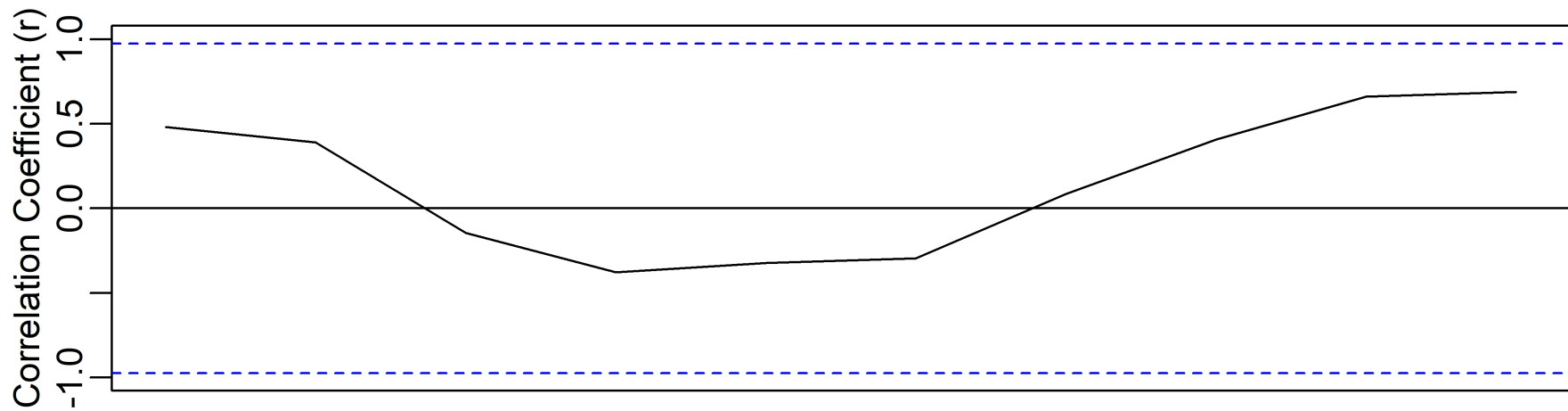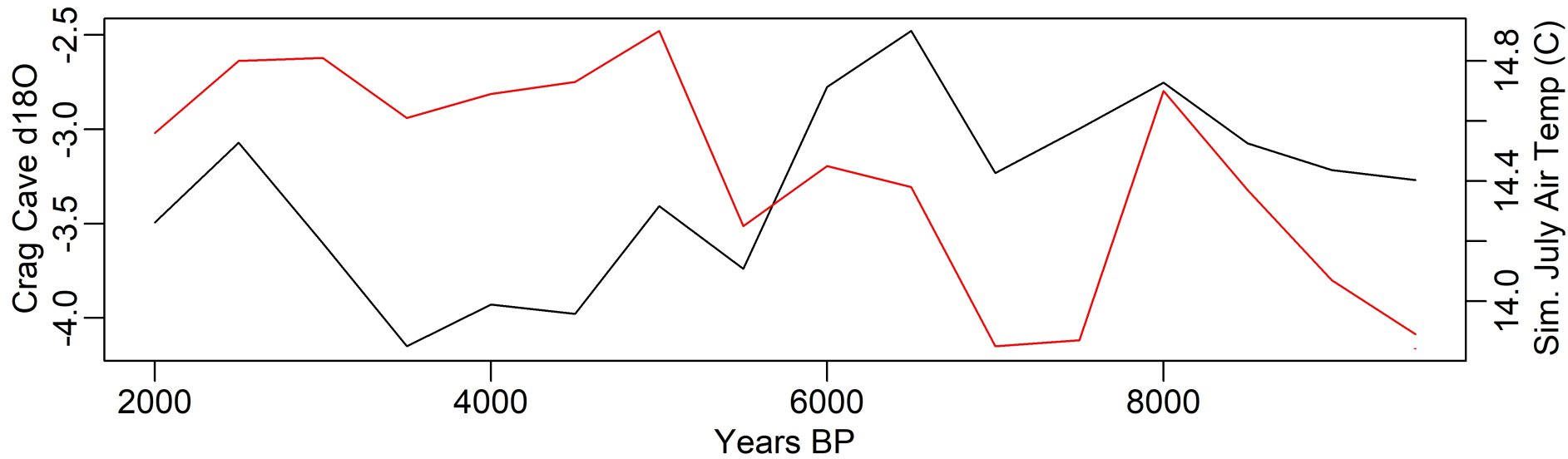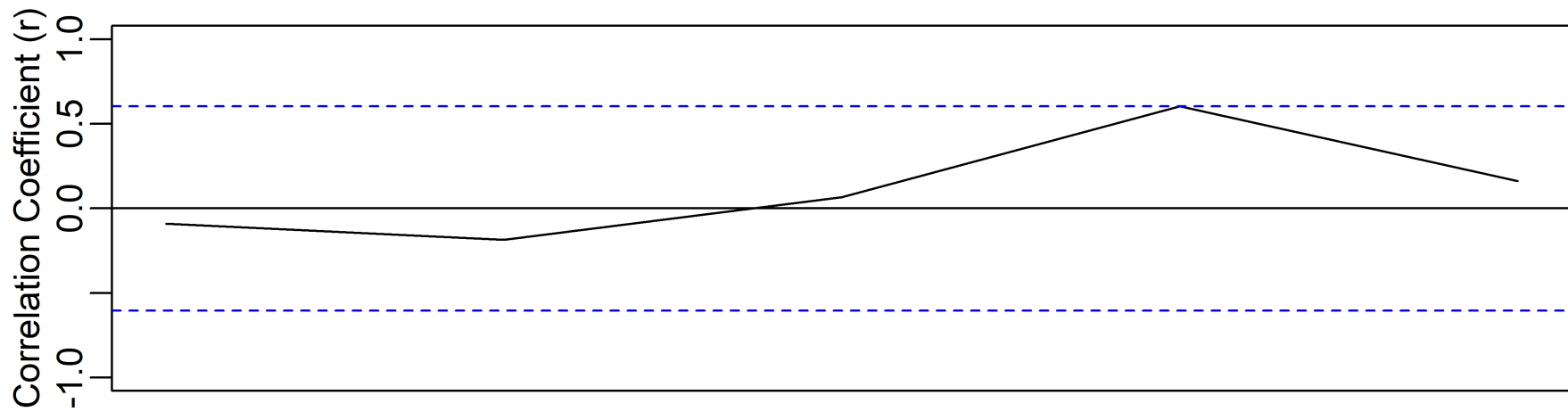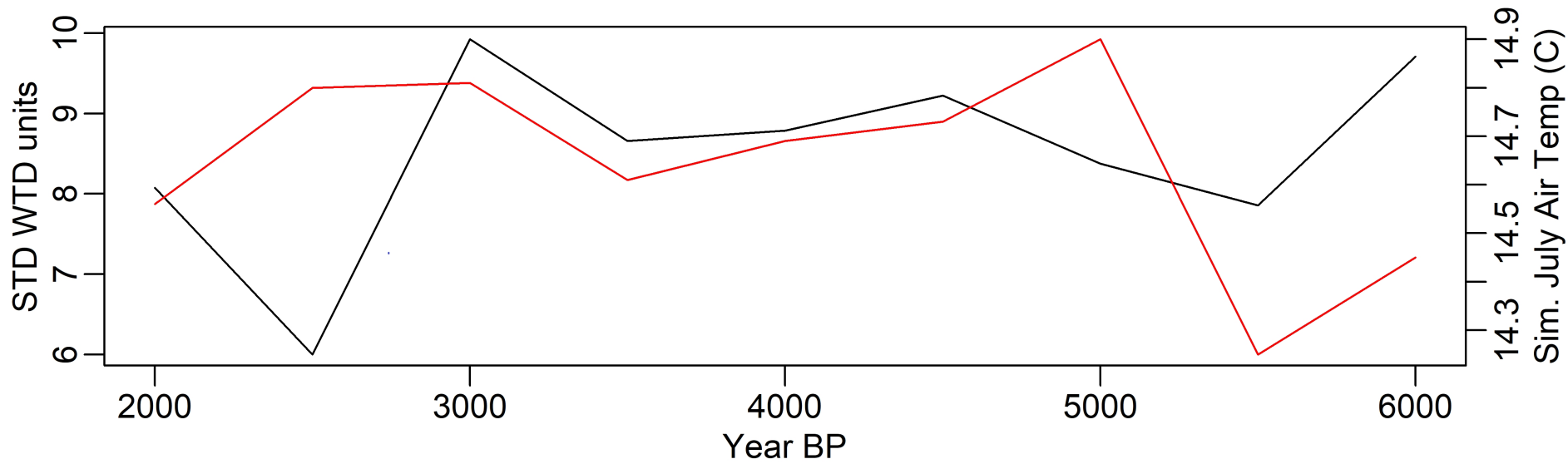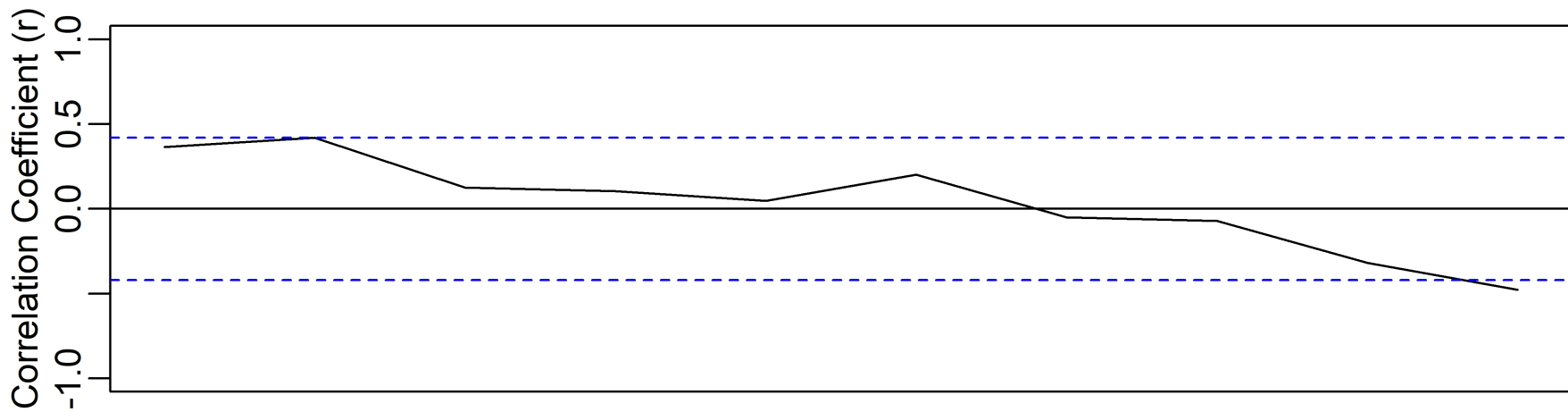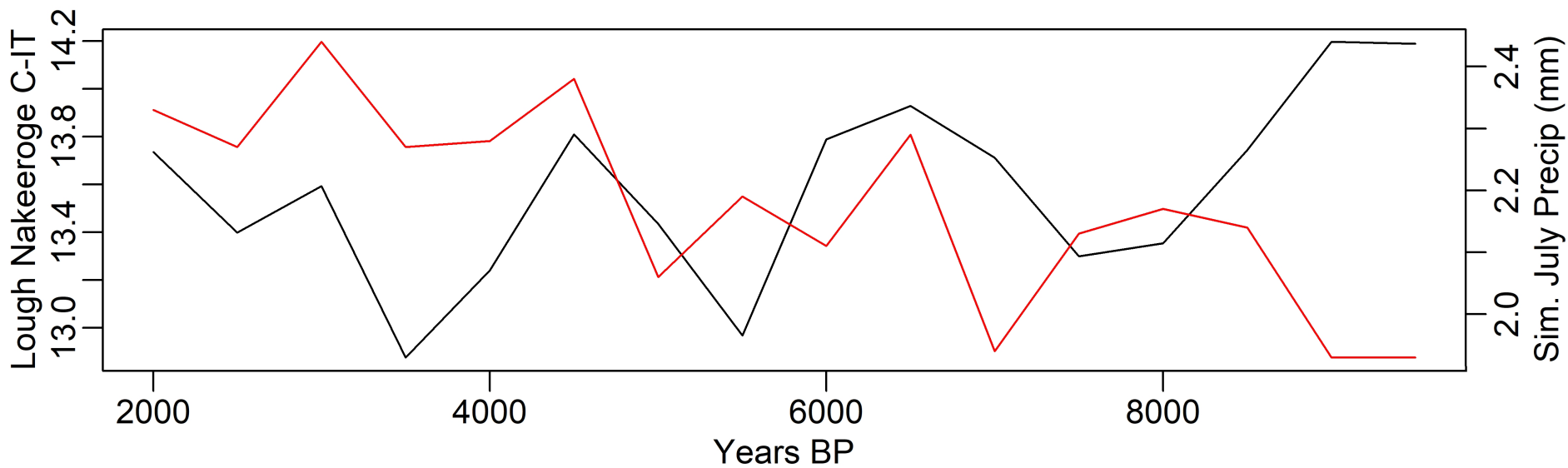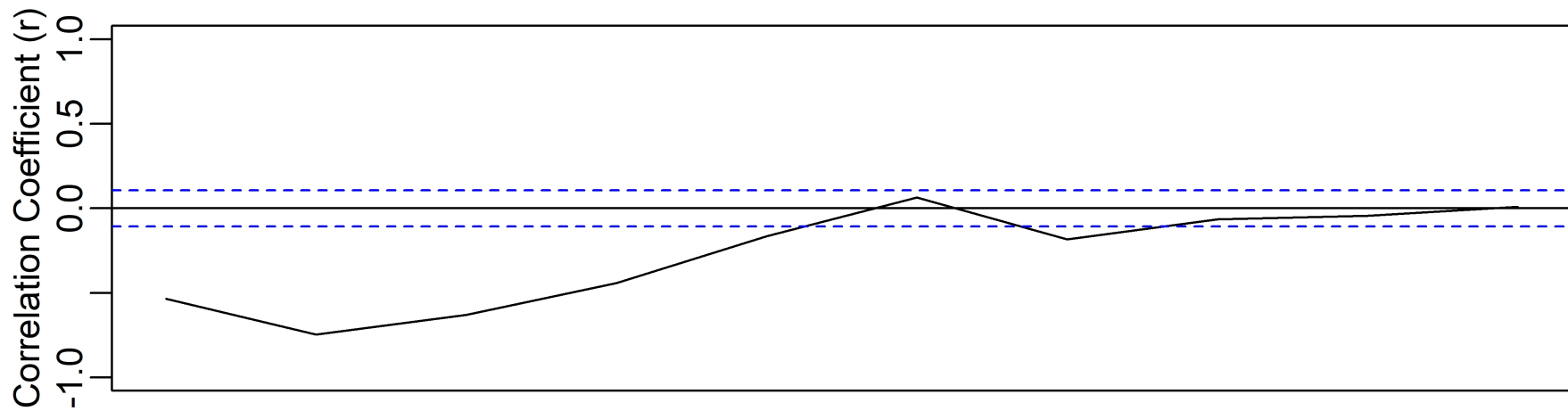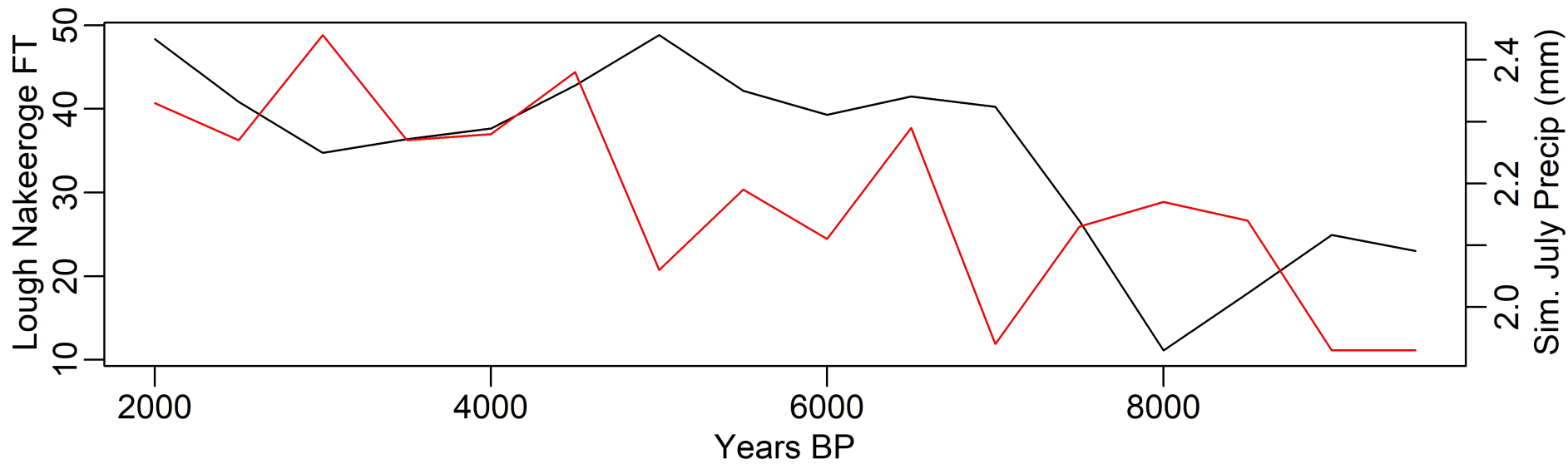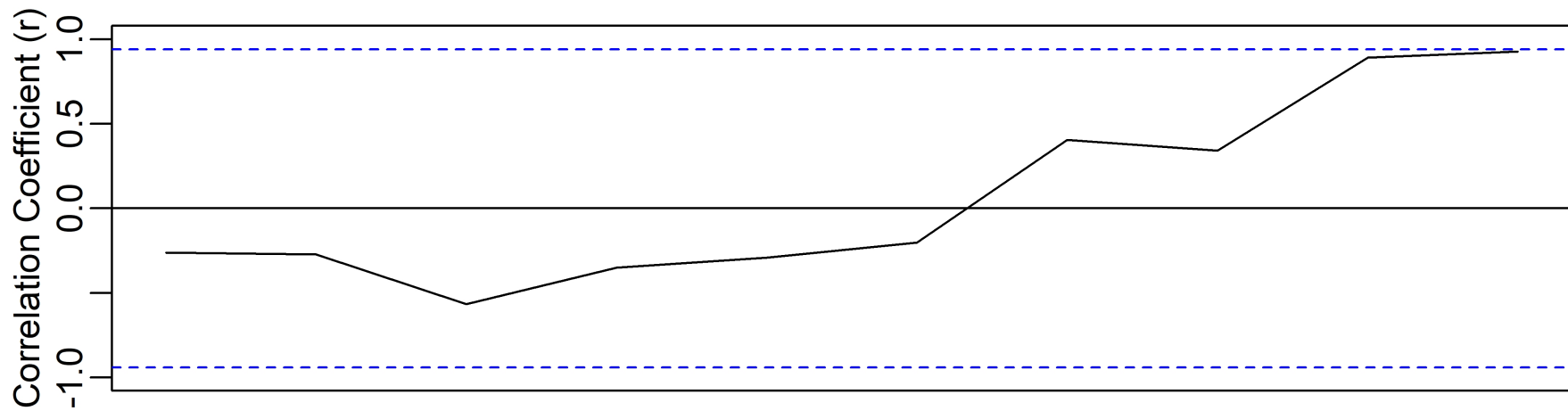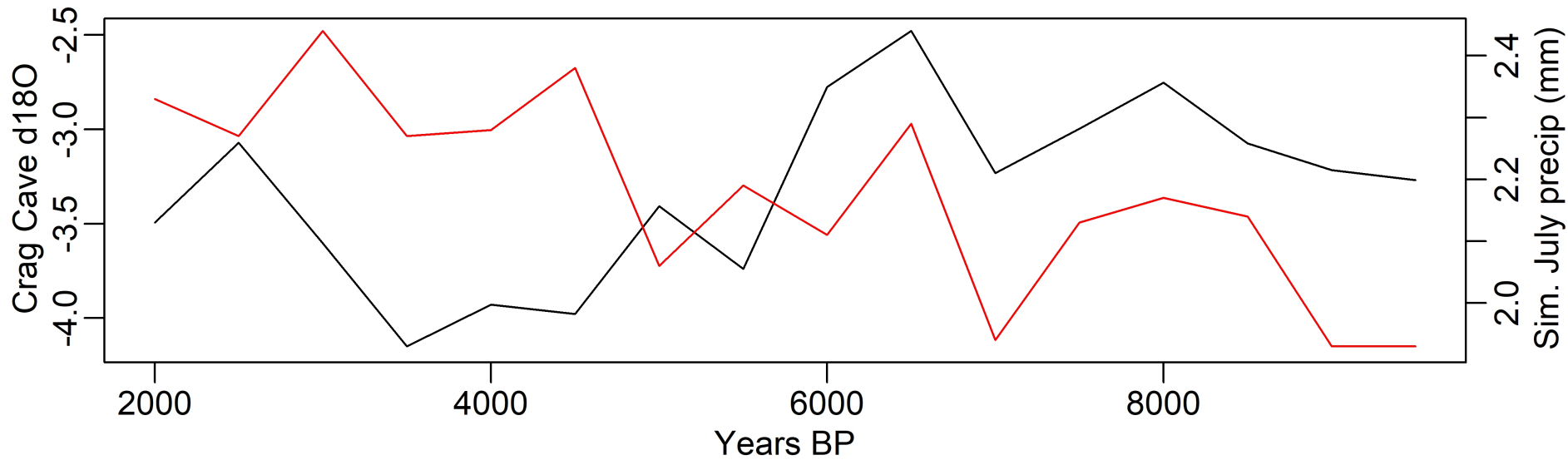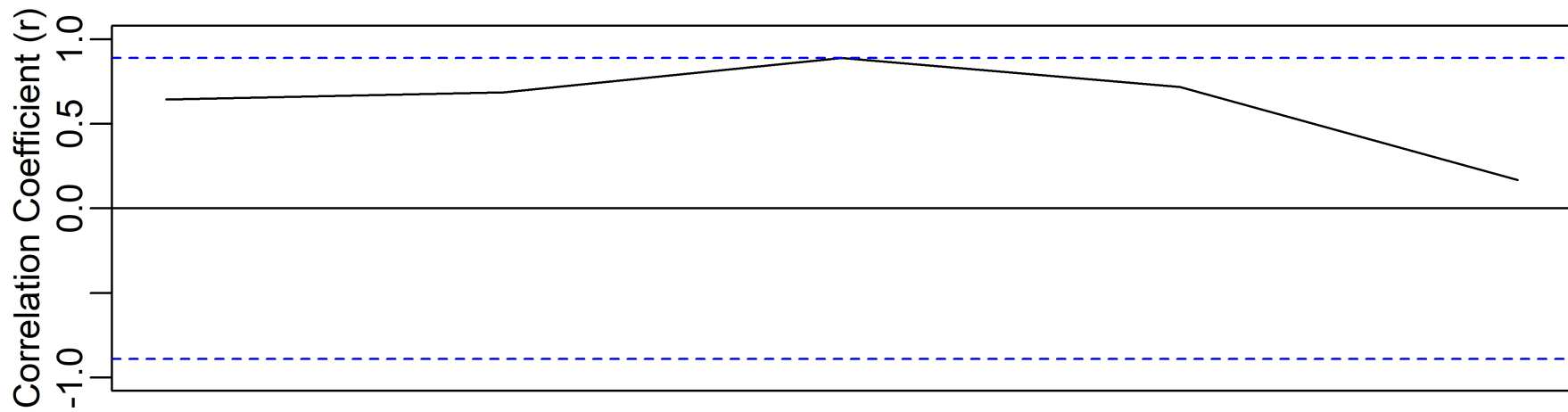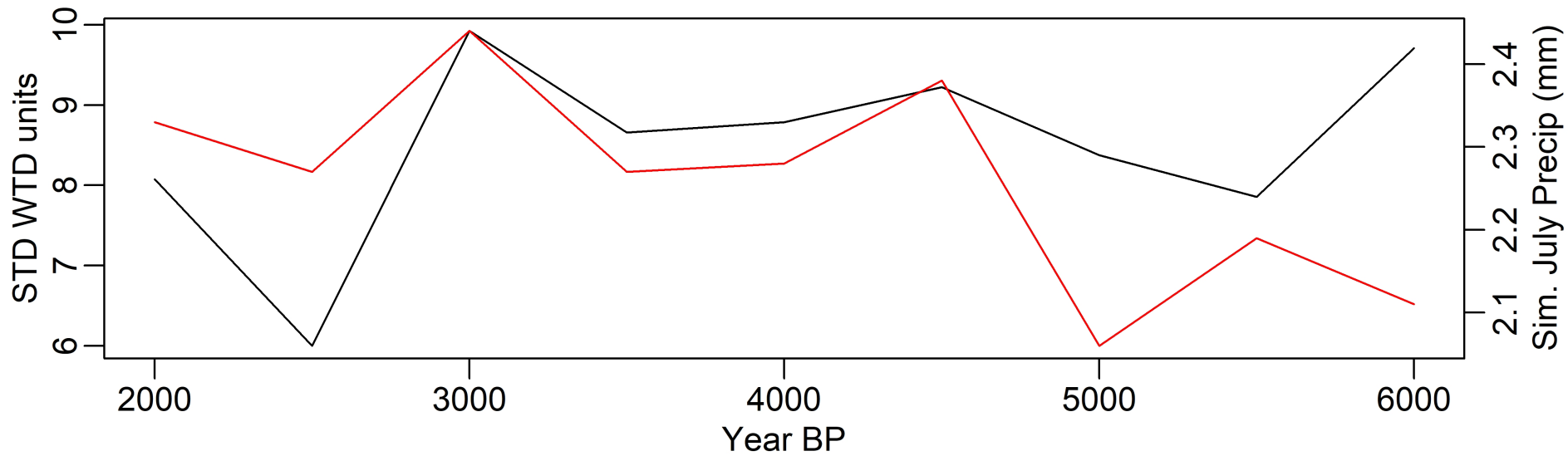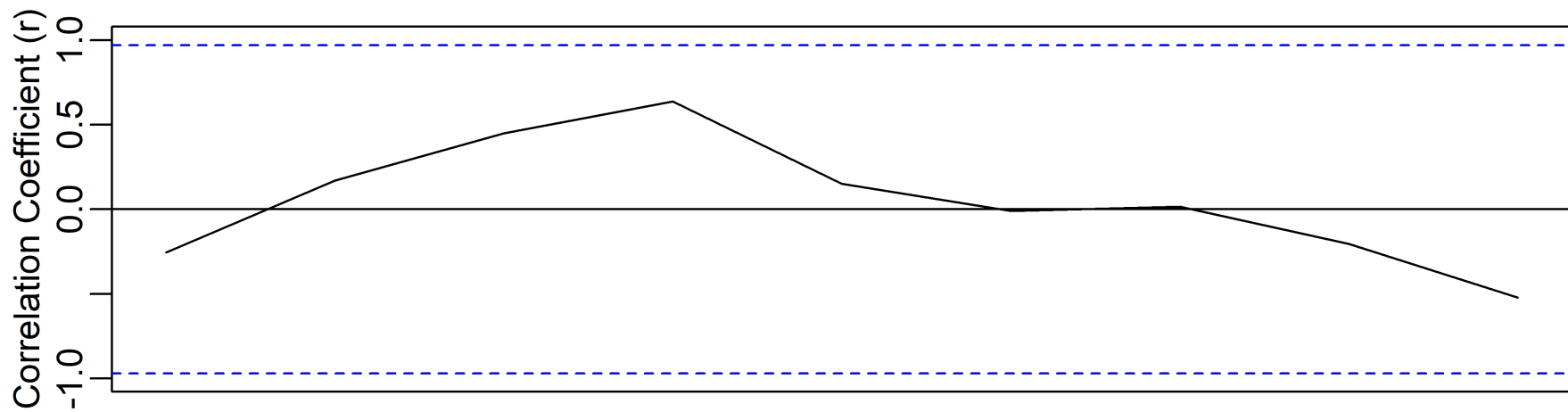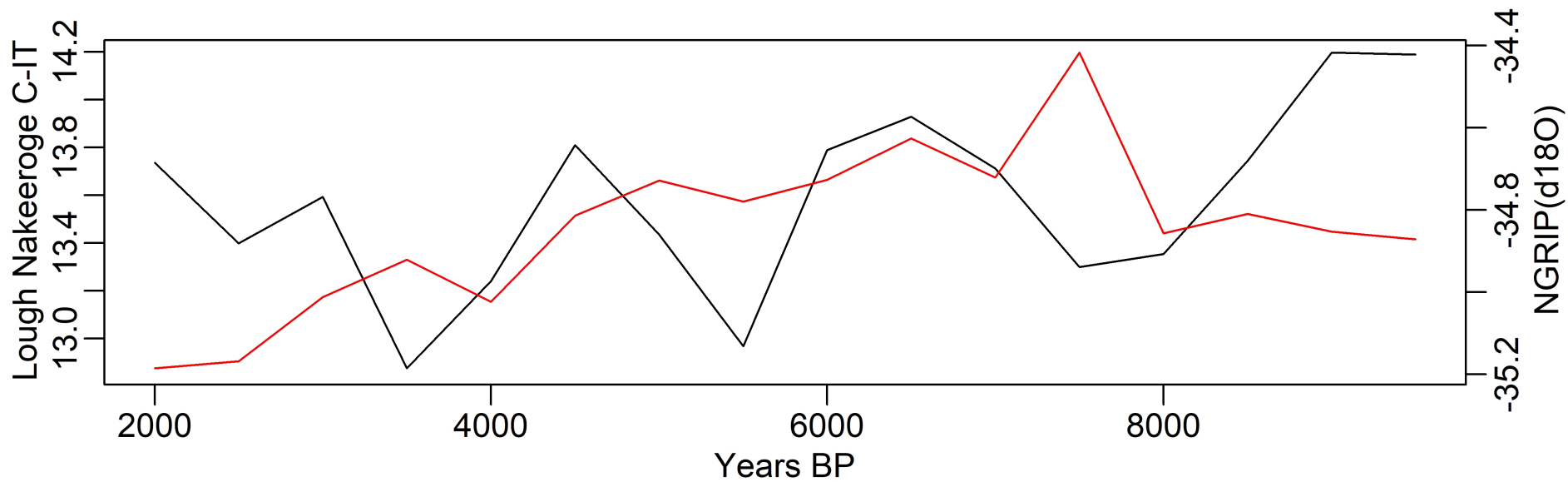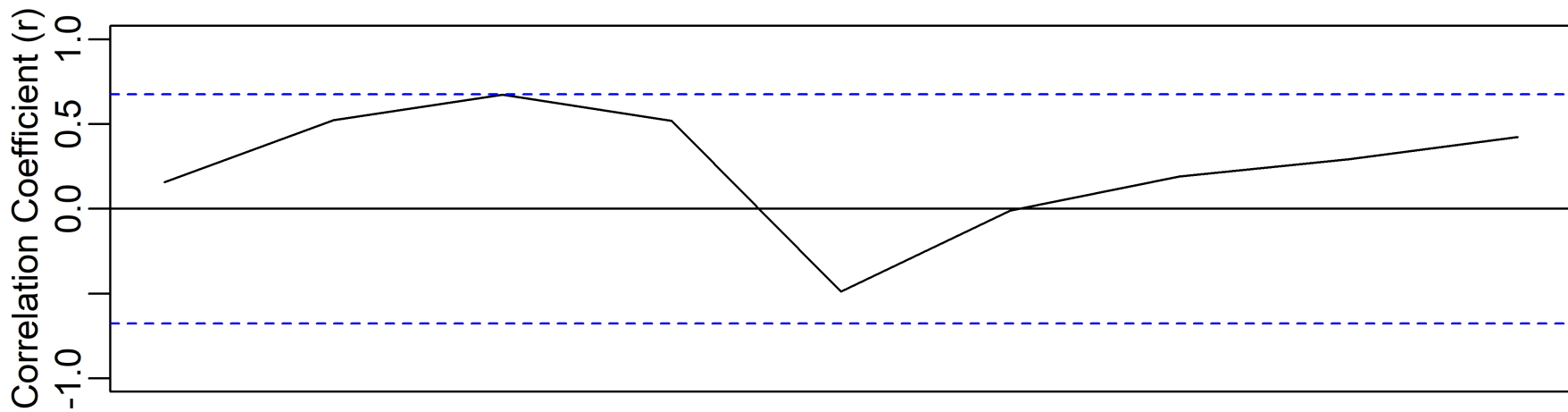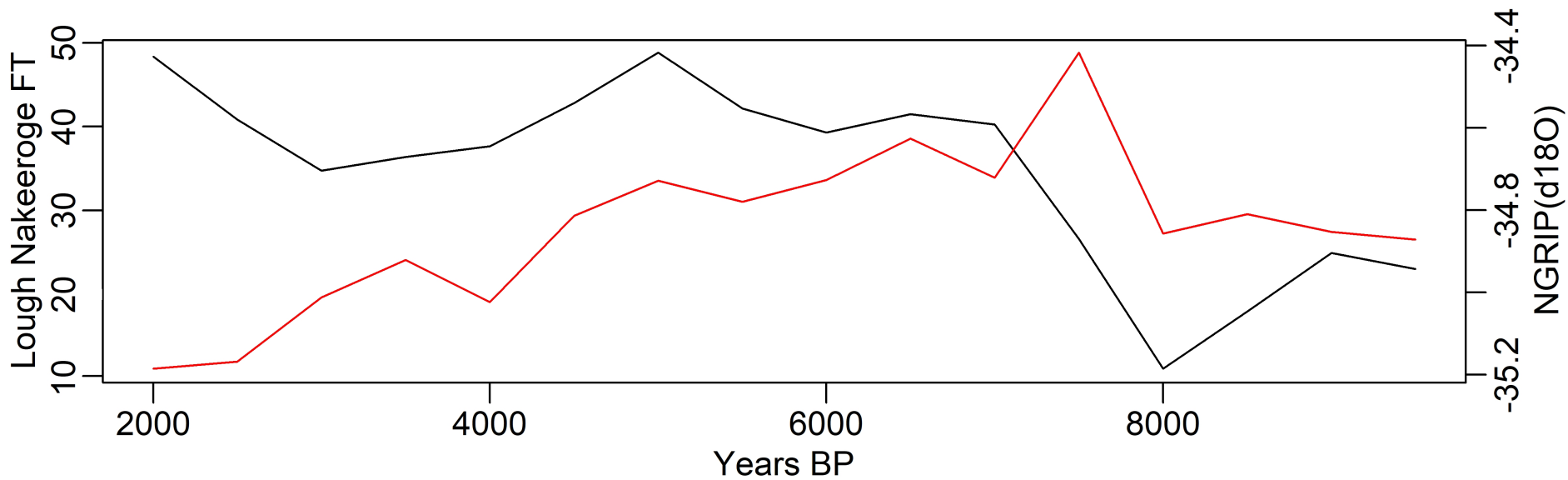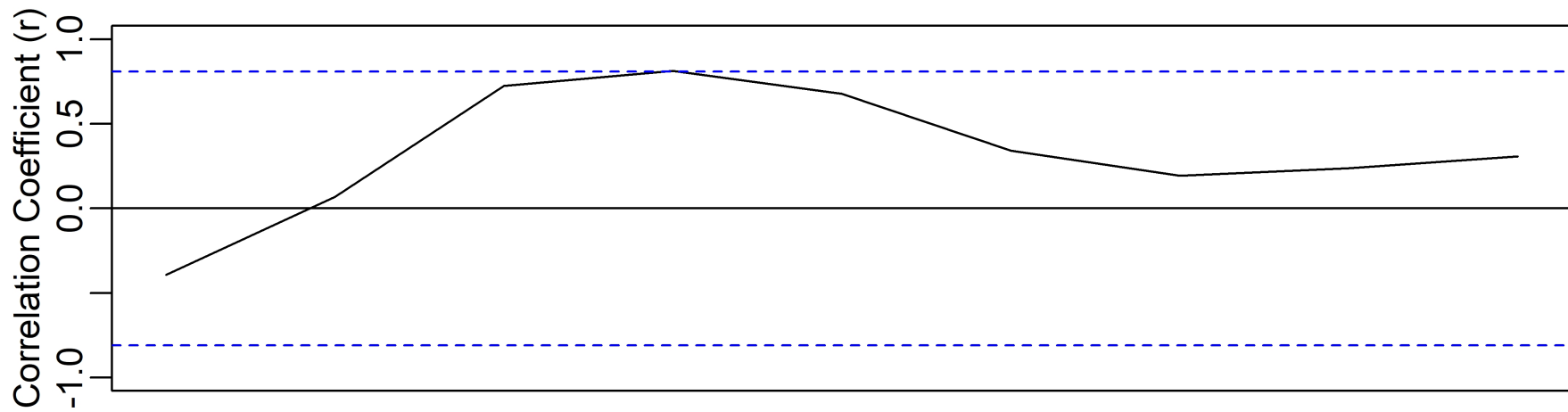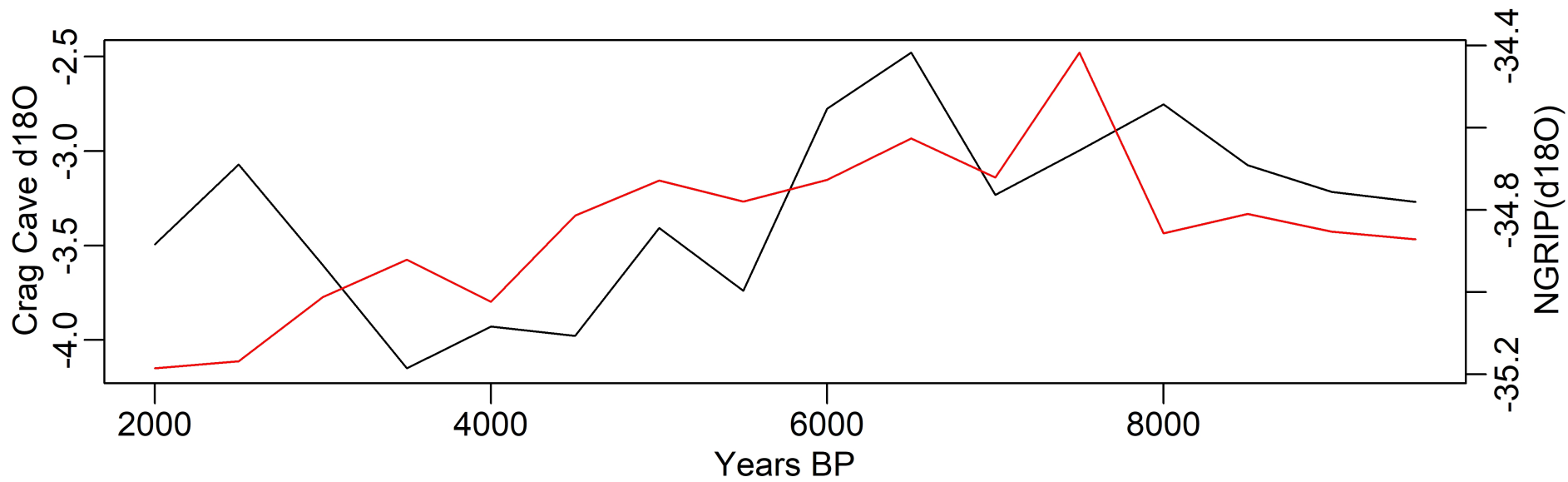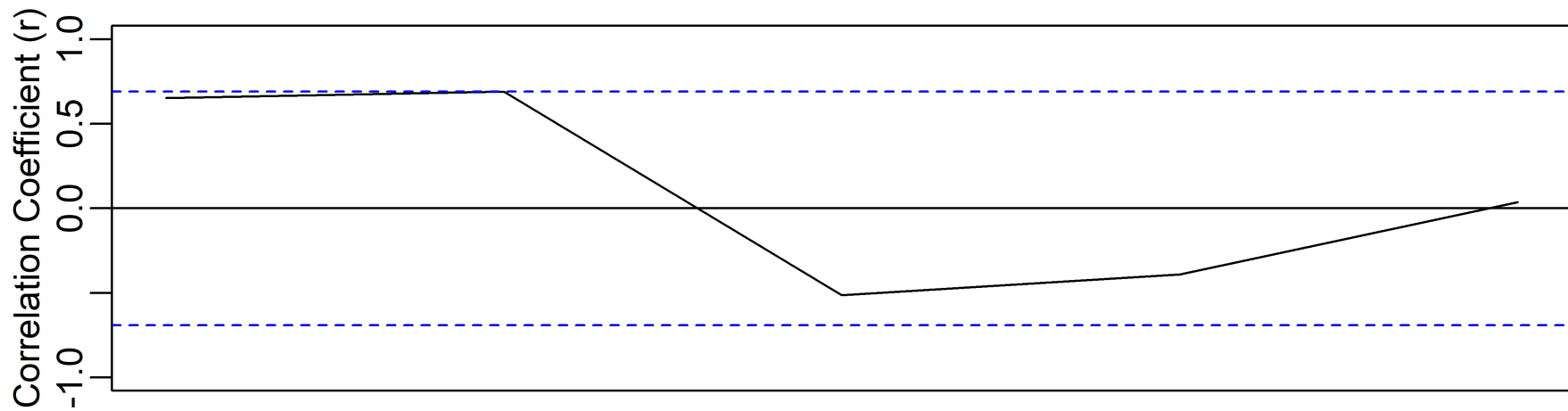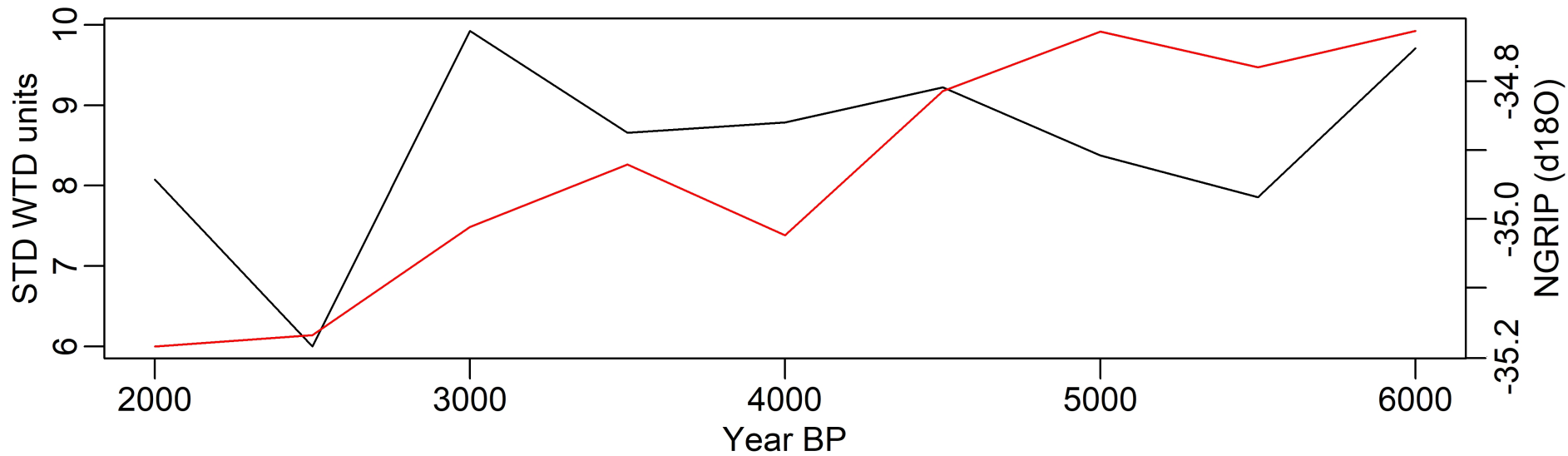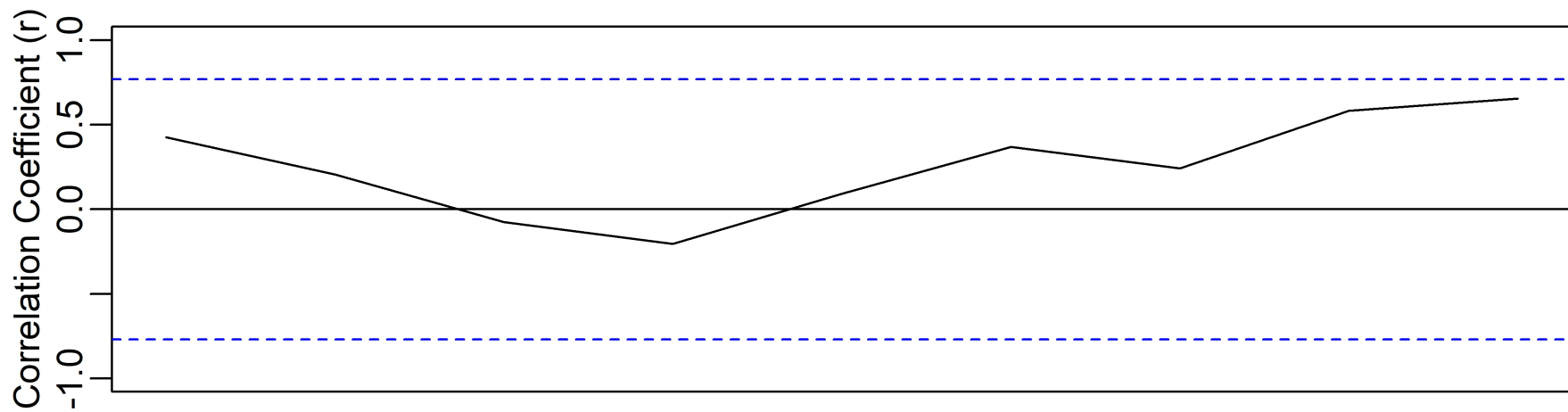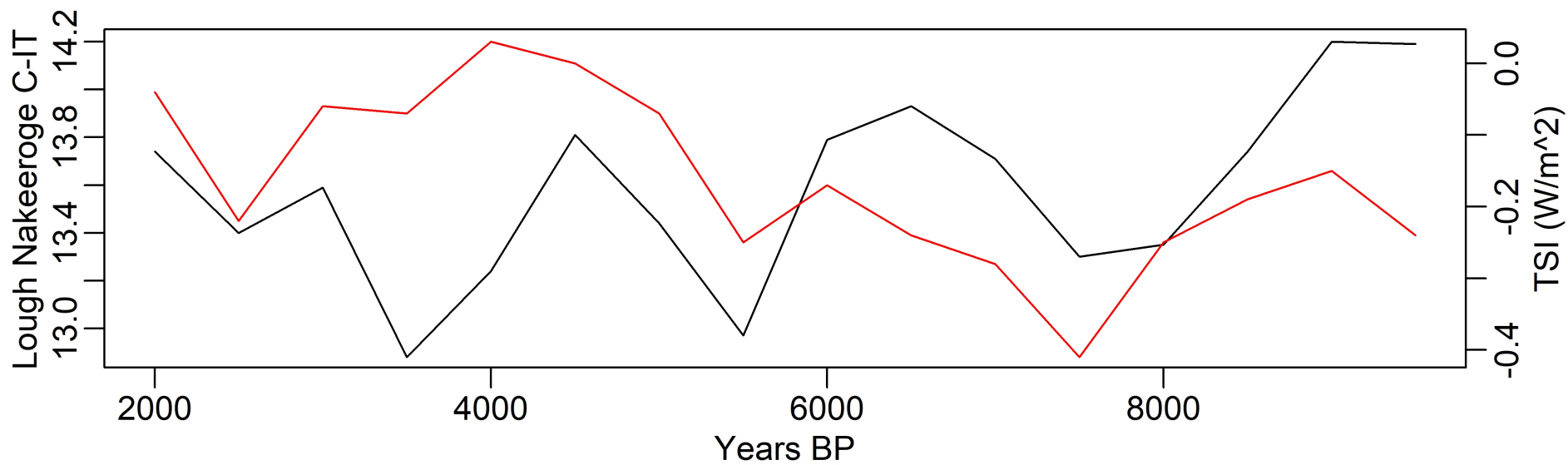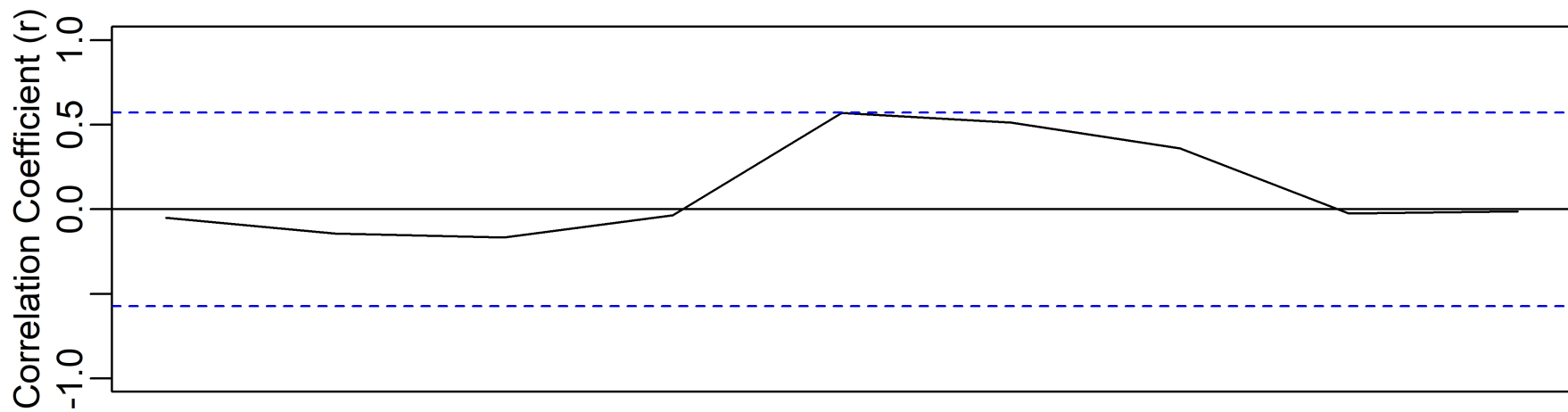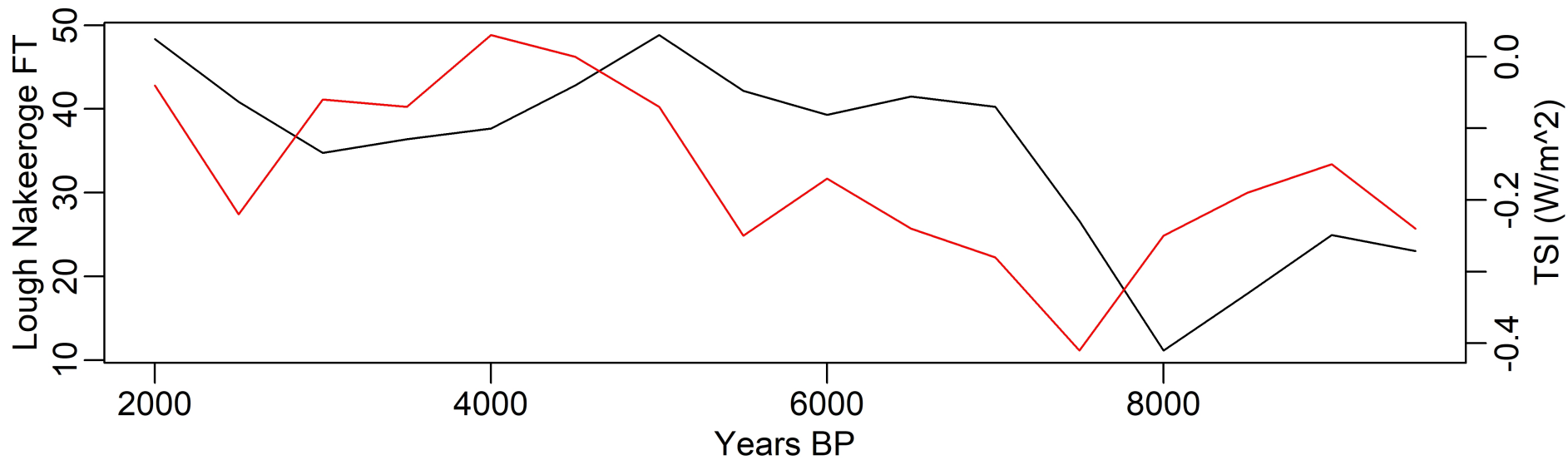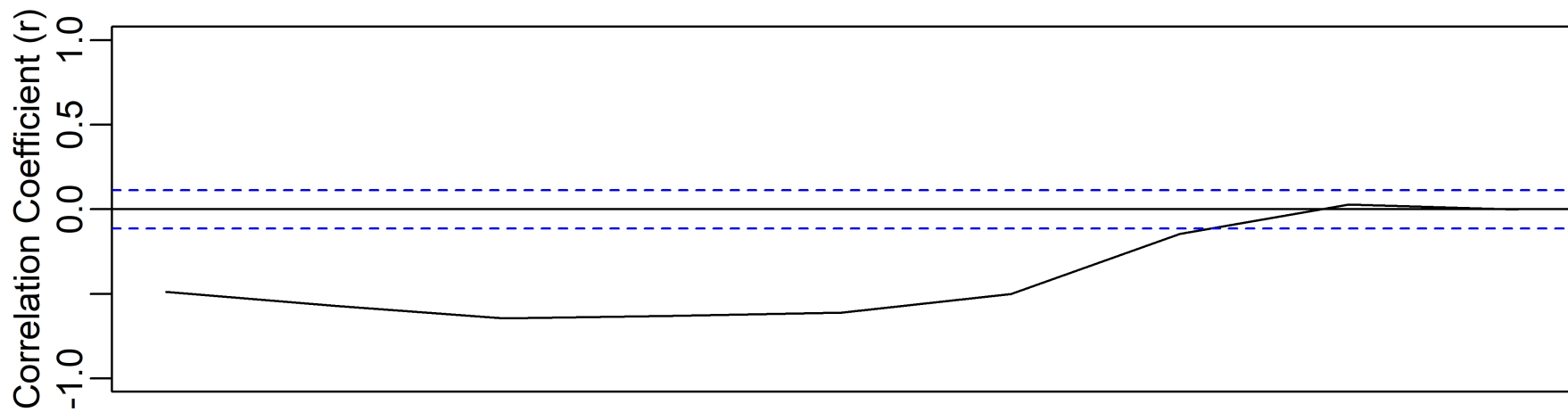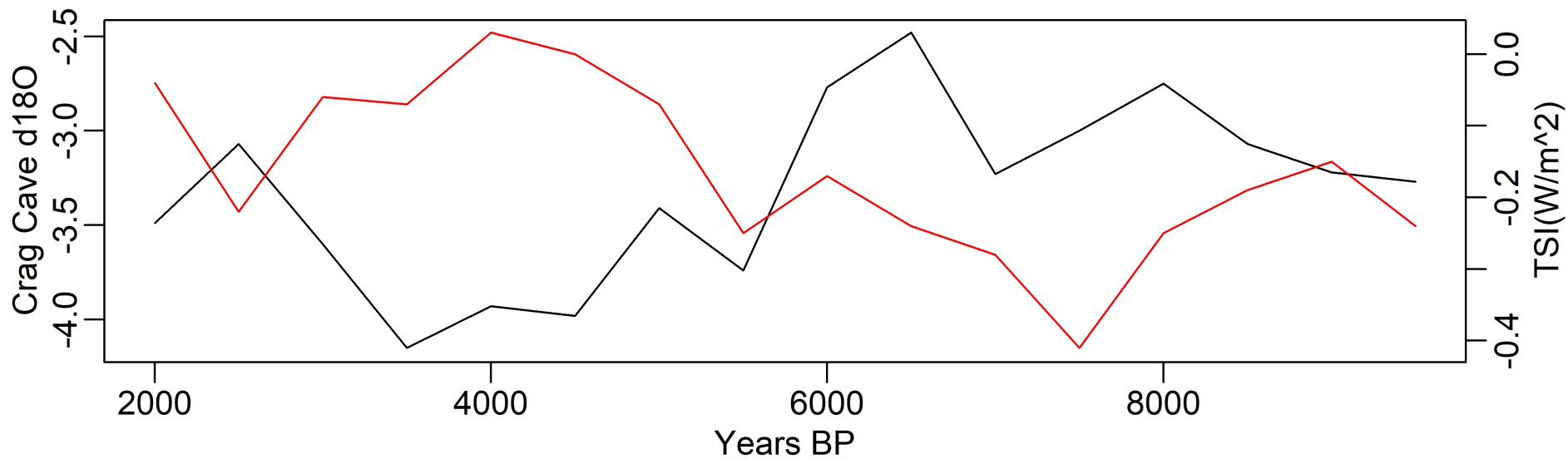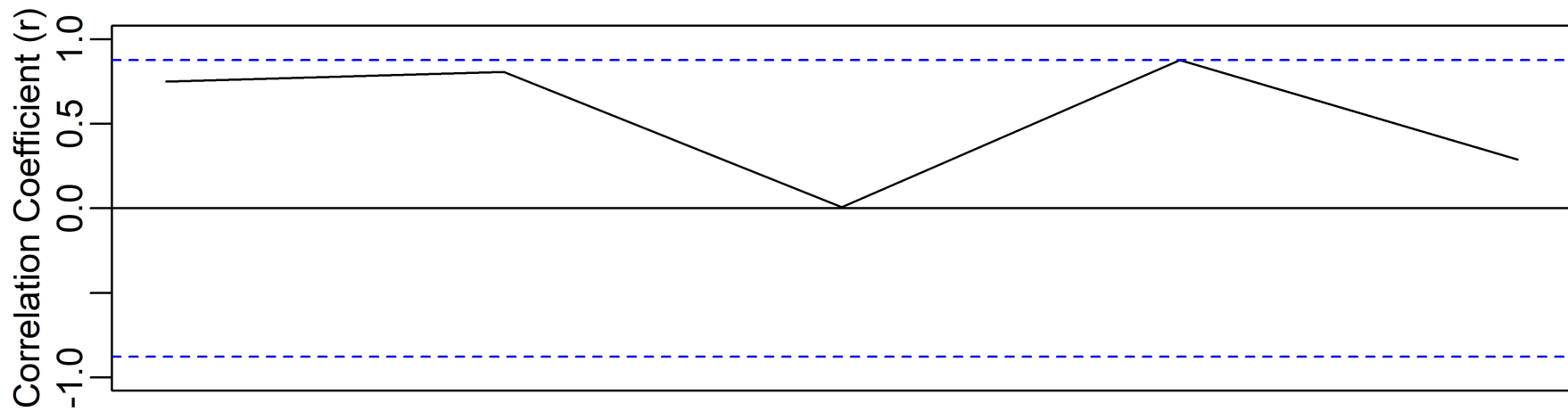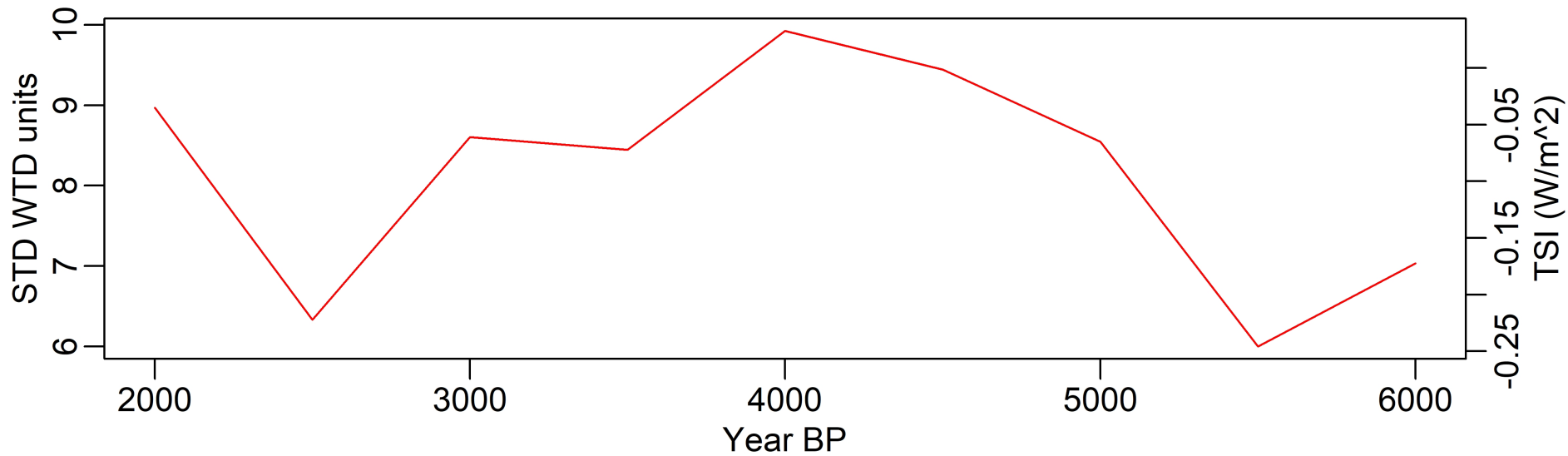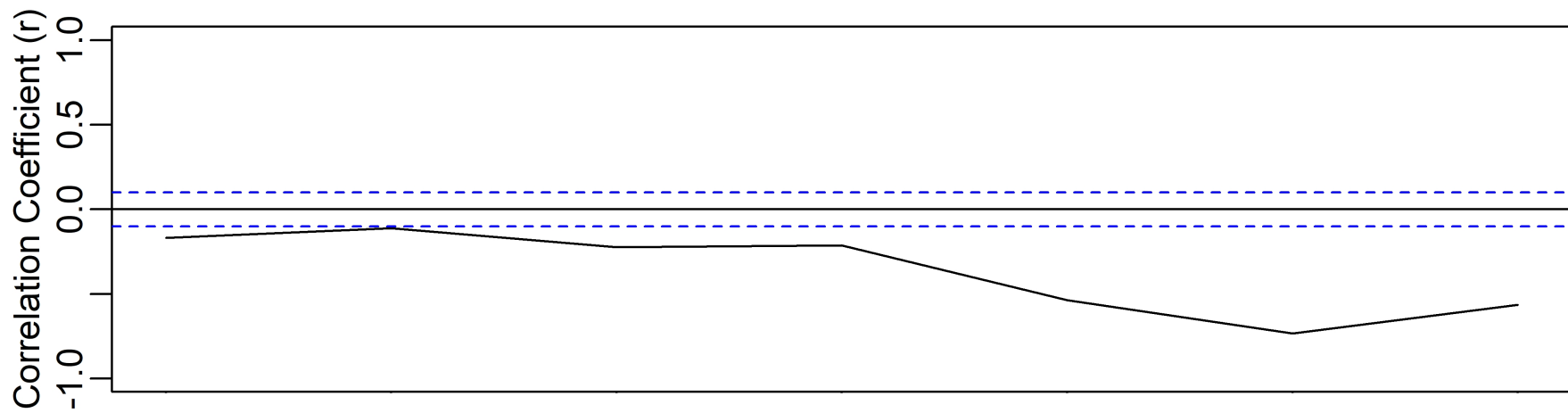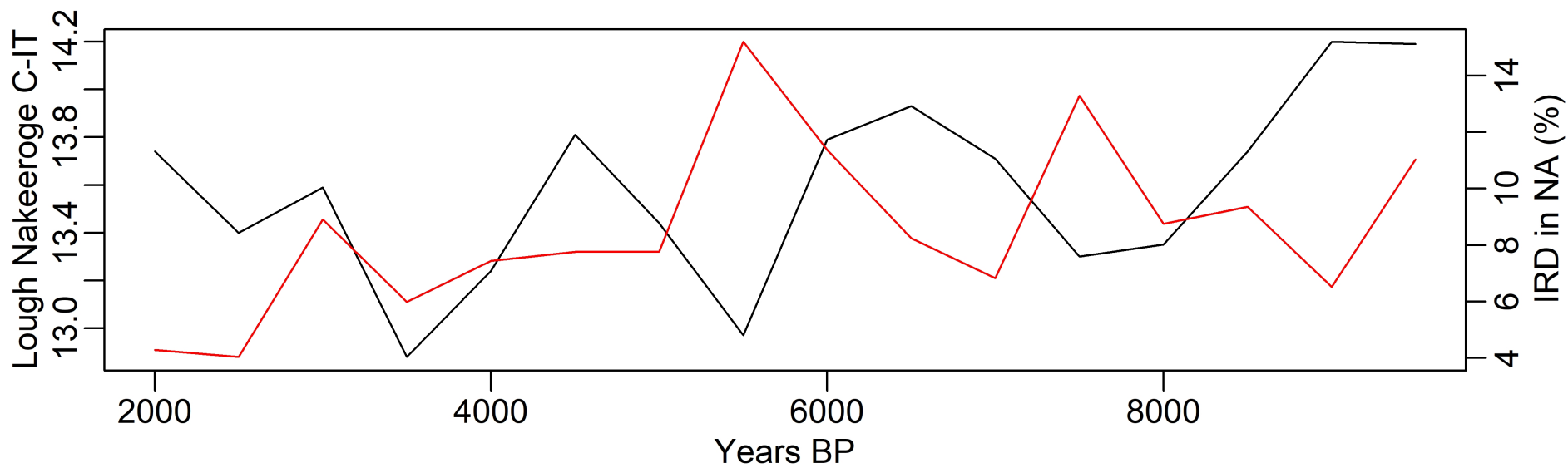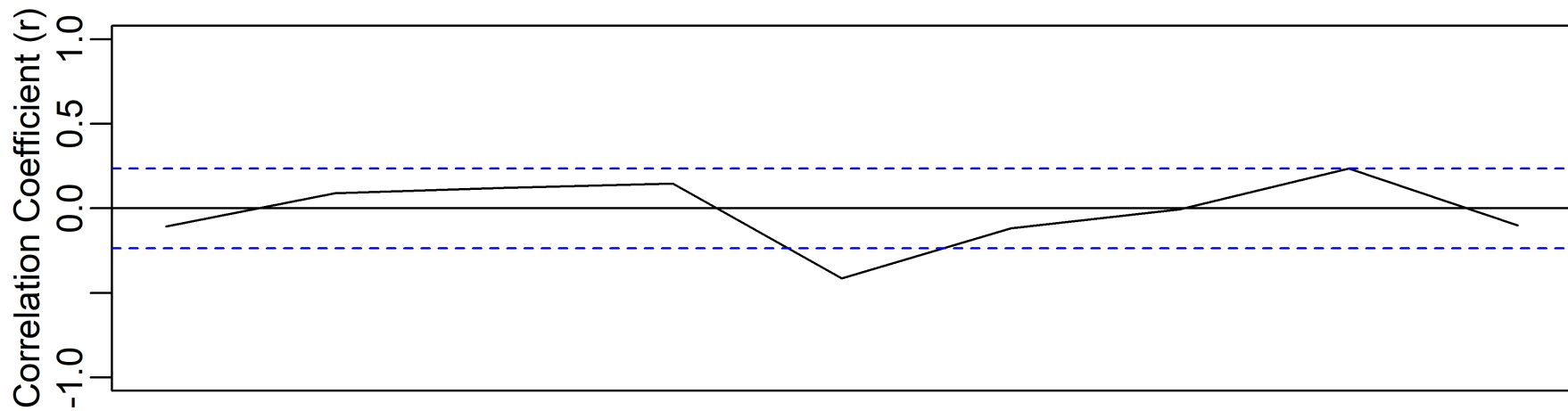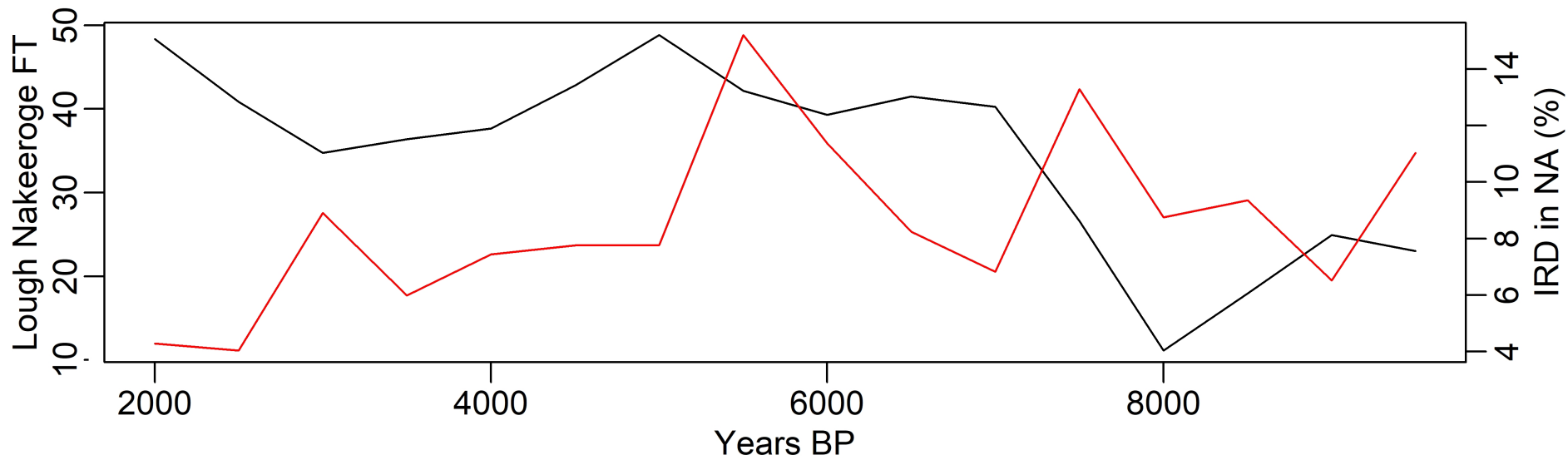
Table 1 Calculated ages of the bulk sediment layers and the corresponding linear accumulation rates. Ages were calibrated using IntCal 13 (Reimer et al. 2013).

Depth (cm)	Core segment	Conventional radiocarbon age (years BP ± 1σ)	Calibrated 2σ age range	Mid-point 2σ age range
76-77	A	2068 ± 37	2254-1884	2027
168-169*	B	4349 ± 35	5328-4515	4932
180-181	A	3874 ± 38	4459-4102	4311
224-225	A	4835 ± 36	5721-5373	5577
279-280	B	6586 ± 40	7462-6838	7214
380-381	B	8993 ± 45	10170-9387	9832

*This date from the top of core B was discounted

Table 2. Pearson's correlations. C-IT = chironomid-inferred temperature, FT = chironomid collector-filterer guild, CC = Crag Cave $\delta^{18}O$, LM = An Loch Mor $CaCO_3$, DWT = Depth to Water table compiled and standardised from Irish peatland records, NGRIP = Greenland Ice NGRIP $\delta180$, TSI = Total Solar Irradiance, IRD = Ice Rafted Debris in N. Atlantic.

	C-IT	FT	CC	LM	DWT	Ann Temp	Ann Precip	Ann PotEvap	July Temp	July Precip	NGRIP	TSI	IRD
C-IT		-0.16	0.43	-0.4	0.32	-0.55*	-0.54*	-0.58*	-0.34	-0.37	0.05	-0.03	-0.15
FT	-0.16		-0.36	0.42	-0.34	0.51*	0.31	0.31	0.32	0.34	-0.18	-0.42	-0.25
CC	0.43	-0.36		0.43	-0.18	-0.51*	-0.52*	-0.36	-0.28	0.33	0.38	-0.66*	0.14
LM	-0.4	0.42	0.43		0.07	0.06	<0.01	0.03	-0.04	0.1	0.33	-0.26	0.39
DWT	0.32	-0.34	-0.18	0.07		<-0.01	0.34	-0.51	-0.03	0.16	0.46	0.49	0.35
Ann Temp	-0.55*	0.51*	-0.51*	0.06	<-0.01						-0.39	0.55*	-0.30
Ann Precip	-0.54*	0.31	-0.52*	<0.01	0.34						-0.18	0.6*	-0.03
Ann PotEvap	-0.58*	0.31	-0.36	0.03	-0.51						-0.6*	0.48*	-0.33
July Temp	-0.34	0.32	-0.28	-0.04	-0.03						-0.53*	0.68*	-0.43
July Precip	-0.37	0.34	0.33	0.1	0.16						-0.4	0.49*	-0.21
NGRIP	0.05	-0.18	0.38	0.33	0.46	-0.39	-0.18	-0.6*	-0.53*	-0.4			
TSI	-0.03	-0.42	-0.66*	-0.26	0.49	0.55*	0.6*	0.48*	0.68*	0.49*			
IRD	-0.15	-0.25	0.14	0.39	0.35	-0.30	-0.03	-0.33	-0.43	-0.21			

*P significance level for Monte Carlo permutation tests (999 unrestricted permutations). $P < 0.05$